ESTIMATING THE HUMAN HEALTH RISKS ASSOCIATED WITH EXPOSURES TO HARMFUL CONSTITUENTS EMITTED FROM ELECTRONIC CIGARETTES

By

YEONGKWON SON

A dissertation submitted to the

School of Public Health

and the

School of Graduate Studies

Rutgers, The State University of New Jersey

In partial fulfillment of the requirements

For the degree of

Doctor of Philosophy

Graduate Program in Public Health

Written under the direction of

Qingyu Meng, PhD

And approved by

_____

_____

_____

_____

_____

New Brunswick, New Jersey

January, 2018

ABSTRACT OF THE DISSERTATION

Estimating the Human Health Risks Associated with Exposures to

Harmful Constituents Emitted from Electronic Cigarettes

by YEONGKWON SON

Dissertation Director:

Dr. Qingyu Meng

The use of electronic cigarettes (e-cigarettes) has been rapidly increased because e-cigarettes are believed to be less harmful to health than conventional cigarettes. In the past five years, a few human and rodent *in vivo* and *in vitro* studies have suggested adverse health effects associated with e-cigarette vaping. However, the emission of chemicals and particles from e-cigarettes is still not well understood under "real-world" vaping conditions. This study evaluated the impacts of "real-world" e-cigarette battery power outputs, vaping topographies, and e-liquid compositions on e-cigarette particle size distribution, e-vapor chemical composition, and the vaping-induced human cancer risk.

E-vapors were generated using a smoking machine under various e-cigarette power settings, vaping topographies, and e-liquid compositions. These e-vapor generation conditions reflected the "real-world" e-cigarettes use pattern, and were obtained from the literature and a panel of 23 current e-cigarette users. E-cigarette particle size distributions (10 nm - 5 μm) were measured with a portable aerosol mobility spectrometer and an optical particle counter. E-cigarette particle deposition patterns in human airways were estimated using the Multiple-Path Particle Dosimetry (MPPD) Model. Harmful constitutes in e-vapor were characterized for nicotine and nicotyrine (ultraviolet–visible (UV) spectroscopy), hydroxyl radical (UV fluorescence), and carbonyls (high performance liquid chromatography (HPLC)-UV detection). Human cancer risks associated with e-cigarette vaping were also estimated using Monte Carlo simulations.

The count median diameter (CMD) of e-cigarette particles ranged from 116 to 280. The CMD increased by 46%, when the heating power increased from 6.4 watts to 31.3 watts. The CMD of the particles generated from the vegetable glycerin (VG)-based e-liquid was 44% larger than the CMD of the particles generated from propylene glycol (PG)-based e-liquids. Both longer puff duration and smaller puff volume facilitated the formation of bigger e-cigarette particles. This study, for the first time, discovered that e-cigarette particle measurement results are substantially influenced by measurement temperature and humidity.

The amount of nicotine generated from e-cigarette vaping (ranging from 0.37 μg to 249.02 μg per puff) was comparable to cigarette smoking, especially under high e-cigarette power output, large puff volume, and high e-liquid nicotine levels. E-cigarette coil temperature favored the formation of nicotiyrine, the concentration of which in e-vapor were substantially higher than that in cigarette smoke (55-222 ng per puff for e-cigarette vs. 2-13 ng per puff for cigarette).

Higher e-cigarette power and larger puff volume facilitated the formation of hydroxyl radical in e-vapor. An increase in power output and puff volume resulted in significantly higher levels of $^{\bullet}OH$ formation in e-vapor due to the elevated coil temperature and oxygen supply. VG-based e-liquids generated higher amount of $^{\bullet}OH$ than PG-based e-liquids. Furthermore, e-vapor could induce $^{\bullet}OH$ formation, and the co-exposure to transition metal ions accelerated $^{\bullet}OH$ formation. Flavored e-liquids generated larger amount of $^{\bullet}OH$ in e-vapor than non-flavored e-liquids.

Compared with VG-based e-liquid, PG-based e-liquids increased formaldehyde and acetaldehyde emission by 2 - 12 folds. Other potentially harmful chemicals were also identified in e-vapor, including glyoxal, acrolein, diacetyl and acetylpropionyl. An increase in device power output from 6.4 watts to 31.3 watts resulted in the increase in formaldehyde emission by 39.3% (1257.8 ug per puff) and 142.1% (2318.2 ug per puff) for VG and PG e-liquid, respectively. PG-based e-liquid generated higher levels of formaldehyde and acetaldehyde than VG-based e-liquid by a factor of 2 and 12, respectively. In addition, glyoxal and acrolein were detected in e-vapor

under high power output conditions. Other potentially harmful carbonyls or their precursors, including diacetyl, acetylpropionyl and acetoin, were observed in e-vapor generated from flavored e-liquids.

Cancer risks associated with e-cigarette vaping ranged from 9.55×10^{6} to 7.51×10^{4}, mainly contributed by carbonyls. Vaping under 31.3 watts posed a 2 -3 times higher cancer risk than vaping under 6.4 watts. PG and PG&VG mixture based e-liquids induced 3.9 and 2.3 folds higher cancer risks than VG-based e-liquids. In contrast, if the cancer risks were normalized by e-vapor nicotine concentrations, vaping under 14.7 watts and 31.3 watts posed 7 - 10 folds smaller cancer risks than vaping under 6.4 watts.

ACKOWLEDGEMENT

First of all, I would like to express deepest gratitude to Dr. Qingyu Meng for his expertise, assistance, and patience throughout the course of my doctoral program. This dissertation would not have been possible without your help. I would like to thank my committee members, Dr. Stephan Schwander, Dr. Gediminas Mainelis, Dr. Olivia Wackowski, and Dr. Clifford Weisel, for many generous and helpful comments.

I would like to extend my sincere appreciation to the exceptional faculty and staff members in Rutgers School of Public Health. I would like to thank Dr. Cristine Delnevo, Dr. Junyan Hong, Dr. Howard Kipen, Dr. Jeffry Laskin, Dr. Vladimir Mishin, Dr. Derek Shendell, Dr. Charles Weschler, Chris Ackerman, Mary Ganss, Margaret Mitchell, Alfredo Regala, and Michelle Ruidíaz-Santiago.

I would also like to give special thanks to Dr. Chungyeong Yoon and the remarkable faculty members in Konkuk University, Dr. Illmin Jung, Dr. Soonjin Hwang, Dr. Younju An, Dr. Sechul Chun, Dr. Youngdae Yoon, for your warm advices.

These acknowledgements would not be completed without mentioning my colleagues and friends: Dr. Hyungchul Kim, Dr. Hanpil Rhee, Dr. Jonghwa Haam, Dr. Kwangwook Jung, Dr. Doochul Choi, Dr. Jaehoon Jeong, Dr. Eunsu Park, Dr. Hyosung Kim, Jangwon Son, Jinhee Park, Kyuhwan Lim, Nan Ji, Uma Bruen, Mawuena Quarcoo, and Thanawat Rattanawitoon.

Last of all, my deepest appreciation belongs to my wife and daughter, Eunju Choi and Joowon Son, for their patience and understanding. I would like to thank my parents, Ilbum Son and Taisoon Yoo, brother, Seungkwon Son, parents-in-law, Jongryul Choi and Sungrye Kim, brother-in-law, Soohyek Choi, and sister-in-law, Soyeon Park.

TABLE OF CONTENTS

LIST OF TABLES

LIST OF FIGURES

GLOSSARY

ACN	Acetonitrile
AMAH	4-(2-aminooxyethyl)-morpholin-4-ium chloride
Asc	Ascorbic acid
CMD	Count median diameter
CYPs	Cytochromes P450
DMSO	Dimethyl sulfoxide
DMPO-OH	5,5-dimethyl-1-pyrroline N-oxide-OH radical
DNPH	2,4-dinitrophenylhydrazine
ELF	Epithelial lining fluid
ESR	Electron spin (or paramagnetic) resonance
GC/MS/MS	Gas chromatography coupled to tandem mass spectrometry
GSD	Geometric standard deviation
HPLC/UV	High-performance liquid chromatography with UV detector
IC_{50}	Half maximal inhibitory concentration
ICRP	International Commission on Radiological Protection
Kanthal	Iron-chromium-aluminium (FeCrAl) alloys
LOD	Limit of detection
LOQ	Limit of quantification
Nichrome	Nickel-chromium (NiCr) alloys
MNBDH	N-Methyl-4-hydrazino-7-nitrobenzofurazan
MPPD	Multiple-Path Particle Dosimetry model
nAchRs	Nicotinic acetylcholine receptors
NNN	3-(1-nitrosopyrrolidin-2-yl)-pyridine or N-Nitrosonornicotine
NNK	4-(methylnitrosamino)-1-(3-pyridyl)-1-butanone or Nitrosamine-ketone

NOAEL	No-observed-adverse-effect-level
$^{\bullet}OH$	Hydroxyl radical
2OHTA	2-hydroxyterephthalic acid
PAH	Polycyclic aromatic hydrocarbons
PBS	Phosphate buffer saline
PG	Propylene glycol
PM	Particulate matter
Q/QH_2	Quinone/Hydroquinone couple
RFU	Relative fluorescence unit
ROS	Reactive oxygen species
TB region	Tracheobronchial region
THF	Tetrahydrofuran
TPT	Disodium terephthalate
TSNAs	Tobacco specific nitrosamines
VG	Vegetable glycol
VOC	Volatile organic compounds

CHAPTER 1

INTRODUCTION

1.1. BACKGROUND

Electronic cigarettes (e-cigarettes) are battery-powered nicotine delivery devices [1]. A typical e-cigarette device is comprised of a heating element (atomizer), a cartridge or tank with nicotine containing liquid (e-liquid), and a battery. The cartridge type e-cigarettes (i.e. cigarette like closed-system) provide fixed power output and e-liquid, while the tank type e-cigarettes allow the users to change the device setting (e.g. voltage, coil resistance and air hole size) and e-liquids. E-liquids typically consist of humectants [propylene glycol (PG) and/or vegetable glycol (VG)] as base materials, nicotine, flavoring ingredients, and other additives including ethyl alcohol [2]. The use of e-cigarettes is known as "vaping" instead of smoking [3].

With the concepts that vaping is safe or safer than smoking, the use of e-cigarettes has rapidly increased because of the intention to use for quitting smoking, popularity of flavors, cost savings, and its convenience to use [3-6]. Ever use of e-cigarettes increased from 3.3% to 8.5% from 2010 to 2013, and current e-cigarette use in 2010 was 1.0% and in 2013 was 2.6% among U.S. adults [3]. In 2014, 12.6% of U.S. adults had ever tried e-cigarettes at least once in their life time and 3.7% of U.S. adults use e-cigarettes currently (some days or every day) [7]. The use of e-cigarette is most prevalent among current and former regular cigarette smokers [8]. E-cigarette use also increased from 4.5% in 2013 to 13.4% in 2014 among high school students [9].

In spite of the increasing popularity of e-cigarettes, the evidence suggesting potential adverse health effects of e-cigarette vaping emerged in a limited number of *in vitro* studies and, in human and rodent *in vivo* studies only [10-42]. The adverse health impacts reported in the literature include cytotoxicity, DNA damage, inflammation, oxidative stress, and cardiopulmonary effects [10-42]. Although health impact studies are sparse and the findings are inconsistent, cautionary statements have been issued by scientific societies and health

organizations (i.e. the American Association for Cancer Research, the American Society of Clinical Oncology, the American Heart Association, and the World Health Organization) regarding e-cigarette vaping [43-45].

E-cigarettes generate sub-micrometer particles with count median diameters (CMD) ranging from 14 nm to 386 nm [46-48]. The e-vapor particle size distribution is likely a key parameter that determines the deposition of potentially harmful aerosols in the respiratory track system [49, 50]. In addition, previous studies also reported that e-vapor contains nicotine, volatile organic compounds (VOCs, e.g. benzene and toluene), heavy metals, polycyclic aromatic hydrocarbons (PAHs), carbonyls (e.g. acetaldehyde, formaldehyde), and tobacco-specific nitrosamines [TSNAs, e.g. 4-(methylnitrosamino)-1-(3-pyridyl)-1-butanone (NNK)] [2, 41, 51-75]. However, the impacts of e-cigarette users' vaping patterns and e-cigarette device settings on e-vapor particle size distribution and chemical composition have not been fully studied to reflect the real-world use of e-cigarettes.

1.2. KNOWLEDGE GAPS AND MOTIVATION

First, the impact of e-cigarette heating coil temperatures on e-cigarette emissions has not been fully characterized. The e-cigarette heating coil temperature, affects e-vapor aerosol formation and chemistry [64, 71] and is determined by the device coil resistance and the battery voltage (i.e. wattage). Nichrome and Kanthal wire are the most popular materials for making e-cigarette heating coils. A straight Nichrom wire stretched horizontally in free air can generate approximately 400 °C under 2.5 Ω and 3.7 V (5.5 wattage) [76]. Coil temperatures can reach above 800 °C using sub-ohm settings with the same voltage (i.e. the coil resistance < 1 Ω). The air hole area of an e-cigarette atomizer can also affect e-vapor density because the air flow rate can change the coil temperature [77]. Although Jensen et al. reported high formaldehyde emissions from e-cigarettes, the battery output voltage (5 volts) in that study was much higher than the real-world battery output voltage [66, 78]. Another limitation of that study [66] is that the author only presented voltage instead of wattage, which determines coil temperature. Only two other studies reported the emission of particles [71] and/or nicotine [64, 71] in narrow range of e-cigarette power output settings (i.e. between 3 to 10 wattage), which cannot represent current tank type e-cigarettes with variable power outputs ranging from 5 to 50 watts. In this dissertation, e-cigarette particles and a suite of harmful constituents in e-vapor were characterized across a wide range of e-cigarette power output settings [57, 79].

Second, the impact of vaping topography on e-cigarette emission is largely unknown. The impact of the vaping topography on e-cigarette emissions has not been studied under ‘real-world’ vaping conditions. Most preceding studies adopted cigarette smoking topography, rather than vaping topography, for e-cigarette emission testing [46, 50, 65, 66, 72, 74, 80-83]. Compared with conventional cigarette smoking, e-cigarette vaping required larger puff volumes and longer puff durations. The reported ranges of daily puff numbers, puff duration, puff volume, and puff interval were 1-1265 puffs/day, 2.65-4.30 seconds, 51-133 mL, and 17.9-29.6 seconds, respectively [84-89]. Since the vaping topography might affect air flow and e-cigarette coil

temperatures [48], there is a need to characterize e-cigarette emissions across a wide range of e-cigarette vaping topography.

Third, the impact of e-liquid compositions on e-cigarette particle properties and chemical compositions has not been well characterized. The e-liquid composition determines air toxics present (or formed) in e-vapor [50, 71]. For example, higher concentrations of formaldehyde were observed in e-vapor generated from PG-based e-liquids than VG-based e-liquids [75]. The impact of flavoring agents on the formation of air toxics is also largely unknown. Therefore, the emission of air toxics from different types of e-liquids, including the most popular flavored e-liquids, needs to be evaluated.

In addition, a few new air toxics, which had not been reported in the literature, were also studied in this dissertation. Nicotyrine, a major pyrolysis product of nicotine [90], is known as an inhibitor of human cytochrome P450 2A13 and 2A6, which are critical enzymes for nicotine metabolism. Nicotyrine can reduce the oxidation rate of nicotine by inhibiting CYP2A enzyme and result in a higher plasma nicotine concentration [91]. Higher concentrations of nicotyrine are expected to be observed in e-vapor than in conventional cigarette smoke, because the coil temperature of e-cigarette favors the formation of nicotyrine [90]. Hydroxyl radical (·OH), the most destructive reactive oxygen species (ROS), can attack all biological molecules [92]. Although Goel et al. [93] and Lerner et al. [21] observed total ROS in e-vapor, ·OH has not been measured and quantified.

In summary, the U.S. Food and Drug Administration (FDA) called for more research on e-cigarette use, emissions, and e-vapor toxicities, in the final rule to regulate tobacco products including e-cigarettes [94]. However, e-cigarette emissions have not been fully characterized under ‘real-world’ exposure conditions. This dissertation aims at evaluating the impacts of real-world e-cigarette use on the e-cigarette particle properties, harmful constituents in e-vapor, and estimating the human cancer risks associated with exposures to carcinogens through e-cigarette vaping.

1.3. HYPOTHESIS AND STUDY AIMS

1.3.1. Hypothesis

Higher e-cigarette coil temperature (indicated by battery output voltage and coil resistance), larger vaping volume, and flavored E-liquid generate larger amount of air toxics in e-vapor, and impose higher cancer risks due to higher levels of carcinogen exposures.

1.3.2. Specific Aims

This study has three aims, specified below and illustrated in Figure 1.

Aim 1: Study the impacts of e-cigarette device settings, vaping topography and e-liquid composition on e-vapor particle concentration, particle size distribution, and lung deposition pattern (Chapter 2)

Aim 2: Study the impacts of e-cigarette device settings, vaping topography, and e-liquid on the formation of air toxics in e-vapor (Chapter 3, 4, and 5)

Aim 3: Estimate human cancer risks associated with e-cigarette vaping (Chapter 6)

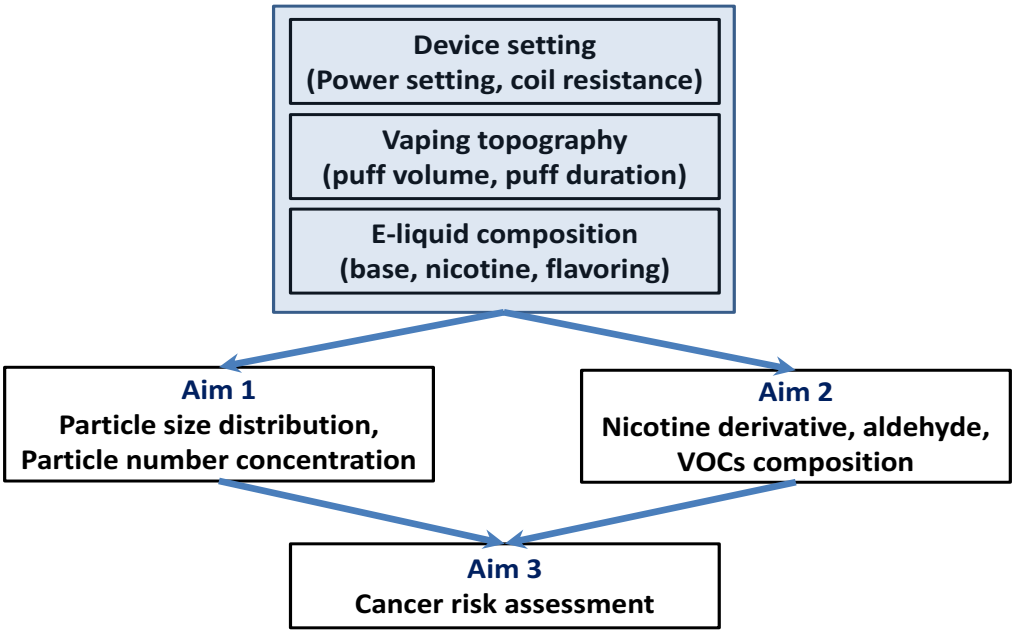

Figure 1-1. The aims of the study

REFERENCES

[1] Trtchounian, A., M. Williams, and P. Talbot, *Conventional and electronic cigarettes (e-cigarettes) have different smoking characteristics.* Nicotine & Tobacco Research, 2010. **12**(9): p. 905-912.

[2] Etter, J.F., E. Zäther, and S. Svensson, *Analysis of refill liquids for electronic cigarettes.* Addiction, 2013. **108**(9): p. 1671-1679.

[3] King, B.A., et al., *Trends in awareness and use of electronic cigarettes among US adults, 2010-2013.* Nicotine & Tobacco Research, 2014: p. ntu191.

[4] Pepper, J.K., et al., *Adolescent males' awareness of and willingness to try electronic cigarettes.* Journal of Adolescent Health, 2013. **52**(2): p. 144-150.

[5] Sutfin, E.L., et al., *Electronic cigarette use by college students.* Drug and alcohol dependence, 2013. **131**(3): p. 214-221.

[6] McCarthy, M., *E-cigarette use doubles among US middle and high school students.* BMJ, 2013. **347**.

[7] Schoenborn, C.A. and R.M. Gindi, *Electronic cigarette use among adults: United States, 2014.* NCHS data brief, 2015. **217**: p. 1-8.

[8] Schoenborn, C.A. and R.M. Gindi, *Cigarette Smoking Status Among Current Adult E-cigarette Users, by Age Group-National Health Interview Survey, United States, 2015.* 2016, CENTERS DISEASE CONTROL 1600 CLIFTON RD, ATLANTA, GA 30333 USA.

[9] Arrazola, R.A., et al., *Tobacco use among middle and high school students—United States, 2011-2014.* MMWR Morb Mortal Wkly Rep, 2015. **64**(14): p. 381-5.

[10] Flouris, A.D., et al., *Acute impact of active and passive electronic cigarette smoking on serum cotinine and lung function.* Inhalation toxicology, 2013. **25**(2): p. 91-101.

[11] Hecht, S.S., et al., *Evaluation of toxicant and carcinogen metabolites in the urine of e-cigarette users versus cigarette smokers.* Nicotine & Tobacco Research, 2015. **17**(6): p. 704-709.

[12] Ramôa, C.P., et al., *Electronic cigarette nicotine delivery can exceed that of combustible cigarettes: a preliminary report.* Tobacco control, 2015: p. tobaccocontrol-2015-052447.

[13] Spindle, T.R., et al., *Preliminary results of an examination of electronic cigarette user puff topography: The effect of a mouthpiece-based topography measurement device on plasma nicotine and subjective effects.* Nicotine & Tobacco Research, 2014: p. ntu186.

[14] Farsalinos, K., et al., *Effect of continuous smoking reduction and abstinence on blood pressure and heart rate in smokers switching to electronic cigarettes.* Internal and

emergency medicine, 2016: p. 1-10.

[15] Rosbrook, K. and B.G. Green, *Sensory effects of menthol and nicotine in an E-cigarette.* Nicotine & Tobacco Research, 2016: p. ntw019.

[16] Schober, W., et al., *Use of electronic cigarettes (e-cigarettes) impairs indoor air quality and increases FeNO levels of e-cigarette consumers.* International journal of hygiene and environmental health, 2014. **217**(6): p. 628-637.

[17] Wang, M.P., et al., *Electronic Cigarette Use and Respiratory Symptoms in Chinese Adolescents in Hong Kong.* JAMA pediatrics, 2016: p. 1-2.

[18] Bahl, V., et al., *Comparison of electronic cigarette refill fluid cytotoxicity using embryonic and adult models.* Reproductive toxicology, 2012. **34**(4): p. 529-537.

[19] Behar, R., et al., *Identification of toxicants in cinnamon-flavored electronic cigarette refill fluids.* Toxicology in Vitro, 2014. **28**(2): p. 198-208.

[20] Cervellati, F., et al., *Comparative effects between electronic and cigarette smoke in human keratinocytes and epithelial lung cells.* Toxicology in Vitro, 2014. **28**(5): p. 999-1005.

[21] Lerner, C.A., et al., *Environmental health hazards of e-cigarettes and their components: Oxidants and copper in e-cigarette aerosols.* Environmental Pollution, 2015. **198**: p. 100-107.

[22] Lerner, C.A., et al., *Vapors produced by electronic cigarettes and e-juices with flavorings induce toxicity, oxidative stress, and inflammatory response in lung epithelial cells and in mouse lung.* PloS one, 2015. **10**(2).

[23] McGrath-Morrow, S.A., et al., *The effects of electronic cigarette emissions on systemic cotinine levels, weight and postnatal lung growth in neonatal mice.* PloS one, 2015. **10**(2): p. e0118344.

[24] Meng, Q., et al., *Has the mist been peered through? Revisiting the building blocks of human health risk assessment for electronic cigarette use.* Human and Ecological Risk Assessment: An International Journal, 2015(just-accepted): p. 00-00.

[25] Romagna, G., et al., *Cytotoxicity evaluation of electronic cigarette vapor extract on cultured mammalian fibroblasts (ClearStream-LIFE): comparison with tobacco cigarette smoke extract.* Inhalation toxicology, 2013. **25**(6): p. 354-361.

[26] Rubenstein, D.A., et al., *Tobacco and e-cigarette products initiate Kupffer cell inflammatory responses.* Molecular immunology, 2015. **67**(2): p. 652-660.

[27] Scheffler, S., et al., *Cytotoxic evaluation of e-liquid aerosol using different lung-derived cell models.* International journal of environmental research and public health, 2015.

12(10): p. 12466-12474.

[28] Scheffler, S., et al., *Evaluation of E-Cigarette Liquid Vapor and Mainstream Cigarette Smoke after Direct Exposure of Primary Human Bronchial Epithelial Cells.* International journal of environmental research and public health, 2015. **12**(4): p. 3915-3925.

[29] Willershausen, I., et al., *Influence of E-smoking liquids on human periodontal ligament fibroblasts.* Head & face medicine, 2014. **10**(1): p. 39.

[30] Glynos, C., et al., *Comparison of the effects of e-cigarette vapor vs cigarette smoke on lung function and inflammation in mice.* European Respiratory Journal, 2015. **46**(suppl 59): p. OA279.

[31] Lim, H.B. and S.H. Kim, *Inhallation of e-Cigarette Cartridge Solution Aggravates Allergen-induced Airway Inflammation and Hyper-responsiveness in Mice.* Toxicological research, 2014. **30**(1): p. 13.

[32] Sussan, T.E., et al., *Exposure to Electronic Cigarettes Impairs Pulmonary Anti-Bacterial and Anti-Viral Defenses in a Mouse Model.* PloS one, 2015. **10**(2): p. e0116861.

[33] Golli, N.E., et al., *Comparison between electronic cigarette refill liquid and nicotine on metabolic parameters in rats.* Life sciences, 2016. **146**: p. 131-138.

[34] Werley, M.S., et al., *Toxicological assessment of a prototype e-cigaret device and three flavor formulations: a 90-day inhalation study in rats.* Inhalation Toxicology, 2016: p. 1-17.

[35] Palpant, N.J., et al., *Cardiac development in zebrafish and human embryonic stem cells is inhibited by exposure to tobacco cigarettes and e-cigarettes.* PloS one, 2015. **10**(5): p. e0126259.

[36] Ponzoni, L., et al., *Different physiological and behavioural effects of e-cigarette vapour and cigarette smoke in mice.* European Neuropsychopharmacology, 2015. **25**(10): p. 1775-1786.

[37] Wu, Q., et al., *Electronic cigarette liquid increases inflammation and virus infection in primary human airway epithelial cells.* 2014.

[38] Alexander, L.C., et al., *E-Cigarette Vapor Decreases Antimicrobial Function Of Macrophages, Neutrophils And Airway Epithelial Cells.* Am J Respir Crit Care Med, 2015. **191**: p. A3680.

[39] Noerager, B., et al., *Mechanical And Chemical Components Of Electronic Cigarettes Affect Combustion Product Formation And Biological Pathways Of Inflammation.* Am J Respir Crit Care Med, 2015. **191**: p. A2712.

[40] Schweitzer, K.S., et al., *Endothelial disruptive pro-inflammatory effects of nicotine and*

e-cigarette vapor exposures. American Journal of Physiology-Lung Cellular and Molecular Physiology, 2015: p. ajplung. 00411.2015.

[41] Williams, M., et al., *Metal and silicate particles including nanoparticles are present in electronic cigarette cartomizer fluid and aerosol.* 2013.

[42] Yu, V., et al., *Electronic cigarettes induce DNA strand breaks and cell death independently of nicotine in cell lines.* Oral oncology, 2016. **52**: p. 58-65.

[43] Bhatnagar, A., et al., *Electronic Cigarettes A Policy Statement From the American Heart Association.* Circulation, 2014. **130**(16): p. 1418-1436.

[44] WHO, *Electronic nicotine delivery systems*. 2014: Moscow, Russian Federation.

[45] Printz, C., *AACR, ASCO issue statement on E-cigarette regulation.* Cancer, 2015. **121**(11): p. 1723-1723.

[46] Ingebrethsen, B.J., S.K. Cole, and S.L. Alderman, *Electronic cigarette aerosol particle size distribution measurements.* Inhalation toxicology, 2012. **24**(14): p. 976-984.

[47] Sosnowski, T.R. and K. Kramek-Romanowska, *Predicted Deposition of E-Cigarette Aerosol in the Human Lungs.* Journal of aerosol medicine and pulmonary drug delivery, 2016.

[48] Zhao, T., et al., *Effects of design parameters and puff topography on heating coil temperature and mainstream aerosols in electronic cigarettes.* Atmospheric Environment, 2016. **134**: p. 61-69.

[49] Asgharian, B., W. Hofmann, and R. Bergmann, *Particle deposition in a multiple-path model of the human lung.* Aerosol Science & Technology, 2001. **34**(4): p. 332-339.

[50] Zhang, Y., W. Sumner, and D.-R. Chen, *In vitro particle size distributions in electronic and conventional cigarette aerosols suggest comparable deposition patterns.* Nicotine & tobacco research, 2013. **15**(2): p. 501-508.

[51] Kavvalakis, M.P., et al., *Multicomponent analysis of replacement liquids of electronic cigarettes using chromatographic techniques.* Journal of analytical toxicology, 2015. **39**(4): p. 262-269.

[52] Kim, H.-J. and H.-S. Shin, *Determination of tobacco-specific nitrosamines in replacement liquids of electronic cigarettes by liquid chromatography–tandem mass spectrometry.* Journal of Chromatography A, 2013. **1291**: p. 48-55.

[53] Kubica, P., et al., *An evaluation of sucrose as a possible contaminant in e-liquids for electronic cigarettes by hydrophilic interaction liquid chromatography–tandem mass spectrometry.* Analytical and bioanalytical chemistry, 2014. **406**(13): p. 3013-3018.

[54] Lim, H.-H. and H.-S. Shin, *Measurement of aldehydes in replacement liquids of*

electronic cigarettes by headspace gas chromatography-mass spectrometry. B Kor Chem Soc, 2013. **34**(9): p. 2691-2696.

[55] Lisko, J.G., et al., *Chemical composition and evaluation of nicotine, tobacco alkaloids, pH, and selected flavors in e-cigarette cartridges and refill solutions.* Nicotine & Tobacco Research, 2015. **17**(10): p. 1270-1278.

[56] Varlet, V., et al., *Toxicity assessment of refill liquids for electronic cigarettes.* International journal of environmental research and public health, 2015. **12**(5): p. 4796-4815.

[57] Gillman, I., et al., *Effect of variable power levels on the yield of total aerosol mass and formation of aldehydes in e-cigarette aerosols.* Regulatory Toxicology and Pharmacology, 2016. **75**: p. 58-65.

[58] Goniewicz, M.L., et al., *Levels of selected carcinogens and toxicants in vapour from electronic cigarettes.* Tobacco control, 2014. **23**(2): p. 133-139.

[59] Goniewicz, M.L., et al., *Nicotine levels in electronic cigarettes.* Nicotine & Tobacco Research, 2012: p. nts103.

[60] Allen, J.G., et al., *Flavoring Chemicals in E-Cigarettes: Diacetyl, 2, 3-Pentanedione, and Acetoin in a Sample of 51 Products, Including Fruit-, Candy-, and Cocktail-Flavored E-Cigarettes.* Environ Health Perspect, 2015.

[61] Czogala, J., et al., *Secondhand exposure to vapors from electronic cigarettes.* nicotine & tobacco research, 2014. **16**(6): p. 655-662.

[62] Farsalinos, K.E., et al., *Tobacco-Specific Nitrosamines in Electronic Cigarettes: Comparison between Liquid and Aerosol Levels.* International journal of environmental research and public health, 2015. **12**(8): p. 9046-9053.

[63] Farsalinos, K.E., V. Voudris, and K. Poulas, *E-cigarettes generate high levels of aldehydes only in 'dry puff'conditions.* Addiction, 2015.

[64] Farsalinos, K.E., et al., *Protocol proposal for, and evaluation of, consistency in nicotine delivery from the liquid to the aerosol of electronic cigarettes atomizers: regulatory implications.* Addiction, 2016.

[65] Herrington, J.S. and C. Myers, *Electronic cigarette solutions and resultant aerosol profiles.* Journal of Chromatography A, 2015. **1418**: p. 192-199.

[66] Jensen, R.P., et al., *Hidden formaldehyde in e-cigarette aerosols.* New England Journal of Medicine, 2015. **372**(4): p. 392-394.

[67] Martinez, R.E., et al., *On-line chemical composition analysis of refillable electronic cigarette aerosol—measurement of nicotine and nicotyrine.* Nicotine & Tobacco

Research, 2015. **17**(10): p. 1263-1269.

[68] McAuley, T.R., et al., *Comparison of the effects of e-cigarette vapor and cigarette smoke on indoor air quality.* Inhalation toxicology, 2012. **24**(12): p. 850-857.

[69] Pellegrino, R., et al., *Electronic cigarettes: an evaluation of exposure to chemicals and fine particulate matter (PM).* Ann Ig, 2012. **24**(4): p. 279-288.

[70] Schripp, T., et al., *Does e-cigarette consumption cause passive vaping?* Indoor air, 2013. **23**(1): p. 25-31.

[71] Talih, S., et al., *Effects of user puff topography, device voltage, and liquid nicotine concentration on electronic cigarette nicotine yield: measurements and model predictions.* Nicotine & Tobacco Research, 2015. **17**(2): p. 150-157.

[72] Tayyarah, R. and G.A. Long, *Comparison of select analytes in aerosol from e-cigarettes with smoke from conventional cigarettes and with ambient air.* Regulatory Toxicology and Pharmacology, 2014. **70**(3): p. 704-710.

[73] Trehy, M.L., et al., *Analysis of electronic cigarette cartridges, refill solutions, and smoke for nicotine and nicotine related impurities.* Journal of Liquid Chromatography & Related Technologies, 2011. **34**(14): p. 1442-1458.

[74] Uchiyama, S., Y. Inaba, and N. Kunugita, *Determination of acrolein and other carbonyls in cigarette smoke using coupled silica cartridges impregnated with hydroquinone and 2, 4-dinitrophenylhydrazine.* Journal of Chromatography A, 2010. **1217**(26): p. 4383-4388.

[75] Kosmider, L., et al., *Carbonyl compounds in electronic cigarette vapors—effects of nicotine solvent and battery output voltage.* Nicotine & Tobacco Research, 2014: p. ntu078.

[76] Pelican Wire Company, I. *Category Archives: Formulas, Conversions & Calculations*. 2011 [cited 2015 Nov 12]; Available from: www.pelicanwire.com/category/formulas-resistance.

[77] Williams, M. and P. Talbot, *Variability among electronic cigarettes in the pressure drop, airflow rate, and aerosol production.* Nicotine & Tobacco Research, 2011. **13**(12): p. 1276-1283.

[78] Jensen, R., et al., *More on hidden formaldehyde in e-cigarette aerosols.* N Engl J Med, 2015. **372**: p. 1575-7.

[79] Alexander, L.E.C., et al., *Electronic cigarettes: the new face of nicotine delivery and addiction.* Journal of thoracic disease, 2015. **7**(8): p. E248.

[80] Fuoco, F., et al., *Influential parameters on particle concentration and size distribution in the mainstream of e-cigarettes.* Environmental Pollution, 2014. **184**: p. 523-529.

[81] Laugesen, M. *Ruyan e-cigarette bench-top tests*. in *Poster presented to the joint conference of the Society for Research on Nicotine and Tobacco and Society for Research on Nicotine and Tobacco-Europe*. 2009.

[82] Manigrasso, M., et al., *Aerosol deposition doses in the human respiratory tree of electronic cigarette smokers.* Environmental Pollution, 2015. **196**: p. 257-267.

[83] Manigrasso, M., et al., *Particle doses in the pulmonary lobes of electronic and conventional cigarette users.* Environmental Pollution, 2015. **202**: p. 24-31.

[84] Farsalinos, K.E., et al., *Evaluation of electronic cigarette use (vaping) topography and estimation of liquid consumption: implications for research protocol standards definition and for public health authorities' regulation.* International journal of environmental research and public health, 2013. **10**(6): p. 2500-2514.

[85] Hua, M., H. Yip, and P. Talbot, *Mining data on usage of electronic nicotine delivery systems (ENDS) from YouTube videos.* Tobacco Control, 2013. **22**(2): p. 103-106.

[86] Behar, R.Z., M. Hua, and P. Talbot, *Puffing Topography and Nicotine Intake of Electronic Cigarette Users.* PloS one, 2015. **10**(2): p. e0117222.

[87] Dautzenberg, B. and D. Bricard, *Real-Time Characterization of E-Cigarettes Use: The 1 Million Puffs Study.* Journal of Addiction Research & Therapy, 2015. **2015**.

[88] Norton, K.J., K.M. June, and R.J. O'Connor, *Initial puffing behaviors and subjective responses differ between an electronic nicotine delivery system and traditional cigarettes.* Tobacco induced diseases, 2014. **12**(1): p. 17.

[89] Robinson, R., et al., *Electronic cigarette topography in the natural environment.* PloS one, 2015. **10**(6): p. e0129296.

[90] Clayton, P., A. Lu, and L. Bishop, *The pyrolysis of (−)-(S)-nicotine: Racemization and decomposition.* Chirality, 2010. **22**(4): p. 442-446.

[91] Kramlinger, V.M., L.B. von Weymarn, and S.E. Murphy, *Inhibition and inactivation of cytochrome P450 2A6 and cytochrome P450 2A13 by menthofuran, β-nicotyrine and menthol.* Chemico-biological interactions, 2012. **197**(2): p. 87-92.

[92] Ayres, J.G., et al., *Evaluating the toxicity of airborne particulate matter and nanoparticles by measuring oxidative stress potential - A workshop report and consensus statement.* Inhalation Toxicology, 2008. **20**(1): p. 75-99.

[93] Goel, R., et al., *Highly reactive free radicals in electronic cigarette aerosols.* Chemical Research in Toxicology, 2015. **28**(9): p. 1675-1677.

[94] FDA, U., *Deeming Tobacco Products To Be Subject to the Federal Food, Drug, and Cosmetic Act, as Amended by the Family Smoking Prevention and Tobacco Control Act;*

Restrictions on the Sale and Distribution of Tobacco Products and Required Warning Statements for Tobacco Products. 2016, Food and Drug Administration.

CHAPTER 2

PARTICLES GENERATED FROM E-CIGARETTE VAPING

2.1. INTRODUCTION

Electronic cigarettes (e-cigarettes), i.e. battery-powered nicotine delivery system, are believed to be substantially less harmful to human health than combusted tobacco cigarettes, and have been increasingly used in the U.S. [1-3]. However, the health risks of e-cigarette vaping are still not well understood, although a limited number of *in vitro*, and *in vivo* rodent and human studies have suggested cardiopulmonary effects of e-cigarette vaping [4, 5]. The lack of knowledge of the physical and chemical properties of e-cigarette particles contributes to the insufficient understanding of e-cigarette health impacts [6]. Indeed, some funding agencies and organizations, including the Food and Drug Administration (FDA), have called for more research on the e-cigarette particles and associated human health impacts [7].

Although studies have begun to examine the chemical composition of e-liquids and aerosols created by vaping, little research has focused on the e-cigarette particle size distributions. Measuring the size and concentration of e-cigarette particles is the first step to characterize the deposition of e-cigarette particles in the human respiratory system and subsequent health effects [8]. However, this is a challenge for many reasons. First, e-cigarettes are diverse products (including “cigalikes”, “vape pens”, “tanks”, and “mods”) that have quickly evolved. E-cigarettes are consumer-driven products and are produced by numerous small vendors and by consumers [9]. As a result, e-cigarettes vary greatly in terms of their heating power and e-liquids (e.g. flavorings, nicotine contents and base material compositions). It is largely unknown how the diversity of e-cigarette vaping patterns influences the formation and the size distribution of e-cigarette particles.

Second, the formation and properties of e-cigarette particles may also be determined by the way e-cigarette users employ their devices, i.e. generating aerosol from a variety of e-liquids,

under various heating powers and different vaping topographies [10-12]. However, preceding studies have only generated and measured e-cigarette particles using a narrow range of heating powers and under vaping topographies that are not necessarily representative of actual vaping behaviors [11-13]. Further, it is not yet well understood how different e-liquid components affect e-cigarette particle sizes.

Furthermore, the measured size of e-cigarette particles may be highly affected by measurement conditions, such as dilution, temperature and humidity. Unlike traditional cigarette particles, e-cigarette particles are primarily composed of propylene glycol (PG) and/or vegetable glycerin (VG) [2]. The evaporation and condensation of both PG and VG are affected by environmental conditions, such as the partial pressures of VG and PG in the air, temperature and humidity [14]. Previous studies reported a wide range of e-cigarette particle sizes, with the count median diameter ranging from 18 nm to 386 nm [10, 12, 13, 15-17]. We hypothesize that the reported inconsistencies in the measured e-cigarette particle sizes in previous studies can be at least partially interpreted by their measurement conditions (i.e. dilution, temperature and humidity). However, the impact of measurement conditions on e-cigarette particle measurements has not been studied to date.

In summary, the measurement of e-cigarette particles needs to reflect the vaping diversity, i.e. what people use for vaping (various e-cigarette device settings and e-liquids) and how people vape (a wide range of vaping topographies), and needs to be conducted under well-controlled environmental conditions. Indeed, in a timely guidance, the U.S. FDA requires the vaping industry to incorporate the real-world vaping diversity in e-cigarette testing [18]. This study examined the impacts of vaping diversity (i.e. e-cigarette heating power, vaping topography, and e-liquid components) on the size distribution and concentrations of e-cigarette particles. This study also evaluated the impact of environmental conditions (i.e. dilution, temperature and humidity) on e-cigarette particle measurements.

2.2. MATERIAL AND METHODS

2.2.1. E-cigarette Device and E-liquids

The e-cigarette device used in the study contained a cartomizer and a battery box. The cartomizer (The Council of Vapor, Walnut, CA, USA) had an adjustable air hole (1-2 mm in diameter) and an adjustable Nichrome heating coil, with the electric resistance ranging from 0.8 to 2.0 Ω. The battery box contained two batteries, an Apollo Valiant battery (Apolo e-cigarette, Concord, CA, USA) and a Sigelei-100 watts battery (Sigelei US, Pomona, CA, USA), permitting the output voltages ranging from 1 to 8.4 volts. The combinations of the battery voltage and the coil resistance provided a wide range of heating power of 3-80 watts. The coil temperature under each heating power was measured with a K-type thermocouple (Fisher Scientific, Pittsburgh, PA).

E-liquids tested in this study were prepared freshly in the lab for quality control purposes [19], with propylene glycol (USP grade, Sigma-Aldrich, St. Louis, MO), vegetable glycol (USP grade, J.T. Baker, Phillipsburg, NJ), nicotine (>99%, Sigma-Aldrich, St. Louis, MO), and flavoring agents.

The selected flavoring agents included in the study were strawberry, dragon fruit, menthol, sweet cream, Bavarian, cinnamon, bubble gum, and graham cracker, and represent the most popular flavors used currently on the market, based on a comprehensive review of 941,914 e-liquid recipes appearing from e-cigarette forums and online vaping shops [20]. The eight flavors appeared in 21.5% of all the e-liquid recipes we reviewed. Flavoring ingredients were purchased from The Perfumer's Apprentice (Scotts Valley, CA, USA), which supplies flavoring agents for more than half of the e-liquid recipes [20]. The ingredients, provided by The Perfumer's Apprentice, are detailed in the online Supporting Information for each of the eight flavors.

2.2.2. Vaping Topography Measurements

At the time when we initiated this research in 2015, there were almost no vaping topography

data available in the literature. Therefore, a preliminary e-cigarette topography study was conducted to inform the vaping topography settings for particle generation.

E-cigarette vaping topographies were measured in a convenience sample of 23 e-cigarette users recruited on Rutgers campuses, with the approval of Rutgers Institutional Review Board (Pro20140000589). Study participants were healthy adults (18-65 years old), who had used e-cigarettes daily for a total of at least 50 days at the time of the study, and had not used any other forms of combusted tobacco or marijuana in the past 30 days. Demographic details of the study participants are presented in Table S2-1.

Each study participant was instructed to perform a 30-minute *ad lib* vaping in an office setting, using his/her own e-cigarette. During this vaping session, the study participant was allowed to engage in other activities, such as reading a book or surfing the internet. Vaping topographies (i.e. puff volumes, puff durations, and inter-puff intervals) were measured using a CReSS Pocket device (Borgwaldt KC Incorporated, North Chesterfield, VA, USA).

The e-cigarette use patterns of the 23 study participants are detailed in Table S2-2. Vaping topographies measured in our study are consistent with later published topography data: The reported puff volumes ranged from 51 to 133 ml, and the puff durations ranged from 2.6 to 4.3 seconds [21-26]. In addition, a square shape topography was used instead of a bell shape topography which was used for the conventional cigarette smoking (Figure S2-1).

2.2.3. E-cigarette Particle Generation

E-cigarette particles were generated from a variety of e-liquids, using a LX1 smoking machine (Borgwaldt KC Incorporated, Hamburg, Germany), under various e-cigarette device settings and vaping topographies. The particle generation conditions are briefly described below and the in details are tabulated in Table S2-3.

Throughout the experiments, the median power output (6.8 watts), puff volume (90 ml), puff duration (3.8 seconds) from the 23 study participants were selected as a default vaping pattern.

VG based e-liquid was used as a baseline because 14 out of 23 study participants were used VG e-liquid. The observed median concentration of nicotine (12 mg/ml) was used as a default concentration in subsequent experiments, unless specified.

The impacts of e-cigarette device settings on e-cigarette particles were tested under a total of 9 conditions, with the selected combinations of 3 levels of coil heating powers (6.4, 14.7 and 31.3 watts) and 3 different cartomizer air hole sizes (1, 1.5, and 2 mm). The selected power outputs represent the observed median, average, and 95^{th} % for the 23 study participants which are compatible with safe, hot, and extremely hot range, respectively, for e-cigarette vaping [27]. A designated coil heating power was achieved by adjusting coil resistance and battery output voltage. Available air hole sizes were used to test the impact of air hole size on particle formation.

To test the impacts of e-liquid compositions on the e-cigarette particle size distribution, particles were generated under 15 conditions, with the combination of 5 nicotine concentrations (0, 3, 12, 24 and 36 mg/ml) and 3 types of e-liquid base solutions [100% PG, 100% VG, and 50% PG + 50% VG (v/v)]. The wide ranges of nicotine level and base material reflect the variety of e-liquid compositions used by the 23 study participants and published e-liquid recipes [20]. In addition, the eight flavoring ingredients mentioned above were added into VG-based e-liquids, to test their impacts on e-cigarette particle size distribution. Based on the ranges of flavoring agent concentrations in 941,914 e-liquid recipes [20], flavored e-liquids containing both high (10%) and low (1%) levels of flavoring agents were used for particle generation (1% and 0.1% for cinnamon flavor).

The impacts of the vaping topography on e-cigarette particles were tested under 6 conditions, with the combination of 3 puff volumes (35, 90, and 170 ml) and 2 puff durations (2 and 3.8 seconds). Besides the median puff volume (90 ml) and duration (3.8 seconds), conventional cigarette smoking regime (i.e. 35 ml and 2 seconds) and 95% puff volume (170 ml) for the 23 study participants were included to generate e-vapor.

2.2.4. E-cigarette Particle Size Distribution and Number Concentration Measurements

The size distributions and number concentrations of e-cigarette particles were measured with a portable scanning mobility particle sizer (Kanomax PAMS, KANOMAX USA, Andover, NJ), and an optical particle counter (Kanomax 3886, KANOMAX USA, Andover, NJ) to cover a wide range of e-cigarette particle sizes (10 nm-5.0 μm). Five replicate experiments and measurements were performed under each e-cigarette particle generation condition, and all measurements were conducted under 37°C and 95% relative humidity (RH) to represent human respiratory track condition. E-cigarette particles, generated under various conditions, were diluted in two 10 L chambers, in order to keep the particle concentrations below the coincidence and saturation limits of the instruments. Then, the particle size distributions obtained from the portable SMPS (10-436 nm) and OPC (0.3-5.0 μm) were combined using weighted averages (Figure S2-2). Mass median diameters were calculated based on the measured particle count distribution and the density of e-liquids used for e-vapor generation (see Appendix for details). Before introducing e-cigarette particles, dilution chambers were purged with dilution air passing through a HEPA-Cap filter (Whatman, Florham Park, NJ), until the background particle (> 10 nm) concentration was non-detectable. E-cigarette particles were then introduced into the chamber and mixed with the dilution air in the chambers by two fans.

The impact of dilution on the size of e-cigarette particles was evaluated by measuring particle size distributions and number concentrations under various dilution ratios, ranging from 396 to 15,907. The measured particle counts and particle sizes were adjusted for dilution using nonlinear regressions (Equation S2-1 and Table S2-10), and are reported as undiluted particle sizes and concentrations unless the dilution ratio is specified.

In addition, the impact of temperature and humidity on e-cigarette particle size distribution was characterized by measuring e-cigarette particles at 20°C and 30% RH, and at 37°C and 95% RH. The two conditions represent room condition and conditions in the human airway.

Temperature was controlled by a water bath and humidity by introducing humidified air through a series of bubblers.

2.2.5. Deposition of E-cigarette Particles in Human Airways

The deposition of e-cigarette particles in the tracheobronchial (TB) region and the bronchoalveolar (BA) regions of the human lung was estimated using a modified multiple path particle dosimetry (MPPD) model [8]. The modified MPPD model simulates not only particle impaction, sedimentation, and diffusion, but also particle evaporation and coagulation [8, 28]. The detailed assumptions and input parameters for the MPPD model are tabulated in Table S2-11.

In addition, the cloud effect, which is the movement of dense e-cigarette particles within a small volume and governs the proximal respiratory track deposition [i.e. the oropharyngeal and the TB regions] [28, 29], was accounted for by calculating a cloud-equivalent particle diameter. It was assumed that a particle with the cloud-equivalent particle diameter would have the same terminal settling velocity as the particle cloud. The procedure to calculate the cloud-equivalent particle diameter is detailed in the online Supporting Information (Equations S2-2, -3, and -4).

2.3. RESULTS AND DISCUSSION

2.3.1. Impacts of Dilution and Environmental Conditions on E-cigarette Particle Measurements

Figure 2-1 illustrates the impact of varying dilution ratios (i.e. the ratio of the dilution air volume and the puff volume) on the measured count median diameters (CMD) of e-cigarette particles. For comparison, Figure 2-1 includes not only the CMDs measured in our study, but also the CMDs reported in previous e-cigarette studies [10, 12, 13, 16, 17, 30].

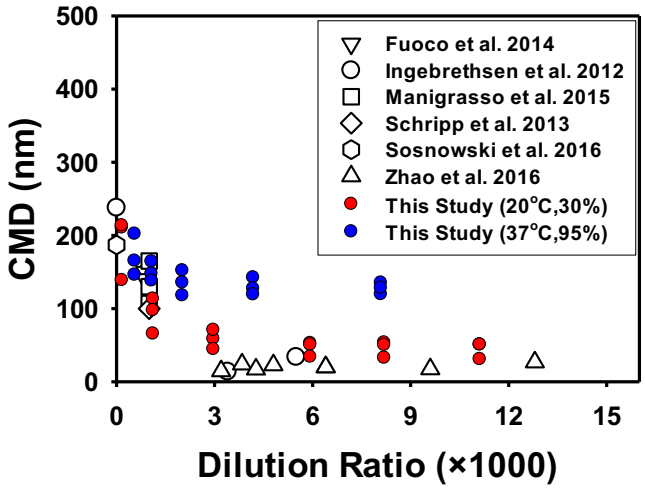

Figure 2-1. The relationship between the count median diameters (CMD) of e-cigarette particles and the dilution ratio during particle measurements, based on the e-cigarette CMD reported in the literature and measurements made in this study under various dilution conditions (37°C/95% RH and 20°C/30% RH)

Dilution ratios substantially influenced the measured e-cigarette particle sizes: The CMD decreased with increasing dilution ratio until approximately 3,000 dilution. For example, in the case of particles generated from VG-based e-liquids under 6.4 watts, when the dilution ratio increased from 548 to 8,087, the CMD decreased from 202 ± 21 nm (mean ± sd, N=5) to 136 ± 13 nm. The measured CMD, mass median diameter (MMD), geometric standard deviation (GSD) and particle number concentrations at each dilution ratio are presented in Tables S1-5-S1-9. A

wide range of CMDs of e-cigarette particles have been reported in the literature, ranging from 18 nm to 386 nm across a broad dilution ratio of 0-12,800 [12, 16]. We found that the measured CMD was highly affected by dilution: Dilution shrank e-cigarette particles due to the evaporation of PG or VG. We developed a statistical model to quantify the impact of dilution on the size of e-cigarette particles (Equation S2-1 and Table S2-10).

Table 1-1. The impact of testing temperature and relative humidity on the measured count median diameters (CMD) and number concentrations (mean ± sd) of e-cigarette particles

E-liquid	Parameter	Temperature and Relative Humidity (RH)	
		20°C and 30% RH	37°C and 95% RH
VG	CMD (nm)	158 ± 10	164 ± 4
	MMD (μm)	2.72 ± 0.05	3.35 ± 0.24
	Geometric Standard Deviation	1.79 ± 0.21	1.89 ± 0.09
	Number Concentration (#/cm^3)	$(9.35 \pm 1.38) \times 10^7$	$(1.61 \pm 0.11) \times 10^8$
PG:VG=1:1 (v:v)	CMD (nm)	127 ± 16	148 ± 12
	MMD (μm)	2.68 ± 0.06	3.39 ± 0.60
	Geometric Standard Deviation	1.75 ± 0.28	2.27 ± 0.10
	Number Concentration (#/cm^3)	$(7.64 \pm 0.70) \times 10^7$	$(1.60 \pm 0.24) \times 10^8$
PG	CMD (nm)	96 ± 7	139 ± 6
	MMD (μm)	2.62 ± 0.03	3.03 ± 0.29
	Geometric Standard Deviation	2.14 ± 0.25	2.39 ± 0.29
	Number Concentration (#/cm^3)	$(3.20 \pm 0.23) \times 10^7$	$(8.62 \pm 0.67) \times 10^7$

The impacts of temperature and RH on e-cigarette particle properties are shown in Table 1-1. E-cigarette particles were measured at both 20°C and 30% RH, and 37°C and 95% RH, at a dilution ratio of 1068. When the measurement condition switched from a typical room condition (20°C and 30% RH) to the physiologically relevant condition (37°C and 95% RH), the measured CMD increased by 4.0%-44%. The particle size increase was driven by water condensation on

PG or VG particles [14, 31]. At the same time, the particle number concentration showed an average increase of 117% (p-value < 0.001, t-tests).

The CMD of e-cigarette particles is sensitive to measurement conditions, indicating that e-cigarette emissions need to be tested under rigorously controlled environmental conditions, and that measurement conditions need to be considered to interpret the results of e-cigarette particle sizes and inhalation dosimetry.

2.3.2. Impacts of Device Settings on Particle Concentrations and Size Distributions

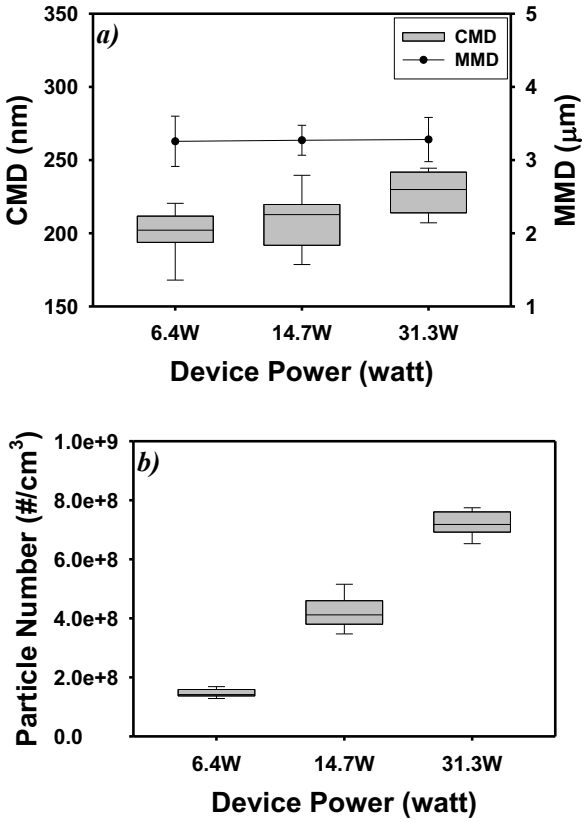

Figure 2-2. The impact of e-cigarette device power on e-cigarette particle count median diameters, mass median diameters (a), and particle counts (b). Particles were measured under 90 ml puff volume, 3.8 sec puff duration, and VG based e-liquid with 12 mg/mL nicotine. (N = 5, and error bars are standard deviations of the 5 independent measurements)

Figure 2-2 illustrates the impacts of e-cigarette device settings on the CMD and the number concentrations of e-cigarette particles. Higher coil heating powers generated higher coil temperatures and larger e-cigarette particles (i.e. larger CMD) compared to lower heating power. The measured coil temperatures were 130.6 ˚C at 6.4 watts, 199.1 ˚C at 14.7 watts, and 223.9 ˚C at 31.3 watts, respectively. When the heating power increased from 6.4 watts to 31.3 watts, the CMD increased from 200 ± 16 nm to 228 ± 14 nm. The CMD observed at 31.3 watts was statistically significantly larger than the CMD observed at 6.4 watts (p-value < 0.001, t-test), but the heating power didn't significantly affect MMD.

Higher e-cigarette heating powers were also associated with higher particle number concentrations. The observed number concentrations were $(1.46 \pm 0.14) \times 10^8/cm^3$, $(4.21 \pm 0.58) \times 10^8/cm^3$, and $(7.20 \pm 0.42) \times 10^8/cm^3$ at 6.4 watts, 14.7 watts and 31.3 watts, respectively. From 6.4 watts to 31.3 watts, the increase in particle number concentration was statistically significant (p-value < 0.001, t-tests). No significant differences in CMDs or particle number concentrations were observed among different air hole sizes (1.0-2.0 mm) tested in our study (data not shown).

Although the impacts of heating power on nicotine yield, aldehyde formation and total aerosol mass have been reported [11, 32, 33], the impacts on e-cigarette particle size distribution have not been studied to date. We, therefore, measured e-cigarette particle size distributions at a wide range of e-cigarette heating power settings, representing e-cigarette devices from the 1st generation (6.4 watts) to the 3rd and 4th generation, i.e. the tank systems with sub-ohm heating coils (> 30 watts). The increase in heating power results in higher heating temperatures, faster evaporation of e-liquids, and eventually high levels of particle condensation and coagulation, leading to bigger particle sizes [34].

2.3.3. Impacts of E-liquid Compositions on Particle Concentrations and Size Distributions

Figure 2-3 shows the change in e-cigarette particle size and number concentrations across

different e-liquids. Compared with PG-based e-liquids, VG-based e-liquids produced larger e-cigarette particles and higher particle number concentrations.

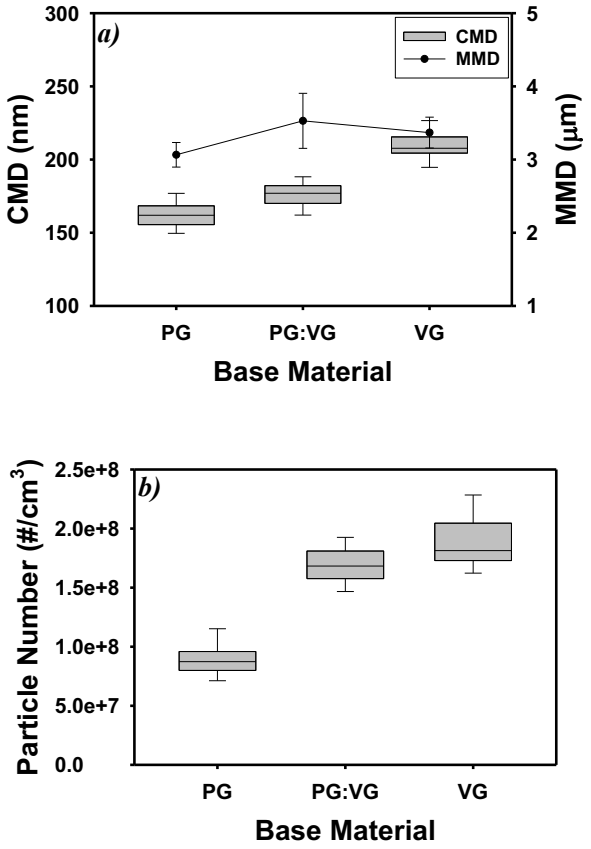

Figure 2-3. The impact e-liquid composition on e-cigarette particle count median diameters, mass median diameters (a) and particle counts (b). Particles were generated under 6.4 watts e-cigarette battery power output, 90 ml puff volume, and 3.8 sec puff duration. (N = 5, and error bars are standard deviations of the 5 independent measurements)

Across all nicotine levels, the mean CMDs of e-cigarette particles were 162 ± 10 nm for PG-based e-liquids and 175 ± 9 nm for PG:VG (v:v=1:1) based e-liquids, significantly smaller than 209 ± 10 nm for VG-based e-liquids (p-value < 0.001, t-tests). In addition, the MMDs of VG and PG:VG (v:v=1:1) based e-liquids were significantly higher than PG e-liquid (p-value < 0.001, t-tests). The particle number concentration for VG-based e-liquids was $(1.89 \pm 0.25) \times 10^8/cm^3$, which is significantly higher than the particle number concentration for PG-based e-liquids [$(9.00 \pm 1.53) \times 10^7/cm^3$] (P-value < 0.001, t-test).

Nicotine, another bulk chemical in e-liquids, had insignificant impacts on e-cigarette particle sizes and number concentrations (data not shown). The differences in CMDs, MMDs, and number concentrations across different nicotine levels were usually less than 8.2%, 5.5%, and 14.3%, respectively.

Table 2-2. The count median diameters, mass median diameters, and number concentrations (mean ± sd) of e-cigarette particles, generated from different flavored e-juice

Flavored e-juice	Count Median Diameter (nm)		Mass Median Diameter (μm)		Particle Number Concentration (#/cm^3)	
	Low level	High level	Low level	High level	Low level	High level
No flavor	209 ± 10		3.37 ± 0.21		(1.89 ± 0.25) × 10^8	
Strawberry	183 ± 12	203 ± 24	3.18 ± 0.09	3.14 ± 0.08	(1.75 ± 0.59) × 10^8	(1.09 ± 0.42) × 10^8
Dragon fruit	185 ± 11	180 ± 18	3.20 ± 0.09	3.13 ± 0.04	(1.41 ± 0.62) × 10^8	(1.41 ± 0.42) × 10^8
Menthol	183 ± 11	187 ± 14	3.22 ± 0.08	3.20 ± 0.02	(1.09 ± 0.18) × 10^8	(9.19 ± 1.91) × 10^7
Cinnamon	186 ± 15	184 ± 13	3.20 ± 0.06	3.24 ± 0.02	(1.11 ± 0.21) × 10^8	(1.27 ± 0.05) × 10^8
Bubble gum	184 ± 16	182 ± 11	3.21 ± 0.05	3.21 ± 0.06	(1.08 ± 0.21) × 10^8	(9.82 ± 1.12) × 10^7
Bavarian	181 ± 12	188 ± 11	3.19 ± 0.07	3.20 ± 0.10	(1.31 ± 0.07) × 10^8	(1.09 ± 0.18) × 10^8
Sweet cream	187 ± 13	184 ± 8	3.19 ± 0.04	3.23 ± 0.07	(1.14 ± 0.23) × 10^8	(1.22 ± 0.17) × 10^8
Graham	186 ± 13	184 ± 11	3.23 ± 0.06	3.25 ± 0.07	(1.11 ± 0.28) × 10^8	(1.07 ± 0.21) × 10^8

Note: Low level and high level indicates 1% and 10% of flavoring agents in e-liquid, except for the cinnamon flavor (0.1% and 1% in e-liquid for low and high contents, respectively).

The CMDs, MMDs, and number concentrations of e-cigarette particles, generated from flavored e-liquids, are presented in Table 2-2. In general, compared with the non-flavored e-liquids, flavored e-liquids generated slightly smaller particles, although the differences in CMDs were not statistically significant between flavored and non-flavored e-liquids. Compared with non-flavored e-liquids, flavored e-liquids [except for fruit-flavored e-liquids (strawberry and dragon fruit flavors)] led to significantly lower particle number concentrations (p-value < 0.001,

t-tests).

The type of base material (i.e. VG or PG) in e-liquids was another factor determining e-cigarette particle size distribution. VG has a much lower vapor pressure (0.01 Pa) than PG (20 Pa), and therefore, tends to condense more on the particle phase than PG, leading to larger particle size and higher particle number concentrations. Most of the flavoring ingredients contain PG, and therefore, adding flavoring ingredients into VG-based solution increases PG contents, leading to smaller particles and possibly deeper lung deposition.

2.3.4. Impacts of Vaping Topographies on Particle Concentrations and Size Distributions

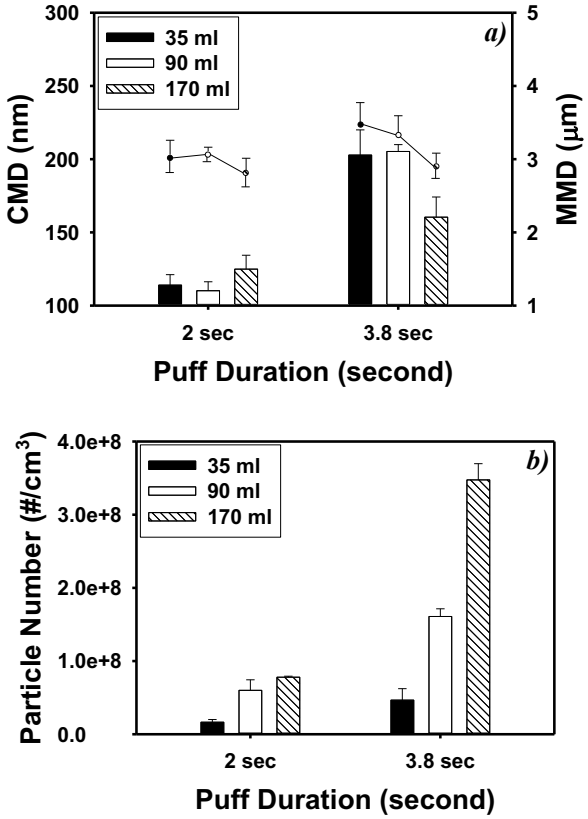

Figure 2-4. The impact of vaping topography on e-cigarette particle count median diameters (bar plots), mass median diameters (dot plots) (a) and particle counts (b). Particles were generated under 6.4 watts e-cigarette battery power output, 1.5 mm cartomizer air hole size, and VG based e-liquid with 12 mg/mL nicotine. (N = 5, and error bars are standard deviations of the 5 independent measurements)

Figure 2-4 demonstrates the impacts of puff volumes and puff durations on e-cigarette particle size and concentrations. Longer puff durations generated significantly larger particles and higher particle number concentrations (p-values < 0.001, t-tests). The CMDs of a 2-sec puff and a 3.8-sec puff were 114 ± 7 and 203 ± 17 nm, 110 ± 6 and 205 ± 5 nm, and 125 ± 10 and 160 ± 14 nm, for 35 ml, 90 ml and 170 ml puffs, respectively. When puff duration increased from 2 sec to 3.8 sec, particle number concentrations increased from $(1.64 \pm 0.37) \times 10^7$ to $(4.66 \pm 1.56) \times 10^7/cm^3$, from $(5.99 \pm 1.44) \times 10^7$ to $(1.61 \pm 0.11) \times 10^8/cm^3$, and from $(7.79 \pm 0.14) \times 10^7$ to $(3.47 \pm 0.22) \times 10^8/cm^3$ for 35 mL, 90 mL and 170 mL puffs, respectively.

Larger puff volumes significantly increased particle number concentrations, but reduced CMDs and MMDs at longer puff durations. The particle number concentration of a 170 ml puff was 1.3-7.5 times higher than that of a 35 ml or a 90 ml puff (p-values < 0.024, t-tests). When the puff duration was 3.8 sec, the CMD decreased from 203 ± 17 nm for a 35 ml puff to 160 ± 14 nm for a 170 ml puff (p-values < 0.003, t-tests).

Vaping topography influenced the size of e-cigarette particles through modifying the air flow rate and the residential time of e-cigarette particles in the cartomizer. We observed bigger e-cigarette particles under longer puff durations and smaller puff volumes, which is consistent with what Ingebrethsen et al [13] reported, i.e. the CMD of e-cigarette particles increased from 296 nm to 386 nm when the puff duration (55 ml puffs) increased from 2-sec to 4-sec. Both longer puff duration and smaller puff volumes can decrease the air flow through e-cigarettes and increase the particle residential time in the cartomizer. Decreased air flow facilitates a stable and higher coil temperature, which can increase the evaporation of e-liquids [12, 33]. Increased particle residential time increased particle coagulation, leading to bigger particles [35]. The theoretical thermal coagulation coefficient is 6.3×10^{10} cm^3/sec for particles with a CMD of 200 nm and a GSD of 1.5, and the kinematic coagulation, due to the air flow passing through the cartomizer,

could be an order of magnitude higher than thermal coagulation [35]. The coagulation rate in our study, i.e. 76.4×10^{10} cm^3/sec, was similar to the theoretical kinematic coagulation rate.

It should be pointed out that e-cigarette vaping topography is generally different from that of cigarette smoking. E-cigarette users need longer puff durations (and/or puff volumes) in order to warm up the heating coil of an e-cigarette device [33]. However, it is still a popular practice to use cigarette smoking topographies to assess e-cigarettes under the conventional cigarette smoking regimes (i.e. 35-55 ml and 2 seconds puffs). Our study and a few other studies have clearly shown the impact of vaping topography on e-cigarette particle size distributions [13, 15, 17, 36]. Therefore, it is imperative to factor real-world vaping topographies into e-cigarette particle measurements.

2.3.5. E-cigarette Particle Deposition in Human Airways

Figure 2-5 shows the mass deposition of e-cigarette particles in the TB and the BA regions of the human lungs, under different e-cigarette device settings, vaping topographies, and e-liquid compositions. The percent depositions of e-cigarette particles in the TB and the BA regions are summarized in Tables S2-5-S2-8.

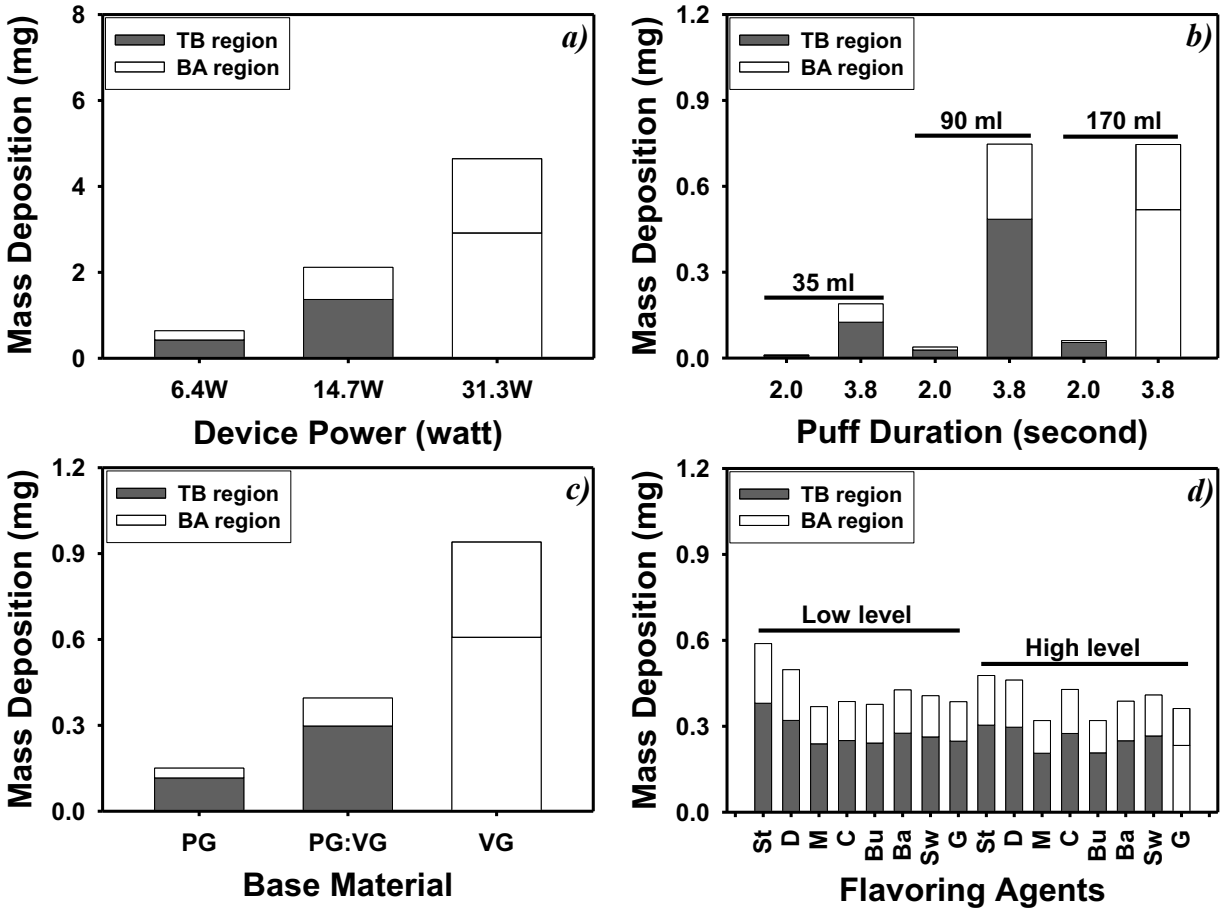

Figure 2-5. The impact of e-cigarette device power output (a), vaping topography (b), e-liquid base material (c), and e-liquid flavoring agents (d), on lung deposition of e-cigarette particles. In panel (d), St, D, M, C, Bu, Ba, Sw, and G represent strawberry, dragon fruit, menthol, cinnamon, bubble gum, Bavarian, sweet cream, and graham flavors, respectively; low level and high level indicate 1% and 10% of flavoring agents except for the cinnamon flavor (0.1% and 1%, respectively). (N = 5, and error bars are standard deviations of the 5 independent measurements)

The total mass deposition per puff of e-cigarette particles in human airways was 3.3-7.3 times higher under high power settings (4.64 mg for 31.3 watts and 2.12 mg for 14.7 watts) than under low power settings (638 μg for 6.4 watts) (p-value < 0.001, t-tests).

Increased puff volume and puff duration resulted in higher particle depositions in both the TB and the BA regions. The total mass deposition of a 90 ml (3.8 seconds) puff was 747 μg, which was 72 times higher than that of puffs generated under the International Organization for

Standardization (ISO) puffing regime (35 ml and 2 seconds) (p-value < 0.001, t-tests). In addition, higher puff volumes showed higher deposition in the TB region: the deposition fractions in the TB region were 0.506, 0.530, and 0.543, for 35 ml, 90 ml, and 170 ml puffs (3.8 seconds puff duration), respectively.

The total mass depositions for VG- and PG:VG mixture-based e-liquids were 940 µg and 395 µg, which was 2.6-6.3 times higher than the deposition of particles generated from PG-based e-liquids (150 µg) (p-value < 0.001, t-tests). Flavored e-liquids resulted in significantly lower particle mass deposition than non-flavored e-liquids (p-value < 0.011, t-tests) except for fruit-flavored e-liquids (strawberry and dragon fruit).

We estimate that 7%-31% of e-cigarette particles are deposited in the BA regions and about 50% in the TB region of the human lungs, and our estimates are different from the findings in previous studies. Zhang et al [37] estimated a 10% and a 17% deposition of e-cigarette particles in the BA regions and the TB region, respectively; and Manigrasso et al [36] reported that the BA deposition of e-cigarette particles was two times higher than that in the TB region. However, none of the previous studies considered particle cloud effects, which is critical for e-cigarette particle deposition in the upper human airways. Neither were particle measurement artifacts corrected in previous studies. Figure S2-3 illustrates the calculated e-cigarette particle deposition in human airways with and without cloud effects. The total deposition and the TB region deposition of e-cigarette particles significantly increased from 33% and 10% *without* cloud effects, to 80% and 52% *with* cloud effects, respectively. Our estimates are consistent with a recently published report on nicotine retain for e-cigarettes vaping: About 90% of the inhaled nicotine from e-cigarettes retains in the human respiratory system [38].

2.3.6. Public Health Implications

This work contributes to a greater understanding of the impacts of measurement conditions and a wide range of vaping diversity on the size and the human airway deposition of e-cigarette

particles, which has critical implications for e-cigarette product testing and the safety evaluation of e-cigarette vaping.

First, this study, for the first time, reports how the measurement conditions (i.e. dilution, temperature, and humidity) influence e-cigarette particle measurements. We observed that the size of e-cigarette particles was substantially influenced by these measurement conditions. This indicates that e-cigarette emissions need to be tested in rigorously controlled environments with minimum dilution, so that the measured CMDs of e-cigarette particles can be compared across different studies and be used to determine inhalation dosimetry.

Second, this is the first study to systematically evaluate the impacts of e-cigarette heating power, vaping topography, and e-liquid components on the size distribution of e-cigarette particles. Our study uncovered the impacts of e-cigarette device power, e-liquid composition and vaping topography on the size and the human airway deposition of e-cigarette particles. Our findings provide key information on e-cigarette regulation and harm reduction. This would, for example, allow e-cigarette device power and e-liquid composition to be regulated to optimize nicotine and flavor delivery with limited harmful chemical emission. In addition, estimated e-vapor deposition patterns may contribute to predict potential adverse effect hotspots associated with various vaping patterns.

Third, our study indicates that particles generated from e-cigarette vaping and from cigarette smoking are in the same size range (Table 2-3). Particles generated from e-cigarette vaping and from cigarette smoking also deposit at similar locations in the human airway (Table 2-3), although the amount of e-cigarette particles (i.e. particle mass and number) deposited is an order of magnitude lower than cigarette particles. Our findings are critically important to evaluate inhalation exposures to e-cigarette particles and human health risks associated with e-cigarette vaping, which is much needed to map the position of e-cigarettes on the risk continuum of tobacco products and to inform the FDA for e-cigarette regulation [18].

Table 2-3. The CMDs and human airway deposition patterns of particles generated from cigarettes and e-cigarettes

Parameters	E-cigarette[a]	Cigarette
CMD (nm)	110-228	180-340[41]
Particle number concentration (#/cm^3)	0.16×10^8 - 7.04×10^8	3.67×10^9 - 6.12×10^9 [41]
Mass deposition (mg/puff)		
TB	0.008-3.1	6.4-56.6[29], b
Pulmonary	0.002-1.8	3.5-31.2[29], b
Total	0.010-4.9	10.0-87.8[29], b
		4.3-25.1[42]
		2.5-5.8[43]
Deposition fraction		
TB	0.51-0.55	0.46-0.63[29]
Pulmonary	0.07-0.31	0.26-0.35[29]
Total	0.60-0.84	0.32-0.89[29]

[a]E-cigarette data presented in Table 3 were measured in this study.
[b]Back calculated from deposition fraction

At last, the impact of hygroscopic growth needs to be further evaluated because deposition of the hydrophilic e-vapor particles in the proximal respiratory track (i.e. oropharynx and TB region) could be much larger than cigarette smoke. Hygroscopic growth factor of VG was 1.5 fold higher than that of cigarette smoke [14, 39]. Therefore, e-vapor particles more quickly swell in proximal airway, which result in more particle deposition than conventional cigarette smoke. Broday and Georgopoulos [40] showed that 25 folds more hygroscopic particles deposited in the lung than stable particles. Moreover, deposition of VG e-vapor could be dramatically affected by the hygroscopic growth compared to PG e-vapor because larger particles have much higher growth rates than smaller particles [35].

The limitations of this work come from 1) limited coverage of flavored e-liquids, 2) possible diffusion loss of e-cigarette particles during measurements, and 4) the uncertainties of the MPPD model. We were unable to assess all possible flavored e-liquids on the market, and had to limit our assessments to the most frequently used eight flavors that appear in more than 20% of the

941,914 e-liquid recipes we collected. Nano-sized e-cigarette particles might be subject to diffusion loss during measurements. This confounder was, however, minimized in our study through the use of conductive materials for the sampling line and by making the sampling line as short as possible. In addition, the deposition of e-cigarette particles in human airways, estimated by the MPPD model, needs to be verified by *in vivo* dosimetry studies.

REFERENCES

[1] Arrazola, R.A., et al., *Tobacco use among middle and high school students-United States, 2011-2014.* MMWR. Morbidity and mortality weekly report, 2015. **64**(14): p. 381-385.

[2] King, B.A., et al., *Trends in awareness and use of electronic cigarettes among US adults, 2010-2013.* Nicotine & Tobacco Research, 2014: p. ntu191.

[3] Trtchounian, A., M. Williams, and P. Talbot, *Conventional and electronic cigarettes (e-cigarettes) have different smoking characteristics.* Nicotine & Tobacco Research, 2010. **12**(9): p. 905-912.

[4] Burstyn, I., *Peering through the mist: systematic review of what the chemistry of contaminants in electronic cigarettes tells us about health risks.* BMC public health, 2014. **14**(1): p. 18.

[5] Farsalinos, K.E. and R. Polosa, *Safety evaluation and risk assessment of electronic cigarettes as tobacco cigarette substitutes: a systematic review.* Therapeutic advances in drug safety, 2014. **5**(2): p. 67-86.

[6] FDA, U., *Deeming Tobacco Products To Be Subject to the Federal Food, Drug, and Cosmetic Act, as Amended by the Family Smoking Prevention and Tobacco Control Act; Restrictions on the Sale and Distribution of Tobacco Products and Required Warning Statements for Tobacco Products*. 2016, Food and Drug Administration.

[7] Grana, R., N. Benowitz, and S.A. Glantz, *E-cigarettes: A Scientific Review.* Circulation, 2014. **129**(19): p. 1972-1986.

[8] Kane, D.B., et al., *Effect of smoking parameters on the particle size distribution and predicted airway deposition of mainstream cigarette smoke.* Inhalation toxicology, 2010. **22**(3): p. 199-209.

[9] Seidenberg, A.B., C.L. Jo, and K.M. Ribisl, *Differences in the design and sale of e-cigarettes by cigarette manufacturers and non-cigarette manufacturers in the USA.* Tobacco control, 2016. **25**(e1): p. e3-e5.

[10] Fuoco, F., et al., *Influential parameters on particle concentration and size distribution in the mainstream of e-cigarettes.* Environmental Pollution, 2014. **184**: p. 523-529.

[11] Talih, S., et al., *Effects of user puff topography, device voltage, and liquid nicotine concentration on electronic cigarette nicotine yield: measurements and model predictions.* Nicotine & Tobacco Research, 2015. **17**(2): p. 150-157.

[12] Zhao, T., et al., *Effects of design parameters and puff topography on heating coil temperature and mainstream aerosols in electronic cigarettes.* Atmospheric Environment, 2016. **134**: p. 61-69.

[13] Ingebrethsen, B.J., S.K. Cole, and S.L. Alderman, *Electronic cigarette aerosol particle size distribution measurements.* Inhalation toxicology, 2012. **24**(14): p. 976-984.

[14] Wright, T.P., et al., *Thermodynamic and kinetic behavior of glycerol aerosol.* Aerosol Science and Technology, 2016. **50**(12): p. 1385-1396.

[15] Laugesen, M. *Ruyan e-cigarette bench-top tests*. in *Poster presented to the joint conference of the Society for Research on Nicotine and Tobacco and Society for Research on Nicotine and Tobacco-Europe*. 2009.

[16] Sosnowski, T.R. and K. Kramek-Romanowska, *Predicted Deposition of E-Cigarette Aerosol in the Human Lungs.* Journal of aerosol medicine and pulmonary drug delivery, 2016.

[17] Manigrasso, M., et al., *Particle doses in the pulmonary lobes of electronic and conventional cigarette users.* Environmental Pollution, 2015. **202**: p. 24-31.

[18] FDA, U., *Premarket Tobacco Product Applications for Electronic Nicotine Delivery Systems*. 2016, Food and Drug Administration: Silver Spring, MD.

[19] Farsalinos, K.E., et al., *Protocol proposal for, and evaluation of, consistency in nicotine delivery from the liquid to the aerosol of electronic cigarettes atomizers: regulatory implications.* Addiction, 2016.

[20] ELiquidRecipes. *e-Liquid Recipes*. 2017 [cited 2017 May 31]; Available from: http://e-liquid-recipes.com/.

[21] Dautzenberg, B. and D. Bricard, *Real-Time Characterization of E-Cigarettes Use: The 1 Million Puffs Study.* Journal of Addiction Research & Therapy, 2015. **2015**.

[22] Hua, M. and P. Talbot, *Potential health effects of electronic cigarettes: a systematic review of case reports.* Preventive medicine reports, 2016. **4**: p. 169-178.

[23] Meng, Q., et al., *Has the mist been peered through? Revisiting the building blocks of human health risk assessment for electronic cigarette use.* Human and Ecological Risk Assessment: An International Journal, 2016. **22**(2): p. 558-579.

[24] Norton, K.J., K.M. June, and R.J. O'Connor, *Initial puffing behaviors and subjective responses differ between an electronic nicotine delivery system and traditional cigarettes.* Tobacco induced diseases, 2014. **12**(1): p. 17.

[25] Robinson, R., et al., *Electronic cigarette topography in the natural environment.* PloS one, 2015. **10**(6): p. e0129296.

[26] Spindle, T.R., et al., *Preliminary results of an examination of electronic cigarette user puff topography: The effect of a mouthpiece-based topography measurement device on plasma nicotine and subjective effects.* Nicotine & Tobacco Research, 2014: p. ntu186.

[27] Misthub. *Tutorial: Variable Voltage and Vaping Power Chart*. 2013 [cited 2017 Oct 30]; Available from: https://www.misthub.com/blogs/vape-tutorials/76788421-tutorial-variable-voltage-and-vaping-power-chart.

[28] Asgharian, B., W. Hofmann, and R. Bergmann, *Particle deposition in a multiple-path model of the human lung.* Aerosol Science & Technology, 2001. **34**(4): p. 332-339.

[29] Broday, D.M. and R. Robinson, *Application of cloud dynamics to dosimetry of cigarette smoke particles in the lungs.* Aerosol Science & Technology, 2003. **37**(6): p. 510-527.

[30] Schripp, T., et al., *Does e-cigarette consumption cause passive vaping?* Indoor air, 2013. **23**(1): p. 25-31.

[31] Byron, P.R., et al., *Pharmaceutical implications of particle growth at high relative humidities.* Pesticide Science, 1977. **8**(5): p. 521-526.

[32] Geiss, O., I. Bianchi, and J. Barrero-Moreno, *Correlation of volatile carbonyl yields emitted by e-cigarettes with the temperature of the heating coil and the perceived sensorial quality of the generated vapours.* International journal of hygiene and environmental health, 2016. **219**(3): p. 268-277.

[33] Gillman, I., et al., *Effect of variable power levels on the yield of total aerosol mass and formation of aldehydes in e-cigarette aerosols.* Regulatory Toxicology and Pharmacology, 2016. **75**: p. 58-65.

[34] Scheibel, H. and J. Porstendo, *Generation of monodisperse Ag-and NaCl-aerosols with particle diameters between 2 and 300 nm.* Journal of Aerosol Science, 1983. **14**(2): p. 113-126.

[35] Hinds, W.C., *Aerosol technology: properties, behavior, and measurement of airborne particles*. 2012: John Wiley & Sons.

[36] Manigrasso, M., et al., *Aerosol deposition doses in the human respiratory tree of electronic cigarette smokers.* Environmental Pollution, 2015. **196**: p. 257-267.

[37] Zhang, Y., W. Sumner, and D.-R. Chen, *In vitro particle size distributions in electronic and conventional cigarette aerosols suggest comparable deposition patterns.* Nicotine & tobacco research, 2013. **15**(2): p. 501-508.

[38] St Helen, G., et al., *Nicotine delivery, retention and pharmacokinetics from various electronic cigarettes.* Addiction, 2016. **111**(3): p. 535-544.

[39] Johnson, T.J., et al., *Hygroscopic effects on the mobility and mass of cigarette smoke particles.* Journal of Aerosol Science, 2015. **86**: p. 69-78.

[40] Broday, D.M. and P.G. Georgopoulos, *Growth and deposition of hygroscopic particulate matter in the human lungs.* Aerosol Science & Technology, 2001. **34**(1): p. 144-159.

[41] Bernstein, D.M., *A review of the influence of particle size, puff volume, and inhalation pattern on the deposition of cigarette smoke particles in the respiratory tract.* Inhalation toxicology, 2004. **16**(10): p. 675-689.

[42] Polydorova, M., *An attempt to determine the retention of tobacco smoke by means of membrane filters.* Inhaled Particles and Vapours. Pergamon Press, New York, 1961: p. 142-144.

[43] Baumberger, J.P., *The amount of smoke produced from tobacco and its absorption in smoking as determined by electrical precipitation.* Journal of Pharmacology and Experimental Therapeutics, 1923. **21**(1): p. 47-57.

CHAPTER 3

NICOTINE AND NICOTYRINE CONCENTRATIONS OF E-VAPOR

3.1. INTRODUCTION

The use of electronic cigarettes (e-cigarette) has rapidly increased. Nicotine, a principal tobacco alkaloid, is one of the major constituents of e-vapor [1]. Nicotine is not a direct cause of tobacco-related diseases [2], but the addictiveness of nicotine influences e-cigarette users to modify their vaping habits to achieve similar plasma nicotine levels as those reached by cigarette smoking [3]. The vaping habits impacting e-cigarette nicotine delivery include the choice of e-liquids, e-cigarette device power output settings, and the vaping topography [4]. In addition, in 2015, 58.8% of adult e-cigarette users also were current cigarette smokers, and many smokers are using e-cigarettes to quit smoking [5]. The presence and delivery of nicotine in e-cigarettes is important in making e-cigarette as satisfactory smoking alternatives and cessation aids. Furthermore, the plasma nicotine level is affected by nicotine metabolism, which can be altered by other e-vapor components, such as nicotyrine [6].

Nicotyrine may form through the hydrogen abstraction reaction of nicotine during the e-cigarette vaping as shown in Scheme 3-1 [7].

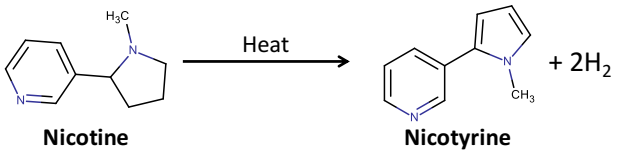

Scheme 3-1. Hydrogen abstraction reaction of nicotine to nicotyrine

E-cigarette vaping is expected to deliver significantly higher amounts of nicotyrine than conventional cigarette products. The coil temperatures of e-cigarettes (200-300 °C) are more favorable to the formation of nicotyrine than the temperatures of cigarette burning (i.e. ~900 °C)

[8]. Nicotyrine itself is non-toxic, but it could inhibit nicotine metabolism through binding to the cytochrome P450 isoforms (i.e. CYP2A6 and CYP2A13), resulting in higher plasma nicotine levels [9].

Although a few studies reported the level of nicotine and nicotiyrine in e-vapor, these studies did not reflect the wide range of real-world vaping behaviors, i.e. the diversity of e-liquid composition, e-cigarette power output, and vaping topography [7, 10]. Therefore, nicotine and nicotyrine emissions under real-world vaping conditions are still not well understood.

This study aimed at evaluating the nicotine and nicotyrine emissions under various real-world vaping conditions by factoring in the impacts of e-liquid composition, e-cigarette power output, and vaping topography on nicotine and nicotyrine concentrations in e-vapor.

3.2. MATERIALS AND METHODS

3.2.1. E-cigarette Device and E-liquids Preparation

A refillable tank type e-cigarette (The Council of Vapor, Walnut, CA, USA) consisting of adjustable Nichrome heating coils (0.8-2.0 Ω) was used to measure nicotine and nicotyrine. Two types of battery box, an Apollo Valiant battery (Apolo E-cigarette, Concord, CA, USA) and a Sigelei-100W battery (Sigelei US, Pomona, CA, USA), were used to provide a wide range of heating power from 3 to 100 watts.

All e-liquids were freshly prepared in our lab using propylene glycol (PG, USP grade, Sigma, St. Louis, MO, USA), vegetable glycol (VG, USP grade, J.T. Baker, Phillipsburg, NJ, USA), and (-)-nicotine (≥99%, Sigma, St. Louis, MO, USA) for quality control purpose.

3.2.2. E-vapor Generation and Collection

E-vapor generation conditions were established based on the e-cigarette use patterns obtained from the 23 current e-cigarette users with the approval of Rutgers IRB (Pro20140000589). Table S2-1 tabulated the demographic details of the 23 study participants. The observed e-cigarette vaping conditions (i.e. device power output, vaping topography, and e-liquid composition) of the 23 study participants are presented in Table S2-2.

To evaluate the impact of e-liquid composition on nicotine and nicotyrine emission, a wide range of nicotine concentrations (0-36 mg/ml) in three base materials [100% PG, 100% VG, and PG&VG mixture (v/v=1:1)] was used.

Three levels of power output (6.4, 14.7, and 31.3 watts) were used to evaluate the impact of e-cigarette power on nicotine and nicotyrine emission. The selected power outputs represented the median, mean, and 95% of the observed power output used by the 23 study participants. These selected power output levels are consistent with the safe, hot, and extremely hot ranges from the e-cigarette vaping power chart [11].

To evaluate the impact of vaping topography on nicotine and nicotyrine emission, the median

puff volume (90 ml) and puff duration (3.8 seconds) obtained from the 23 study participants was employed. In addition, cigarette smoking regime (35 ml puff volume and 2 seconds puff duration) and the 95% puff volume (170 ml) obtained from the 23 study participants were also included. The selected vaping topography was consistent with published vaping topographies: the median puff volume and duration were 91 ml (ranging from 51 ml to 133 ml) and 3.8 seconds (ranging from 3.0 secs to 4.3 secs), respectively [12-17]. Square shape topography was used instead of the bell shape topography which was used for the cigarette smoking (Figure S2-1).

Under each experimental condition (Table S3-1), e-vapor was generated using a LX1 smoking machine (Borgwaldt KC Incorporated, Hamburg, Germany). Twenty puffs of e-vapors were collected on a 47 mm Zefluor Teflon filter (2.0 μm pore size, Pal life sciences, Port Washington, NY, USA). Each Teflon filter was put in a Teflon filter holder submerged into an ice bucket to condense e-vapor. The weight of the collected e-vapor was measured by weighing the Teflon filter and the filter holder before and after each sampling.

3.2.3. Nicotine and Nicotyrine Measurement

E-vapor collected on Teflon filters was extracted using 5 ml of acidified ethanol, prepared by adding 3.75 mL of concentrated hydrochloric acid (37%, Sigma, St. Louis, MO, USA) in a liter of ethanol (≥99.8%, Sigma, St. Louis, MO, USA) [18, 19]. Filter extracts were analyzed by UV absorbance (GENESYS 10 UV-Vis spectrophotometer, Thermo Scientific, Waltham, MA, USA) at the wavelength of 260 nm and 310 nm for nicotine and nicotyrine, respectively [18]. Nicotine did not interfere with nicotyrine measurement, but nicotyrine showed weak absorbance at 260 nm [18]. However, the interference of nicotyrine was neglected because nicotyrine appeared in e-vapor in much lower concentrations than nicotine. The limit of detection (LOD) of nicotine was 290 ng/mL, 303 ng/mL, and 296 ng/mL, respectively, for VG, PG&VG mixture, and PG based e-vapor; and the LOD for nicotyrine was 64 ng/mL, 59 ng/mL, and 45 ng/mL, respectively, for VG, PG&VG mixture, and PG based e-vapor.

The UV spectroscopy method for nicotine and nicotyrine measurement was validated by the GC/MS/MS method. In brief, 20 puffs of e-vapor were generated using VG based e-liquid containing 12 mg/ml nicotine under two different power output conditions (6.4W and 31.3W). The generated e-vapor was collected on the Teflon filter, and 2 µl quinoline was spiked on the filter. Quinoline spiked filters were extracted using 4 ml methanol (HPLC grade, ≥99.9%, Sigma, St. Louis, MO, USA), and analyzed with GC/MS/MS. The detailed experimental procedure and results are presented in the supplemental material. Figure S3-3 show that no significant differences between these two methods, as the average difference between the two measures was less than 10%.

3.2.4. Quality Assurance and Quality Control

Nicotyrine can be formed during the e-liquid storage and the sampling process [7] due to the oxidation of nicotine. Solvent blanks were always checked on the same day of sample collection. The formation of nicotyrine during the sampling process was examined by spiking 50 µL of VG based e-liquid with 3, 12, 24, and 36 mg/mL nicotine on a Teflon filter, and introducing 20 or 50 puffs of clean air through the spiked filter under 35, 90 and 170 mL puff volumes. Nicotine and nicotyrine on the filter were measured before and after introducing air to the filter.

3.2.5. E-vapor pH measurement

It is known that the acidity of e-vapor can be affected by the gas/particle partitioning and the absorption of nicotine in the human respiratory system [20, 21]. To address this, twenty puffs of e-vapor collected on a Teflon filter were dissolved in 5 ml of DI water, and the e-vapor acidity was measured using an OAKTON pH 110 instrument (OAKTON instrument, Vernon Hills, IL, USA).

3.3. RESULTS AND DISCUSSION

3.3.1. Quality Assurance and Quality Control

Nicotyrine content of the pure nicotine solution (≥99%) was less than 1% of nicotine concentration (87±23 ng/ml nicotyrine per 10 μg/mL nicotine). Nicotine, nicotyrine and nicotyrine-nicotine ratio (mass/mass) of the prepared e-liquids are tabulated in Table 3-1. E-liquids with higher nicotine content showed significantly higher nicotyrine concentrations and nicotine-nicotyrine ratios than e-liquids containing lower levels of nicotine (p-values < 0.001, t-tests). On average, nicotyrine-nicotine ratios for e-liquids containing 12 mg/ml, 24 mg/ml, and 36 mg/ml nicotine were 1.6, 1.9, and 2.2 folds higher than the ratio for e-liquids containing 3 mg/ml nicotine. Base materials did not impact on nicotyrine formation.

Table 3-1. Nicotine, nicotyrine concentration, and nicotyrine-nicotine ratio of studied e-liquids

Component	Base material	Nicotine level			
		3 mg/ml	12 mg/ml	24 mg/ml	36 mg/ml
Nicotine (mg/ml)	**VG**	2.954±0.034	11.77±0.163	23.58±0.265	35.45±0.519
	PG:VG=1:1 (v:v)	3.040±0.046	12.09±0.141	24.17±0.304	36.17±0.393
	PG	3.048±0.045	12.10±0.150	24.30±0.377	36.26±0.602
Nicotyrine (μg/ml)	**VG**	25.44±6.345	146.6±7.913	375.6±27.76	642.1±70.59
	PG:VG=1:1 (v:v)	22.36±1.690	150.4±16.74	409.2±20.66	723.1±102.2
	PG	22.20±2.856	198.1±12.62	391.6±18.24	704.8±49.80
Nicotyrine/Nicotine	**VG**	0.009±0.002	0.012±0.001	0.016±0.001	0.018±0.002
	PG:VG=1:1 (v:v)	0.007±0.000	0.012±0.001	0.017±0.001	0.020±0.003
	PG	0.007±0.001	0.016±0.001	0.016±0.001	0.019±0.002

Additional measurement artifacts resulted from the reaction between nicotine and air on the filters during the sampling process. Air exposure facilated the convertion of nicotine to nicotyrine (Figure 3-1a). Nicotyrine levels increased by 60.6% after introducing 20 puffs of 170 ml air (p-values < 0.001, t-tests), while 20 puffs of 35 ml and 90 ml air did not increase nicotyrine levels

(p-values > 0.451, t-tests). E-liquids with lower nicotine concentrations formed more nicotyrine after introducing the same amount of clean air (Figure 3-1b). The average nicotyrine levels after introducing 50 puffs of 90 ml air were 225%, 50%, 38%, and 15% higher than fresh e-liquids containing 3, 12, 24, and 36 mg/mL nicotine, respectively (p-values < 0.007, t-tests). In this study, the reported nicotyrine concentrations are corrected for the measurement artifacts. The correction method is detailed in the supplemental material (Table S3-3).

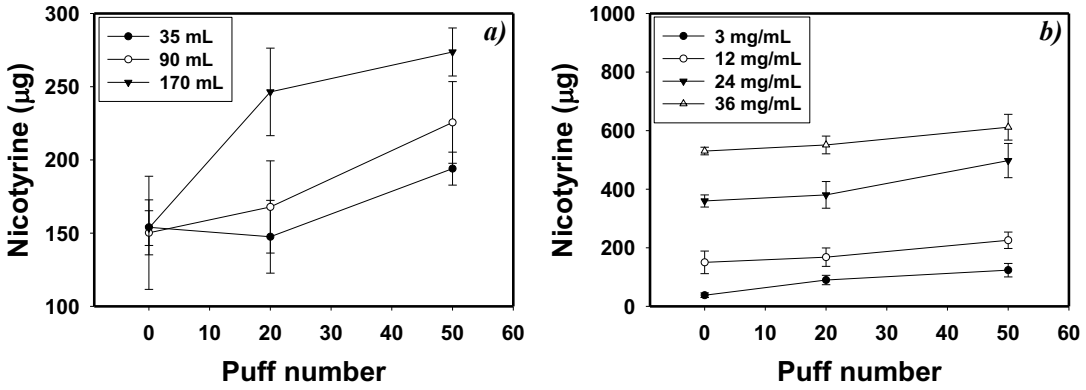

Figure 3-1. Measurement artifacts associated with (a) the air flowing through sample filter and (b) the e-liquids containing different nicotine concentrations (N = 5, and error bars are standard deviations of 5 independent measurements)

3.3.2. Factors affecting e-vapor nicotine and nicotyrine levels

E-liquids with higher nicotine concentrations and VG-based e-liquids emitted higher amounts of nicotine and nicotyrine in e-vapor (Figure 3-2). VG-based e-liquids emitted 8.0 and 10.1-fold more nicotine and nicotyrine, respectively, than PG based e-liquids (p-values < 0.001, t-tests). In general, the amount of nicotine in e-vapor was proportional to the nicotine concentrations in e-liquids. Nicotyrine concentrations of e-vapors from e-liquid with 12 mg/ml nicotine were significantly higher than 3 mg/ml nicotine (p-values < 0.001, t-tests), while e-liquids with 12, 24, and 36 mg/ml nicotine did not show significant differences in nicotyrine concentration. On average, the nicotyrine-nicotine ratios for e-vapor samples were 5.7-fold higher than that of the corresponding e-liquids.

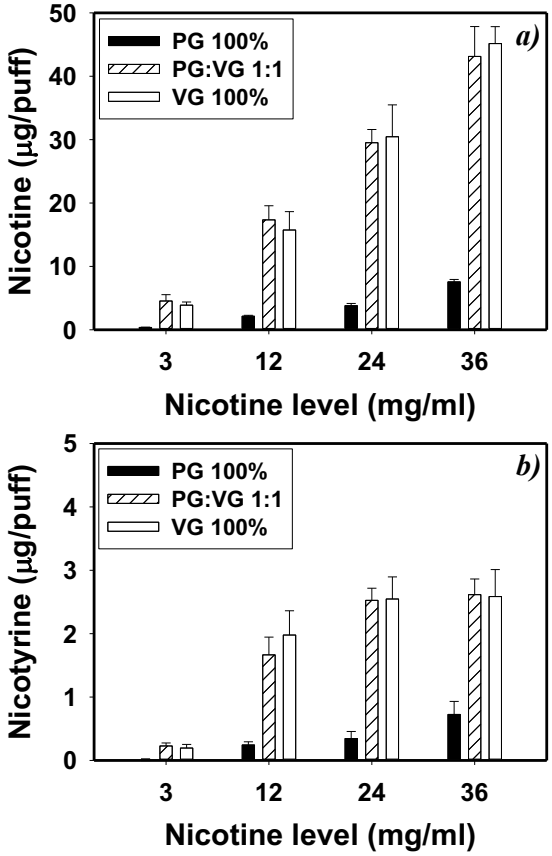

Figure 3-2. The impact of e-liquid composition on (a) nicotine and (b) nicotyrine concentration. E-vapors were generated under 6.4 W power output, 1.5 mm air hole size, and 90 ml puff volume, 3.8 sec puff duration, and 24 sec puff interval (n = 5, and error bars are standard deviations of 5 independent measurements)

Table 3-2. Nicotine, nicotyrine, nicotyrine/nicotine ratio, and e-vapor mass of e-cigarette vapor generated under different E-cigarette device power outputs

Component	Device Power		
	6.4 W	**14.7 W**	**31.3 W**
Nicotine (μg/puff)	16.29±1.436	137.1±6.723	236.3±13.97
Nicotyrine (μg/puff)	2.109±0.509	12.67±0.340	11.64±0.354
Nicotyrine/Nicotine	0.129±0.043	0.092±0.030	0.049±0.005

Higher e-cigarette device powers showed significantly higher e-vapor nicotine and nicotyrine concentrations (p-values < 0.001, t-tests) (Table 3-2). E-vapor nicotine concentration for the 31.3 watts power output was 14.5 and 1.7-fold higher than 6.4 and 14.7 watts conditions, respectively (*p*-values < 0.001, t-tests). 14.7 and 31.3 watts conditions generated 6.0 and 5.5 times more

nicotyrine than 6.4 watts power output (p-values < 0.001, t-tests). Nicotyrine-nicotine ratio under 31.3 W power output was 0.049, and it was significantly lower than 6.4 watts and 14.7 watts power output condition with the ratios of 0.129 and 0.092 (p-values < 0.001, t-tests).

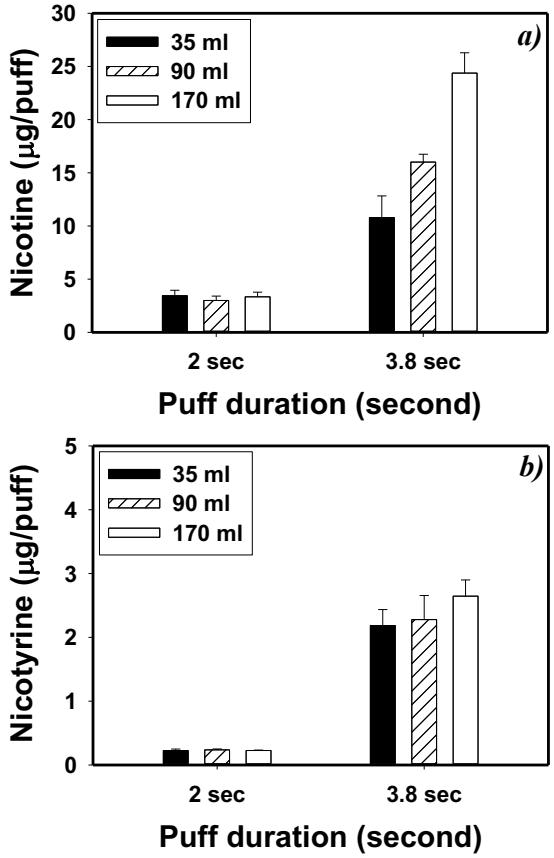

Figure 3-3. The impact of vaping topography on (a) nicotine and (b) nicotyrine concentration. E-vapors were generated under 6.4 W power output, 1.5 mm air hole size, and 24 sec puff interval with VG based E-liquid with 12 mg/mL nicotine (n = 5, and error bars are standard deviations of 5 independent measurements)

Longer puff durations increased e-vapor nicotine and nicotyrine levels (Figure 3-3). 3.8-second puffs generated 3.3-6.9-fold higher nicotine and 9.6-11.7-fold higher nicotyrine than 2-second puffs (p-values < 0.001, t-tests). Higher puff volumes also increased e-vapor nicotine and nicotyrine concentrations. 170 ml puff volume under 3.8 seconds puff duration increased nicotine and nicotyrine concentrations by 125.8% and 21.0% than 35 ml and 2.8 seconds puffs,

respectively (p-values < 0.020, t-tests).

3.3.3. pH Mesaurements

E-vapor pH ranged from 8.09 to 9.51, and higher nicotine level showed significantly higher pH values (p-values < 0.001, t-tests). PG-based e-liquid containing 3, 12, 24, and 36 mg/ml nicotine showed average pH of 8.09±0.02, 8.47±0.01, 8.56±0.01, and 8.98±0.01, respectively. PG&VG mixture and VG-based e-liquid showed higher pH than PG-based e-liquid under the same nicotine level (p-values < 0.001, t-tests). For e-liquids with 3, 12, 24, and 36 mg/ml nicotine, the pH values for PG&VG-based e-liquids were 8.67±0.02, 9.11±0.01, 9.26±0.02, and 9.51±0.01, respectively; and were 8.65±0.02, 9.11±0.02, 9.28±0.02, and 9.52±0.02, respectively, for VG-based e-liquids.

3.3.3. Discussions and Health Implications

This study evaluated the impact of the e-liquid composition, e-cigarette device settings, and vaping topography on nicotine and nicotyrine concentrations in e-vapor. Nicotine is one of the major e-vapor components [3]; and nicotyrine is a major oxidative product of nicotine, could inhibit the nicotine metabolism, increase serum nicotine level, and thus might decrease e-cigarette craving [6]. The inhibited nicotine metabolism might also reduce craving for regular cigarette for the e-cigarette/cigarette dual users, resulting in less risks for relapse. However, nicotyrine formation under different e-cigarette use conditions has not been fully studied before. We therefore examined nicotine and nicotyrine formation under ‘real-world’ e-cigarette use patterns.

Nicotine in e-liquids is the precursor for nicotyrine formation. Nicotyrine-nicotine ratio of pure nicotine solution was less than 0.01, and the nicotyrine-nicotine ratio was 0.01-0.02 for the freshly made e-liquids in our lab (VG based e-liquid with 3-36 mg/mL nicotine without flavor). Nicotyrine might form during the e-liquid preparation through the reaction between nicotine and air [22]. A study also presented that e-liquid (PG:VG mixture with 18 mg/mL nicotine with

tobacco flavor) exposed to air increased nicotyrine-nicotine ratio from 0.03-0.04 to 0.08-0.09 after 65 days [7]. Therefore, measurement artifacts should be considered in the quantification of nicotyrine concentration in e-vapor. The air flowing through the sample filters facilitated nicotyrine formation, and we observed a linear relationship (r^2=0.802) between the nicotyrine increments and the volume of air introduced (Figure S3-4). Measurement artifacts contributed to 6.6-36.7% of measured nicotyrine.

The nicotine and nicotyrine concentrations in the e-vapor were determined by e-liquid base materials and nicotine levels in e-liquid. E-liquids with higher nicotine contents increased nicotine and nicotyrine concentration as expected. VG and PG&VG-based e-liquids generated significantly higher amount of nicotine and nicotyrine than PG-based e-liquid. VG and nicotine have similar evaporation rate due to the similar boiling points: 247 ˚C for nicotine and 290 ˚C for VG. However, PG has a much lower boiling point (188.2 ˚C) than nicotine and can be quickly evaporated, which can decrease the vaporization of nicotine. In addition, nicotine delivery ratio was calculated using the ratios between the nicotine concentrations of e-vapors (mg/ml) and the e-liquid nicotine concentrations (mg/ml). The average nicotine delivery ratio of PG (0.92) was much higher than that of VG (0.72) and PG:VG (0.86) e-liquids. More particle phase VG might be expected than nicotine because the vapor pressure of VG (0.01 Pa) is much lower than nicotine (5 Pa). In contrast, PG tend to be present in the gas phase due to the high vapor pressure (20 Pa). Geiss and Bianchi [23] also reported lower nicotine delievery ratio for VG based e-liquid collected on the filter paper than PG:VG mixed e-liquid.

Higher device power outputs increased nicotine and nicotyrine levels in e-vapor due to higher coil temperatures. Higher coil temperatures have been shown to increase e-liquid evaporation and generated larger amount of nicotine in e-vapor [4]. In addition, our studies show that higher power output increases e-cigarette coil temperatures, resulting in more nicotyrine evaporation and formation. The measured coil temperatures in our study using the K-type thermocouple were 130.6 ˚C, 199.1 ˚C, and 223.9 ˚C at 6.4 W, 14.7 W, and 31.3 W, respectively. Higher coil

temperatures facilitate nicotyrine evaporation in e-vapor. Vaporized nicotyrine contributed 7.3%, 10.3%, and 19.3% of the observed nicotyrine in e-vapor under 6.4, 14.7, 3.13 watts condition, respectively. Furthermore, e-cigarette vaping formed more than 80% of nicotyrine in e-vapor. Nicotine to nicotyrine conversions have been shown to increase with increasing temperatures between 200 ˚C and 400 ˚C. However, above 400 ˚C, the nicotyrine yields are significantly decreased [8]. Temperatures measured by thermocouple are lower than actual temperatures up to 300 ˚C [24]. A previous study using thermal imaging method reprotedthat coil temperatures at 15 watts and 20 watts were approximately 250 ˚C and 300 ˚C after 5 puffs, respectively [25].

Larger puff volume under 3.8 seconds puff duration increase e-vapor nicotine and nicotyrine concentrations. More air flowing through the e-cigarette coils facilitates the evaporation of e-liquids [4]. On the other hand, we observed that lower puff volumes under 3.8 seconds puff duration facilitated nicotyrine formation by changing the retention time within the cartomizer. 95.3%, 93.3%, and 91.2% of nicotyrine were formed during the vaping process at 35, 90, and 170 ml puff volumes with 3.8 seconds duration conditions, respectively. Vaping topography under 35 ml puff volume and 3.8 seconds puff duration has 2.6 and 4.9 times longer retention time within the cartomizer. Increased retention times provide longer reaction times between the vaporized nicotine and the air around the hot cartomizer, and thus form more nicotyrine.

pH is a critical factor that changes gas/particle partitioning of nicotine and its absorption. The measured e-vapor pH values were between 8.09 and 9.51. This coincides with reported pH values that ranged from 7.3 to 9.3 for e-liquids containing 6-24 mg/ml nicotine and other flavors, while e-liquids without nicotine showed much lower pH values (5.1-6.4) [26]. At basic condition ($pH \geq 8$), nicotine ($pKa = 8.02$) is predominantly present in its unprotonated forms (Nic), which facilitate nicotine absorption through biological membranes [20]. In addition, only unprotonated nicotine can be vaporized to gas phase from particles, which facilitates deep lung deposition [21, 27]. In contrast, the pH of cigarette smoke extract is slightly lower than that of e-vapor. Reported cigarette smoke pH rangeed between 5.8 to 7.8 for 11 brands of commercial cigarette and the

1R4F “Kentucky reference cigarette” [21]. Mono-protonated nicotines ($NicH^+$) dominate under this pH range which were mainly presented in the particle phase [20]. Most of the particle phase nicotine was deposited in the buccal region, but the absorption of $NicH^+$ was less efficient than unprotonated nicotine [27].

E-cigarettes could deliver comparable amounts of nicotine per puff to that from combusted tobacco products. We observed nicotine concentrations ranging from 0.37 μg/puff to 249 μg/puff depending on the e-liquid composition, device power settings, and vaping topographies. The reported nicotine concentrations of e-vapor in the literature are comparable with our measurements with the values between 0.107 μg/puff and 530 μg/puff [1, 4, 7, 10, 28]. The cigarette smoke nicotine concentrations of up to 232 μg/puff were reported [29, 30].

It is likely that e-cigarette vaping could deliver significantly higher amount of nicotyrine than conventional cigarette smoking. Previous studies reported that experienced e-cigarette users change their vaping patterns (e.g. number of puffs, e-liquid nicotine concentration, device power output, and vaping topography) to achieve similar levels of plasma nicotine as conventional cigarette smokers [3]. Given the same nicotine intake, e-cigarette users can be exposed to 2-63 times more nicotyrine than conventional cigarette smokers because the nicotyrine-nicotine ratio for e-vapor and for the mainstream tobacco smoke ranged from 0.025 to 0.202 and from 0.003 to 0.013, respectively [7, 10, 29, 31].

In addition, nicotyrine in e-vapor might also indirectly help e-cigarette users to inhale less potentially harmful chemicals emitted from the e-cigarette. Nicotyrine could increase serum nicotine levels by inhibiting human cytochrome P450 isoforms (i.e. CYP2A13 and CYP2A6) [32-34]. Consequently, e-cigarette users might feel satisfaction with fewer number of vaping sessions, resulting in lower harmful chemical exposures such as formaldehyde and acetaldehyde [6]. Nicotyrine in e-vapor and resulting higher serum nicotine level might also help to making e-cigarettes as an effective alternative of regular cigarettes. As a result, nicotyrine might decrease lung cancer risks associated with the tobacco-specific nitrosamines (TSNAs) by inhibiting the

bioactivation of TSNAs [35].

On the other hand, delayed nicotine metabolism could increase cancer risk through the stimulation of nicotinic acetylcholine receptors (nAchRs) [36]. nAchRs were shown to bind with nicotine, N-nitrosonornicotine (NNN), or 4-(methylnitrosamino)-1-(3-pyridyl)-1-butanone (NNK) [37]. Bindings of the nAchRs with these ligands can increase cell growth, inhibit apoptosis, and thus promote malignant cell growth [38]. Therefore, nicotine and/or TSNAs can act as tumor promoters with nAchRs facilitating outgrowth of cells [36]. E-cigarette users might therefore experience higher cancer risks through the nAchRs system than smokers of combusted tobacco, even though e-vapors might expose to less carcinogens [39]. Clearly, the impact of the increased retention time of nicotine in the human body during e-vaping should be further investigated.

It is worth mentioning that several flavoring chemicals were shown to inhibit nicotine metabolism *in vitro* [2]. Menthol is one of the most popular flavors for both e-cigarettes and combusted tobacco products. Menthol flavors could inhibit CYP2A6 and CYP2A13 mediated nicotine metabolism [33]. Other flavoring chemicals including nookatone, coumarin, and tryptamine from grapefruit, cinnamon, and acacia, respectively, could reduce CYP2A6 enzyme activity [2]. The impact of flavoring ingredient on nicotine metabolism also remains to be evaluated. Although, the flavoring chemicals might not be a big concern for regular tobacco products, they are important for e-cigarette products as e-liquids contain a large variety of flavoring components.

In concludion, the nicotine and nicotyrine concenration in e-vapor was measured under real-world vaping conditions. Nicotyrine in e-vapor mainly formed by vaping (≥ 80%), followed by aeration. The amount of nicotine, emitted from e-cigarette under high e-liquid nicotine level, high device power, and large puff volume, was comparable to nicotine levels in cigarette smoke. E-cigarette coil temperature (200-300 ◦C) favored the formation of nicotyrine, and e-cigarette vaping generated 2-63 folds more nicotyrine than conventional cigarette smoking. The impact of

nicotyrine on nicotine metabolism needs to be further accessed due to the kinetics of nicotine is associated with various respiratory diseases.

REFERENCES

[1] Goniewicz, M.L., et al., *Nicotine levels in electronic cigarettes.* Nicotine & Tobacco Research, 2012: p. nts103.

[2] Hukkanen, J., P. Jacob, and N.L. Benowitz, *Metabolism and disposition kinetics of nicotine.* Pharmacological reviews, 2005. **57**(1): p. 79-115.

[3] Dawkins, L.E., et al., *Self-titration by experienced e-cigarette users: blood nicotine delivery and subjective effects.* Psychopharmacology, 2016: p. 1-9.

[4] Talih, S., et al., *Effects of user puff topography, device voltage, and liquid nicotine concentration on electronic cigarette nicotine yield: measurements and model predictions.* Nicotine & Tobacco Research, 2015. **17**(2): p. 150-157.

[5] Schoenborn, C.A. and R.M. Gindi, *Cigarette Smoking Status Among Current Adult E-cigarette Users, by Age Group-National Health Interview Survey, United States, 2015*. 2016, CENTERS DISEASE CONTROL 1600 CLIFTON RD, ATLANTA, GA 30333 USA.

[6] Abramovitz, A., et al., *Electronic cigarettes: The nicotyrine hypothesis.* Medical hypotheses, 2015. **85**(3): p. 305-310.

[7] Martinez, R.E., et al., *On-line chemical composition analysis of refillable electronic cigarette aerosol—measurement of nicotine and nicotyrine.* Nicotine & Tobacco Research, 2015. **17**(10): p. 1263-1269.

[8] Clayton, P., A. Lu, and L. Bishop, *The pyrolysis of (−)-(S)-nicotine: Racemization and decomposition.* Chirality, 2010. **22**(4): p. 442-446.

[9] Stålhandske, T. and P. Slanina, *Nicotyrine inhibits in vivo metabolism of nicotine without increasing its toxicity.* Toxicology and applied pharmacology, 1982. **65**(3): p. 366-372.

[10] Sleiman, M., et al., *Emissions from electronic cigarettes: key parameters affecting the release of harmful chemicals.* Environmental Science & Technology, 2016. **50**(17): p. 9644-9651.

[11] Misthub. *Tutorial: Variable Voltage and Vaping Power Chart*. 2013 [cited 2017 Oct 30]; Available from: https://www.misthub.com/blogs/vape-tutorials/76788421-tutorial-variable-voltage-and-vaping-power-chart.

[12] Dautzenberg, B. and D. Bricard, *Real-Time Characterization of E-Cigarettes Use: The 1 Million Puffs Study.* Journal of Addiction Research & Therapy, 2015. **2015**.

[13] Hua, M. and P. Talbot, *Potential health effects of electronic cigarettes: a systematic review of case reports.* Preventive medicine reports, 2016. **4**: p. 169-178.

[14] Meng, Q., et al., *Has the mist been peered through? Revisiting the building blocks of*

human health risk assessment for electronic cigarette use. Human and Ecological Risk Assessment: An International Journal, 2016. **22**(2): p. 558-579.

[15] Norton, K.J., K.M. June, and R.J. O'Connor, *Initial puffing behaviors and subjective responses differ between an electronic nicotine delivery system and traditional cigarettes.* Tobacco induced diseases, 2014. **12**(1): p. 17.

[16] Robinson, R., et al., *Electronic cigarette topography in the natural environment.* PloS one, 2015. **10**(6): p. e0129296.

[17] Spindle, T.R., et al., *Preliminary results of an examination of electronic cigarette user puff topography: The effect of a mouthpiece-based topography measurement device on plasma nicotine and subjective effects.* Nicotine & Tobacco Research, 2014: p. ntu186.

[18] Swain, M.L., et al., *Ultraviolet absorption spectra of nicotine, nornicotine and some of their derivatives.* Journal of the American Chemical Society, 1949. **71**(4): p. 1341-1345.

[19] Willits, C., et al., *Spectrophotometric determination of nicotine.* Analytical Chemistry, 1950. **22**(3): p. 430-433.

[20] Benowitz, N.L., J. Hukkanen, and P. Jacob III, *Nicotine chemistry, metabolism, kinetics and biomarkers*, in *Nicotine psychopharmacology*. 2009, Springer. p. 29-60.

[21] Pankow, J.F., et al., *Percent free base nicotine in the tobacco smoke particulate matter of selected commercial and reference cigarettes.* Chemical research in toxicology, 2003. **16**(8): p. 1014-1018.

[22] Wada, E., T. Kisaki, and K. Saito, *Autoxidation of nicotine.* Archives of Biochemistry and Biophysics, 1959. **79**: p. 124-130.

[23] Geiss, O., et al., *Characterisation of mainstream and passive vapours emitted by selected electronic cigarettes.* International journal of hygiene and environmental health, 2015. **218**(1): p. 169-180.

[24] Baker, R., *Temperature distribution inside a burning cigarette.* 1974.

[25] Geiss, O., I. Bianchi, and J. Barrero-Moreno, *Correlation of volatile carbonyl yields emitted by e-cigarettes with the temperature of the heating coil and the perceived sensorial quality of the generated vapours.* International journal of hygiene and environmental health, 2016. **219**(3): p. 268-277.

[26] Lisko, J.G., et al., *Chemical Composition and Evaluation of Nicotine, Tobacco Alkaloids, pH, and Selected Flavors in E-Cigarette Cartridges and Refill Solutions.* Nicotine & Tobacco Research, 2015: p. ntu279.

[27] Bergström, M., et al., *Regional deposition of inhaled 11C-nicotine vapor in the human airway as visualized by positron emission tomography.* Clinical Pharmacology &

Therapeutics, 1995. **57**(3): p. 309-317.

[28] Farsalinos, K.E., et al., *Protocol proposal for, and evaluation of, consistency in nicotine delivery from the liquid to the aerosol of electronic cigarettes atomizers: regulatory implications.* Addiction, 2016.

[29] Sakuma, H., et al., *The distribution of cigarette smoke components between mainstream and sidestream smoke: III. Middle and higher boiling components.* Beiträge zur Tabakforschung/Contributions to Tobacco Research, 1984. **12**(5): p. 251-258.

[30] Tayyarah, R. and G.A. Long, *Comparison of select analytes in aerosol from e-cigarettes with smoke from conventional cigarettes and with ambient air.* Regulatory Toxicology and Pharmacology, 2014. **70**(3): p. 704-710.

[31] Cai, J., et al., *Fast analysis of nicotine related alkaloids in tobacco and cigarette smoke by megabore capillary gas chromatography.* Journal of Chromatography A, 2003. **1017**(1): p. 187-193.

[32] Denton, T.T., X. Zhang, and J.R. Cashman, *Nicotine-related alkaloids and metabolites as inhibitors of human cytochrome P-450 2A6.* Biochemical pharmacology, 2004. **67**(4): p. 751-756.

[33] Kramlinger, V.M., L.B. von Weymarn, and S.E. Murphy, *Inhibition and inactivation of cytochrome P450 2A6 and cytochrome P450 2A13 by menthofuran, β-nicotyrine and menthol.* Chemico-biological interactions, 2012. **197**(2): p. 87-92.

[34] Su, T., et al., *Human cytochrome P450 CYP2A13: predominant expression in the respiratory tract and its high efficiency metabolic activation of a tobacco-specific carcinogen, 4-(methylnitrosamino)-1-(3-pyridyl)-1-butanone.* Cancer Research, 2000. **60**(18): p. 5074-5079.

[35] Kamataki, T., et al., *Role of human cytochrome P450 (CYP) in the metabolic activation of nitrosamine derivatives: application of genetically engineered Salmonella expressing human CYP.* Drug metabolism reviews, 2002. **34**(3): p. 667-676.

[36] Minna, J.D., *Nicotine exposure and bronchial epithelial cell nicotinic acetylcholine receptor expression in the pathogenesis of lung cancer.* Journal of Clinical Investigation, 2003. **111**(1): p. 31.

[37] Schuller, H.M., et al., *Interaction of tobacco-specific toxicants with the neuronal α 7 nicotinic acetylcholine receptor and its associated mitogenic signal transduction pathway: potential role in lung carcinogenesis and pediatric lung disorders.* European journal of pharmacology, 2000. **393**(1): p. 265-277.

[38] West, K.A., et al., *Rapid Akt activation by nicotine and a tobacco carcinogen modulates*

the phenotype of normal human airway epithelial cells. The Journal of clinical investigation, 2003. **111**(1): p. 81-90.

[39] Beckmann, J. and K.S. Lips, *The non-neuronal cholinergic system in health and disease.* Pharmacology, 2013. **92**(5-6): p. 286-302.

CHAPTER 4

HYDROXYL RADICALS INDUCED BY E-CIGARETTE VAPING

4.1. INTRODUCTION

The use of e-cigarettes has been rapidly increasing in the US population [1, 2]. However, e-cigarettes are not risk free products. E-vapor contains potentially harmful chemicals including carbonyls and flavoring chemicals [3, 4]. Limited number of studies reported the presence of reactive oxygen species (ROS) in e-vapor [4-6]. Even though the oxygen radical concentrations found in e-vapor might be much lower than that of other potentially harmful chemical species, the radical exposures caused by various e-cigarette vaping conditions need to be understood due to high risk potencies of the some radical species.

In addition, a conventional cigarette study showed that the only 3% of cigarette tar extract (by mass) containing radicals [i.e. Q/QH_2 and hydroxyl radical ($^{\bullet}OH$)] induced 70% of the total DNA damage generated by the whole cigarette tar extract [7]. Among the ROS (i.e. $O_2^{\bullet-}$, H_2O_2, and $^{\bullet}OH$), $^{\bullet}OH$ is the most destructive radical which can damage vital biological components in lung epithelial lining fluid (ELF) [8]. Moreover, there are no $^{\bullet}OH$ specific antioxidant enzymes such as superoxide dismutase or catalase [9]. Therefore, specific ROS needs to be targeted to understand the mechanism of oxidative stress induced by e-cigarette vaping.

$^{\bullet}OH$ formed during the e-cigarette vaping has not been studied to date. The formation of radicals in e-vapor may be affected by the diverse e-cigarette products and use patterns. Device power settings and vaping topographies may affect radical formation through modifying e-cigarette heating coil temperatures and oxygen supplies [10]. In addition, various e-liquid compositions, such as the type of base materials, nicotine levels, and flavoring agents, may contribute to radical formation through thermal degradation [6]. Therefore, the level of radical species needs to be evaluated under wide ranges of e-cigarette use patterns.

Also, the formation of $^{\bullet}OH$, induced by e-vapor components under physiologically relevant

condition (i.e. 37 ˚C, pH 7.4, avoiding light), is unknown. The ELF contains ascorbic acid and iron ions ($Fe^{2+/3+}$) which may interact with the e-vapor components to form ˙OH through the Fenton reaction [11]. Previous studies have been reported that nicotine and several flavoring chemicals were redox cycled, mediated by transition metal ion [12, 13]. However, the level of ˙OH induced by e-vapor was not evaluated so far. Measuring the e-vapor induced ˙OH formation might be the first step to understand longer term oxidative stress associated with e-cigarette vaping.

Therefore, this study was directed on assessments of the level of ˙OH formed under 'real-world' relevant vaping conditions (i.e. device setting, vaping topography, and e-liquid composition). The ˙OH induced by e-vapor with ascorbic acid or Fe^{3+} was also evaluated.

4.2. MATERIAL AND METHODS

4.2.1. E-cigarette and E-liquids Preparation

The refillable tank type e-cigarette (The Council of Vapor, Walnut, CA, USA) consisted of an adjustable air hole (1, 1.5, and 2 mm) and a replaceable Nichrome heating coil head (dual-bottom coil with 0.8, 1.2, and 2.0 Ω), and was used for the different experiment conditions. Two types of battery boxes, an Apollo Valiant battery (Apolo E-cigarette, Concord, CA, USA) and a Sigelei-100W battery (Sigelei US, Pomona, CA, USA), were used to provide a wide range of heating power from 3 to 80 watts.

All e-liquids were freshly prepared in our laboratory using propylene glycol (PG, USP grade, Sigma-Aldrich, MO, USA), vegetable glycol (VG, USP grade, J.T. Baker, NJ, USA), (-)-Nicotine (≥99.0%, Sigma-Aldrich, MO, USA), and flavoring agents. The eight flavoring agents (strawberry, dragon fruit, menthol, sweet cream, Bavarian, cinnamon, bubble gum, and graham cracker flavors) were obtained from The Perfumer's Apprentice (Scotts Valley, CA, USA). These flavors attained most popularity among the e-cigarette forum and in vape shops [14]. The ingredients of the eight flavors have only been partially released by the manufacturer and appeared to be natural/artificial flavors in PG, water or ethyl alcohol.

Flavoring agents usually contains dozens of flavoring chemicals (e.g. strawberry flavor contains anethole, benzyl acetate, ethyl butyrate, maltol, etc). Flavoring chemicals may redox cycle with transition metal ions, and induce $^{\bullet}OH$. Therefore, nine flavoring chemicals were selected based on their popularity in the commercially available e-liquids [4]. Benzyl alcohol (99%), benzyl acetate (99%), ethyl acetate (99%), trans-anethole (≥98%), trans-cinnamaldehyde (≥98), 2,3-butanedione (99%, diacetyl), 2,3-pentanedione (97%, acetylpropionyl) were purchased from Alfa Aesar (Haverhill, MA, USA). Citral (95%) and vanillin (99%) were purchased from Sigma-Aldrich (St. Louis, MO, USA). The nine flavoring chemicals represented fruity, citrus, spicy, and creamy/buttery flavors. Fruity flavoring chemicals consist of hydroxyl and ester functional groups, and other flavoring chemicals usually were aldehydes (Table S4-1).

4.2.2. Hydroxyl Radical Measurements in E-vapor

Real-world vaping conditions are important to understand exposures of e-cigarette users to $^{\bullet}$OH. To obtain vaping conditions, 23 current e-cigarette users (25 ± 10 years old, 21 men and 2 women, and 1.4 ± 0.9 years e-cigarette use history) were recruited to access the vaping pattern using a CReSS Pocket device (Borgwaldt KC Incorporated, North Chesterfield, VA, USA) with the approval of the IRB at Rutgers University. Detailed demographics and observations are shown in Table S2-1 and Table S2-2.

Median values from Table S2-2 were used as a baseline vaping pattern. Baseline device power output was 6.4W which was recommended by the e-cigarette forums as a safe power output, and vaping topography was 90 ml puff volume and 3.8 seconds puff duration. The vaping topography in our experiment is comparable to the vaping topographies reported in the literature: the reported median puff volume and duration was 91 ml (51-133 ml) and 3.8 seconds (2.65-4.3 seconds), respectively [15-20]. VG-based e-liquid containing 12 mg/ml nicotine, which was most popular e-liquid among the 23 study participants, was used throughout the experiment unless otherwise specified.

In order to test the impact of device settings on $^{\bullet}$OH radical formation, the median and the 95% of observed power outputs from the 23 study participants (i.e. 6.4W and 31.3W) were used to generate e-vapor. The selected power outputs represented the safe and the extremely hot ranges of the e-cigarette vaping power chart [21]. Three different air hole sizes (i.e. 1, 1.5, and 2 mm), which were the available air hole diameters from the e-cigarette vendor, were used to evaluate the impact of air flow rate on $^{\bullet}$OH radical formation. To test the impacts of vaping topography, cigarette smoking regime (i.e., 35 ml puff volume and 2 seconds puff duration) and the 95th percentile of the observed puff volume (170 ml) were used to generate e-vapor.

The impact of e-liquid composition (i.e. different base materials, nicotine levels, and flavoring agents) on e-vapor $^{\bullet}$OH concentration was tested because various e-vapor components and their thermal degradation products might have different redox potentials and alter $^{\bullet}$OH

formation. In order to test the impact of base material and nicotine concentrations, nicotine (0, 3, 12, 24, and 36 mg/mL) in VG, PG&VG (v/v=1:1), or PG-based e-liquid were used to generate e-vapor. The levels of nicotine and base materials were observed from the 23 study participants and e-liquid recipes on the market [14]. In addition, e-vapors were generated using freshly prepared e-liquids consisting of eight flavored e-liquids with low and high levels of flavoring agents (1 and 10% by volume except cinnamon flavor, 0.1% and 1% of cinnamon flavored e-liquid was tested). The levels of the flavoring agents were obtained from the 941,914 e-liquid recipes [14]. Detailed experimental conditions are tabulated in Table S4-2.

For each experimental condition, 50 puffs of e-vapor were generated using a LX1 smoking machine (Borgwaldt KC Incorporated, Hamburg, Germany) connected with a mid-jet impinge containing 15 ml of phosphate buffered saline [PBS, pH 7.4, 114 mM sodium chloride (NaCl, ≥99.5%, Sigma-Aldrich, MO, USA), 8 mM sodium phosphate dibasic (Na_2HPO_4, ≥99.0%, Sigma-Aldrich, MO, USA), 2 mM potassium phosphate monobasic (KH_2PO_4, ≥99.995%, Sigma-Aldrich, MO, USA)] with 15 mM of disodium terephthalate (TPT, ≥99.0%, Alfa Aesar, MA, USA) as a stable, $^{\bullet}OH$ specific fluorescence probe [22]. Dimethyl sulfoxide (DMSO, ≥99.9%, Sigma-Aldrich, MO, USA) (50 mM) was added immediately after collecting e-vapor and samples were stored at -20 °C until analysis. PBS and other chemicals were prepared using chelex-100 (50-100 mesh, Sigma-Aldrich, MO, USA) treated deionized water to remove metal ions.

4.2.3. E-vapor-Induced Hydroxyl Radicals

E-vapor components may interact with ascorbic acid (Asc, ≥99.0%, Sigma-Aldrich, MO, USA) in ELF to induce $^{\bullet}OH$. To explore the levels of $^{\bullet}OH$ generated by e-vapor, 50 puffs of e-vapor and 100 μM of ascorbic acid in 15 ml PBS (pH 7.4) were incubated for 2 hours. The selected conditions included three flavored e-liquids representing fruit, spicy, and creamy/fatty flavors (strawberry, cinnamon, and sweet cream flavor), and 0, 3, 12, 24, 36 mg/ml nicotine in VG. The three flavoring agents were selected to represent different flavoring categories. E-vapors

were generated under 6.4W as 90 ml and 3.8 seconds puffs. The ascorbic acid concentration was based on human respiratory ELF studies [23].

E-vapor components may also interact with transition metal ions to induce $^{\bullet}OH$ by initiating the Fenton reaction, transition metals alone cannot induce $^{\bullet}OH$ without a reducing agent [9]. Therefore, to test $^{\bullet}OH$ inducing capacity, 50 puffs of e-vapor and 100 μM of Fe^{3+} (iron(III) nitrate, ≥99%, Sigma-Aldrich, MO, USA) in 15 ml PBS (pH 7.4) was incubated for 2 hours at 37 °C, avoiding light. Testing e-liquids contained strawberry, cinnamon, and sweet cream flavored e-liquids, and e-liquids containing 0, 3, 12, 24, 36 mg/ml nicotine in VG. Other vaping conditions were 6.4W, 90 ml puff volume and 3.8 seconds puff duration. In addition, the level of $^{\bullet}OH$ induced by e-vapors containing flavoring chemical and Fe^{3+} were tested using nine flavoring chemicals, representing fruity (benzyl alcohol, benzyl acetate, and ethyl acetate), sweet (anethole), citrus (citral), spicy (cinnamaldehyde), and creamy/buttery (vanillin, diacetyl, and acetylpropionyl) flavors.

Nicotine was also tested for its ability to generate hydroxyl radicals since it is a redox-active chemical [12]. The induced $^{\bullet}OH$ levels were measured using the nicotine solutions containing 0.1, 0.3, 0.6, and 0.9 mM in PBS (pH 7.4) in the presence of Fe^{3+}. These nicotine concentrations correspond to the e-vapor samples containing 3-36 mg/ml nicotine. The nicotine solutions were incubated with 15 mM of TPT and 100 μM of Fe^{3+} for 2 hours at 37 °C, avoiding light.

4.2.4. Hydroxyl Radical Detection

Hydroxyl radicals in reaction mixes were measured as formation of 2-hydroxyterephthalic acid (2OHTA, 97%, Sigma-Aldrich, MO, USA), the reaction product of $^{\bullet}OH$ and TPT [22]. A high-throughput approach was applied using a 96 well fluorescent microplate reader (BioTek Synergy™ 4 Multi-detection Microplate reader) to measure 2OHTA at ex/em=310/425 nm. A calibration curve was generated using 0.1 to 1.5 μM 2OHTA standard samples in phosphate buffer (pH 7.4) containing 15 mM TPT (Figure S4-1). Limits of detection (LOD) and limits of

quantification (LOQ) were three and ten times the standard deviation of seven blank samples. LOD and LOQ of 2OHTA were 4.1 nM and 13.7 nM, respectively.

4.2.5. Quality Assurance and Quality Control

The amount of TPT in reaction mixes is sufficient to outcompete other •OH scavengers under our experimental conditions [22]. The 15 mM of TPT would be sufficient to capture •OH in e-vapor and •OH induced by e-vapor because the levels of •OH in this experimental conditions were much lower than the •OH concentrations induced by transition metal ion and ascorbic acid in our previously published report [22].

Throughout the •OH formed in e-vapor experiments, lab blanks were obtained for each batch of experiment. Blank samples were 50 puffs of e-vapor generated under the same experimental conditions, and then collected using the mid-jet impinge containing 15 ml of PBS (pH 7.4) with 15 mM of TPT and 50 mM of DMSO. Blank values under each experimental conditions were subtracted from the corresponding measured concentrations.

To validate the sampling system, 50 puffs of air passed through the unpowered e-cigarette were collected using a mid-jet impinge containing 15 ml of PBS (pH 7.4) with 15 mM of TPT. The signals with and without DMSO were 3131±81 RFU and 3025±48 RFU, respectively. The results indicated that the air flow through the e-cigarette did not increase 2OHTA.

4.3. RESULTS AND DISCUSSION

4.3.1. Impact of Device Settings on •OH Formation

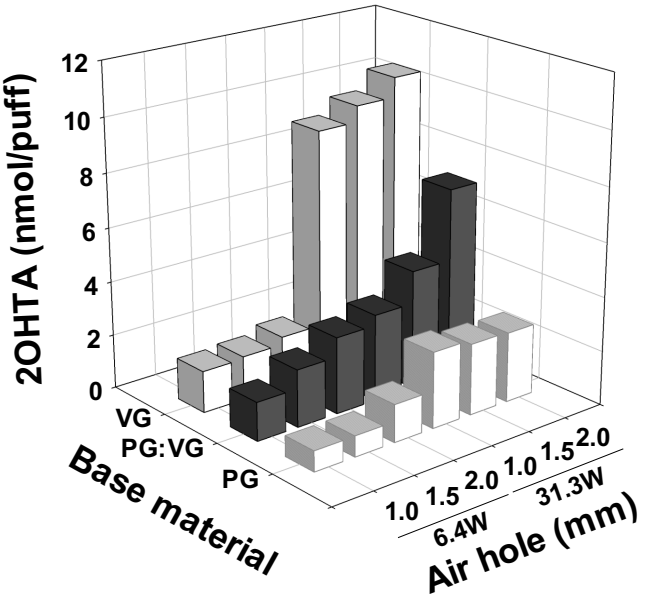

Figure 1. 2OHTA concentrations generated by different device power settings, air hole sizes, and base materials (n=5). 12 mg/ml nicotine was added in all e-liquids. 90 ml puff volume, 3.8 sec puff duration, and 24 sec puff interval was used for vaping topography

Figure 4-1 shows the impact of device power output, air hole size and e-liquid base material on •OH emission in e-vapor. Higher power output significantly increased •OH generation (p-value < 0.001, t-tests). 31.3W power output formed usually 2.7, 2.3, and 5.8 times more •OH than 6.4W conditions for PG, PG&VG, and VG e-liquids, respectively. Furthermore, 31.3W power output with 2 mm air hole size formed 119.1% and 14.3% more •OH than 1 mm air hole atomizers for PG:VG and VG e-liquid, respectively (p-value < 0.027, t-tests).

E-cigarette power output is associated with the amount of e-vapor and its chemical composition. On the one hand, increased power output (i.e. high coil temperature) was shown to generate higher amounts of e-vapor due to the increased e-liquid evaporation rate [24]. Larger e-vapor quantity under higher power output settings might increase the amount of •OH per puff.

$$C_3H_8O_3 + 3/2O_2 \rightarrow 3CO_2 + 4H_2 \quad \text{Equation 4-1}$$

$$C_3H_8O_3 + 7/2O_2 \rightarrow 3CO_2 + 4H_2O \quad \text{Equation 4-2}$$

$$C_3H_8O_3 \rightarrow {}^{\cdot}OHR + H \quad \text{Equation 4-3}$$

On the other hand, increased device power output and oxygen supply facilitates the partial oxidation of e-liquid given by the Equation 4-1 and Equation 4-2 [25]. The partial oxidation (Eq. 1) and combustion reaction (Equation 4-2) of VG are thermodynamically favorable at e-cigarette coil temperatures (i.e. 200-300 ˚C), and higher coil temperatures always favor these reactions [25]. Moreover, higher oxygen supplies due to the larger air hole size could increase the partial oxidation and combustion reactions. In addition, hydrogen abstracting reaction during the thermal degradation of VG and PG can form hydroxyl group radicals including $^{\bullet}OH$, $^{\bullet}CH_2OH$, and $^{\bullet}C_3H_7O_3$ (Equation 4-3) [26, 27]. Reactions between the partial oxidation products (i.e. H_2, CO_2, H_2O, and radicals) and other e-liquid components could lead to the formation of $^{\bullet}OH$ during e-cigarette vaping [9].

4.3.2. $^{\bullet}OH$ formation using Different E-liquids

Table 4-1. Formed 2OHTA in e-vapor (mean ± standard deviation, nmol/puff, n=5) for e-liquids with different base materials and nicotine concentrations[†]

Base material	Nicotine level				
	0mg/ml	3mg/ml	12mg/ml	24mg/ml	36mg/ml
VG	1.43±0.32	1.80±0.30	1.71±0.49	1.10±0.15	1.63±0.62
PG:VG	1.82±0.79	1.78±0.71	1.88±0.62	0.56±0.94	1.48±0.34
PG	1.08±0.21	1.15±0.70	0.89±0.53	0.82±0.54	0.70±0.16

[†]6.48 W power output, 1.5 mm air hole, 90 ml puff volume, 3.8 sec puff duration, and 24 sec puff interval used

Table 4-1 shows $^{\bullet}OH$ species in e-vapor generated with various e-liquids containing different base materials and different levels of nicotine. VG and PG&VG based e-liquids formed usually

1.7 and 1.9 fold higher •OH levels than PG based e-liquids (p-value < 0.015, t-tests). Similarly, Lerner et al [6] reported that the VG-based e-liquid showed higher ROS level compare to PG-based e-liquid. There is no sufficient knowledge to explain the impact of base material on •OH formation, but potential impacting factors could be the difference of the reaction temperature and oxidation product of PG and VG [26]. In the presence of O_2, PG and VG could initiate the reaction at 127 ˚C and 200 ˚C, respectively, to form the oxidation products derived from the carbon-centered radicals. The higher reaction temperature of VG-based e-liquid might produce more intermediate products (e.g. radicals) due to the incomplete oxidation reaction, while PG e-liquid can quickly produce final oxidation products under the same reaction temperature.

Even though the differences of 2OHTA levels were not statistically significant (p-values > 0.05, t-tests), 2OHTA concentrations for e-liquids with higher nicotine concentration were slightly lower than the samples containing less nicotine (Table 4-1). In previous research, e-vapor with 24 mg/ml nicotine showed less ROS concentration than e-vapor without nicotine [6]. Nicotine regarded as an antioxidant agent because nicotine has many oxidation sites that can react with •OH to form electronically neutral radicals [9]. Simultaneously, redox potential of nicotine may facilitate •OH formation [12]. The competing effects of nicotine might result in different e-vapor •OH levels.

Figure 4-2 shows e-vapor •OH levels formed using non-flavored (100% VG) and flavored e-liquids. Flavored e-liquids formed higher levels of •OH in e-vapor than non-flavored e-liquids (p-value < 0.049, t-tests). Ranges of the average 2OHTA concentration for low and high flavored e-liquids were 2.29-2.92 nmol/puff and 2.79-3.66 nmol/puff, respectively; while non-flavored e-liquid (100% VG) induced 1.43±0.32 nmol/puff of 2OHTA. Among the flavored e-liquids, fruit (strawberry, dragonfruit) and sweet (bubble gum) flavored e-liquids formed slightly more •OH than menthol and creamy/buttery (Bavarian cream, sweet cream, and graham cracker) flavored e-liquids (p-value > 0.177, t-tests).

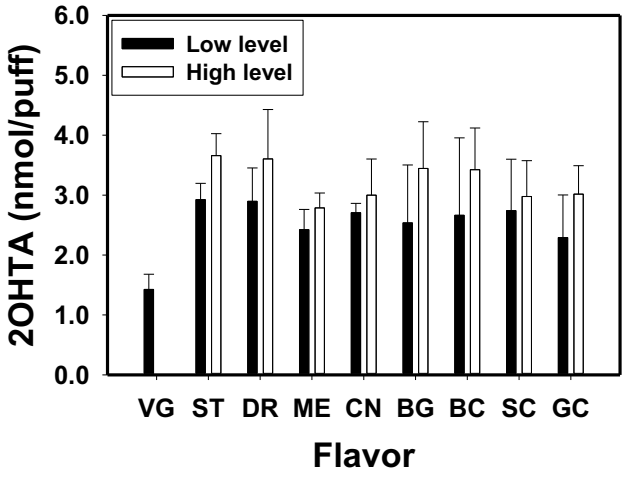

Figure 4-2. 2OHTA concentrations for the non-flavored e-liquid and the eight flavored e-liquids. Low and high indicates 1% and 10% of flavoring ingredient in VG (by volume) except cinnamon flavor (0.1% and 1% for cinnamon flavor) (n=5, error bars indicate standard deviation). VG: non-flavored e-liquid, ST: strawberry, DR: dragon fruit, ME: menthol, CN: cinnamon, BG: bubble gum, BC: Bavarian cream, SC: sweet cream, and GC: graham cracker flavor. Device setting was 6.48 W and 1.5 mm air hole diameter, and vaping topography was 90 ml puff volume, 3.8 sec puff duration, and 24 sec puff interval

4.3.3. Impact of Vaping Topographies on •OH Formation

The impacts of vaping topography on •OH formation in e-vapor are presented in Table 4-2.

Table 2. Formed 2OHTA in e-vapor (mean ± standard deviation, nmol/puff, n=5) for different vaping topographies†

Puff duration	Puff volume		
	35ml	90ml	170ml
2sec	0.66±0.72	1.68±0.96	2.66±0.73
3.8sec	0.34±0.66	1.70±0.40	3.80±0.59

†6.48 W power output, 1.5 mm air hole, VG based e-liquid containing 12 mg/ml nicotine, and 24 sec puff interval used

•OH levels using 35 ml puff volume were not significantly different between with and without the •OH scavenger (p-value > 0.101, t-tests). Therefore, toxicological studies adopting conventional cigarette smoking regime (i.e. 35 ml puff volume and 2 seconds puff duration)

might not reflect the e-cigarette user's •OH exposure. A 90 ml or 170 ml puff (3.8 seconds) generated 4.1 and 10.3 fold more •OH than a 35 ml puff (3.8 seconds), respectively (p-value < 0.004, t-tests). 2OHTA concentrations for a 170 ml and 3.8 seconds puff was significantly higher than a 170 ml and 2 seconds puff (p-value < 0.027, t-tests). Increased puff volume associated with increased air flow rate around the e-cigarette coil which could facilitate e-liquid evaporation [24]. Increased oxygen supply could initiate oxidation of VG/PG at significantly lower temperature compare to anaerobic conditions [26]. In addition, high air flow rate rapidly mixed e-vapor with supplied oxygen that would increase the oxidation rate [25].

4.3.4. E-vapor Induced •OH formation with Ascorbic Acid

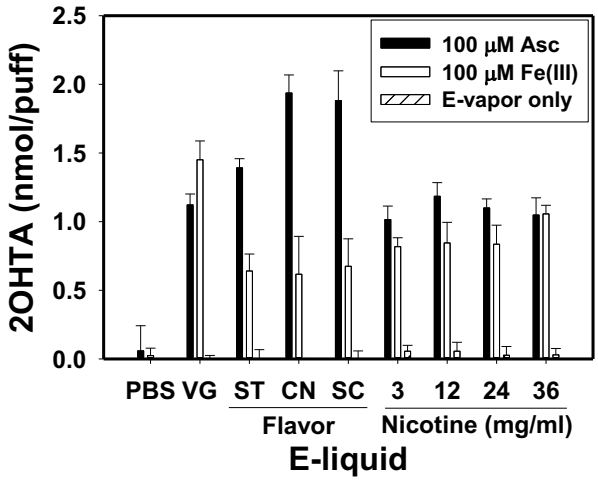

Figure 4-3. 2OHTA concentrations induced by PBS only, 100% VG, flavored (ST: strawberry, CN: cinnamon, SC: sweet cream) and nicotine containing e-vapors (3-36 mg/ml nicotine) with 100 μM ascorbic acid (Asc) or 100 μM Fe^{3+} after 2 hours incubation under 37 ˚C, avoiding light (n=5, error bars indicate standard deviation)

E-vapors generated using flavored e-liquids with ascorbic acid, which is an abundant molecule in human ELF, induced higher •OH under the physiologically relevant incubating condition (37 ˚C, avoiding light) (Figure 4-3). Flavored e-liquids with 100 μM ascorbic acid

generated 1.2-1.7 fold higher •OH than non-flavored (100% VG) e-liquid (p-value < 0.016, t-tests). Among the flavored e-liquids, cinnamon and sweet cream flavor induced 39.1% and 35.1% higher •OH than strawberry flavored e-liquid (p-value < 0.034, t-tests). E-vapor- and ascorbic acid-only samples did not induce •OH.

Flavored e-vapors could induce higher •OH levels due to the higher numbers and amount of redox cycling components (i.e. flavoring chemicals or thermal degradation products of flavoring chemicals) than VG only e-vapor. An e-vapor component (R) might be reduced by ascorbic acid (Asc) through Equation 4-4, and the reduced e-vapor component might increase •OH through the organic Fenton reaction (Equation 4-5).

$$R^+ + AscH_2 \rightarrow R^{\cdot} + Asc^{\cdot -} + 2H^+ \qquad \text{Equation 4-4}$$

$$R^{\cdot} + O_2^{\cdot -} + 2H^+ \rightarrow R^+ + {}^{\cdot}OH + OH^- \qquad \text{Equation 4-5}$$

Redox potentials of flavoring chemicals are still not well understood due to the large varieties of chemical structures. Limited number of studies suggested the reducing capacity of cinnamaldehyde, vanillin and diacetyl which might present in cinnamon and sweet cream flavored e-liquids [28, 29]. Thermal degradation products of vanillin (i.e. vanillic acid) also showed reducing capacity [13]. Therefore, flavored e-liquids might form more chemical compounds which could redox cycle oxygen and hydrogen to form •OH under the presence of ascorbic acid.

4.3.5. E-vapor Redox Cycled Fe^{3+} to Induce •OH

E-vapor induced •OH with Fe^{3+} after 2 hours incubation under 37 ˚C, avoiding light, while e-vapor and Fe^{3+} itself did not induce •OH (Figure 4-3). To generate •OH, Fe^{3+} needs to be reduced to Fe^{2+} by an e-vapor component (R) by Equation 4-6, and then Fe^{2+} in the system could generate •OH through the Fenton reaction (Equation 4-7).

$$Fe^{3+} + R \rightarrow Fe^{2+} + R^{+}$$ Equation 4-6

$$Fe^{2+} + O_2^{\cdot -} + 2H^{+} \rightarrow Fe^{3+} + {}^{\cdot}OH + OH^{-}$$ Equation 4-7

Interestingly, VG only e-vapor with 100 μM Fe^{3+} induced 1.4-2.4 fold higher $^{\bullet}$OH than other conditions (p-value < 0.001, t-tests), while flavored e-vapors with ascorbic acid induced significantly higher amount of $^{\bullet}$OH than VG only e-vapor. Different 2OHTA formation trends might be affected by the redox potentials of e-vapor components, ascorbic acid (E^0=0.33 V, pH=7.0), and $Fe^{3+/2+}$ (E^0=0.77 V, pH=7.0). Redox potential of VG only e-vapor could be more favorable to the reduction of Fe^{3+} to Fe^{2+} than flavored e-liquid samples. In contrast, redox potential of ascorbic acid might facilitate reducing flavored e-vapor constituents to form more $^{\bullet}$OH than VG only e-vapor.

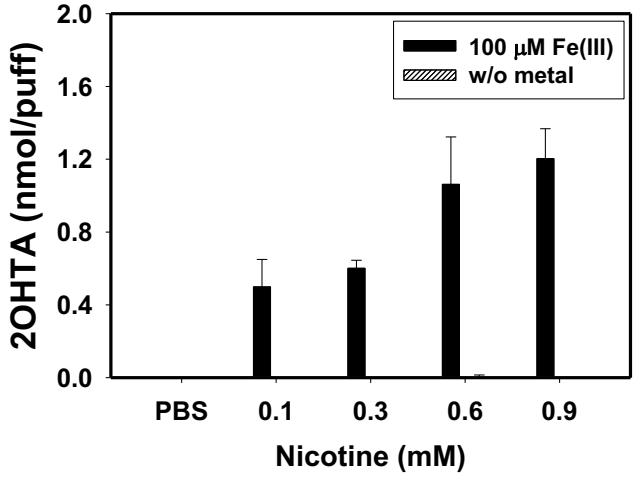

Figure 4-4. 2OHTA concentrations induced by 0.1-0.9 mM nicotine solution in PBS (pH 7.4) with 100 μM of Fe^{3+} after 2 hours incubation under 37 °C, avoiding light (n=5, error bars indicate standard deviation)

Nicotine solution with Fe^{3+} could initiate Fenton reaction to form $^{\bullet}$OH, while nicotine solution without metal ion did not induce $^{\bullet}$OH (Figure 4-4). 0.9 mM nicotine solution with 100

μM Fe^{3+} induced 2.1-fold more •OH than 0.1 mM nicotine solution. The level of •OH for 0.1 and 0.3 mM nicotine solutions with Fe^{3+} were 19.6% and 10.0% lower than the e-vapor containing 3 and 12 mg/ml nicotine with Fe^{3+}, respectively. However, 0.6 and 0.9 mM nicotine solution with Fe^{3+} induced usually 40% more •OH than the e-vapor samples containing 24 and 36 mg/ml nicotine with Fe^{3+} (p-value < 0.019, t-tests). Nicotine (E^0=0.84 V, pH=7.0) might act as either •OH scavengers or competing redox agents with Fe^{3+} in e-vapor samples [12].

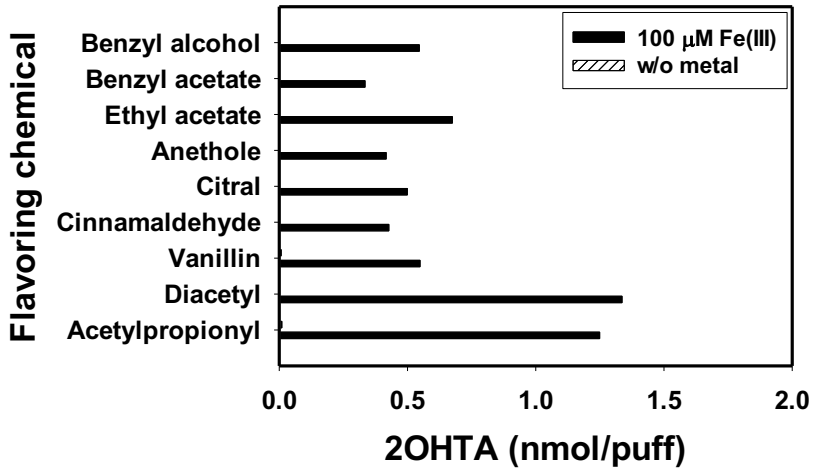

Figure 4-5. 2OHTA generated by e-liquids containing flavoring chemicals with and without 100 μM Fe^{3+} after 2 hours incubation under 37 °C, avoiding light (n=5, error bars indicate standard deviation). Results were normalized by the molar concentration of flavoring chemicals

E-vapors generated using the butter flavoring chemicals (i.e. diacetyl and acetylpropionyl) induced higher •OH with Fe^{3+} than e-vapors containing other flavoring chemicals (Figure 4-5). At the same molar concentrations, diacetyl and acetylpropionyl e-vapors with 100 μM Fe^{3+} formed approximately two times more •OH than the e-vapors incorporating fruit-like flavoring chemicals (benzyl alcohol, benzyl acetate, and ethyl acetate) (p-value < 0.001, t-tests). The results could provide evidences that the flavoring chemicals in e-vapor could redox cycle the transition metal ions to form •OH through the Fenton reaction.

4.3.6. Health Implications

In this study, the impact of real-world vaping patterns (e-cigarette device settings, vaping topographies, and e-liquid compositions) on •OH in e-vapor was assessed for the first time. •OH is one of the most harmful e-vapor components because (1) the risk potency of •OH can be much higher than that of other potentially harmful components in e-vapor [7], and (2) the daily dose of e-vapor free radical can still exceed the dose caused by ambient particulate matter (PM), assuming a vaping frequency of 200 puffs/day [5].

Our study and published results show that e-vapor contains lower levels of radicals per puff than the cigarette smoke [5, 6]. The levels of free radicals in tobacco smoke were 10 to 1000 times higher than that in e-vapor observed in our study (0.86-1.09×10^{14} OH radicals/puff) and in other studies reported before (0.25-1.03×10^{13} radicals/puff or 0.59-2.94 μM H_2O_2 equivalents/puff) [5-7, 9].

However, the daily e-vapor radical exposure can be comparable with the daily dose induced by cigarette smoking depending on the e-cigarette use patterns. In 2015, on average, US smokers smoked 14.2 cigarettes per day (ranging 5-30 cigarettes/day) [30]. Assuming a cigarette can make 10-12 puffs, average •OH exposures associated with cigarette smoking range from 5.0×10^{16} to 3.6×10^{19} OH radicals/day (9.1±1.3×10^{18} OH radicals/day). The daily average radical exposures induced by e-cigarette vaping can be 2.4±2.6×10^{16} OH radicals/day (8.6×10^{14} to 1.1×10^{17} OH radicals/day), assuming a range of puff frequency of 10-1000 puffs/day [15, 16]. The ranges of ROS dosages for e-cigarette vaping overlap the daily ROS dose induced by cigarette smoking.

The •OH induced by e-vapor components through the Fenton reaction is much slower than cigarette smoke. Both cigarette smoke and e-vapor contain •OH and can induce •OH formation. The Q/QH_2 couple in cigarette tar can redox cycle transition metal ion to form •OH [31]. The EPR signal intensity of the DMPO-OH spin adduct was increased by 4-fold by adding 20 μm Fe^{3+} in the cigarette tar extract solution (20 mg/ml, pH 9.5) [7]. We evaluated •OH induced by e-vapor and Fe^{3+}, and the •OH level was 5-10 fold lower than the •OH produced by conventional cigarette

smoke. Therefore, redox activity of e-vapor components might be much lower than the activity of conventional cigarette smoke.

Limited numbers of *in vivo* and *in vitro* studies have shown oxidative stress caused by e-cigarette vaping. *In vivo* mouse studies showed that e-vapor extracts in ELF induced lung glutathione depletion and lipid peroxidation [6, 32], which might indicate the ROS exposure [8]. Limited numbers of *in vitro* studies have also shown that e-vapor exposure increases DNA damage and apoptotic/necrotic cell death [33-35]. Increased DNA damage could support e-vapor induced $^{\bullet}OH$ exposures because $^{\bullet}OH$ might be the only radical species that can damage DNA due to the high reactivity [36]. Therefore, the $^{\bullet}OH$ generation mechanism needs to be further studied to be able to reduce their adverse health impacts.

Oxidative stress responses were observed only after long-term e-vapor exposures (24 hours or longer) [33-35]. Up to 3 hours of e-vapor exposures using human bronchial epithelial cell line (BEAS-2Bs) did not induce DNA damage, while cigarette smoke exposures resulted in significantly higher DNA damage and cytotoxicity after 3 hours [37]. Taylor et al [38] incubated human bronchial epithelial cells (NCI-H292) with e-vapor extracts for 6 hours, and no cell death, ROS formation and glutathione consumption was observed. The evidences suggest that the level of $^{\bullet}OH$ in e-vapor might not be sufficient to induce acute adverse health impacts, but the induced $^{\bullet}OH$ could increase oxidative stress responses. Therefore, it is necessary to study longer-term oxidative stress in order to be able to assess the oxidative potential of e-vapor rather than their acute impacts.

Recent developments in e-cigarette devices may elevate the radical doses. For instance, the combinations of the recently developed sub-ohm coils (e.g. the Clapton, Twisted, Helix, and Staple coils with the resistance of less than 1 ohm) and battery devices can provide over 100 watts power output. The extremely high power output settings might cause elevated oxidative stress due to the induction of enormous amount of e-vapor radicals. Consequently, the safe range of e-cigarette power output and vaping frequency needs to be assessed, promoted, and regulated

to protect public health.

Popular use of flavored e-liquids might increase e-vapor •OH exposures and result in potential health problems. This is a relevant concern as the market share of non-flavored e-cigarettes was decreased by 3% between 2012 and 2013, while the market share of fruit and other flavored e-cigarette were increased at least by 0.8% and 2.6%, respectively [39]. Increased use of the flavored e-liquid is posing a potential health problems due to the higher oxidative potential of flavored e-liquids than non-flavored. In addition, e-cigarettes are the most popular flavored tobacco product among high school students [40]. Vaping flavored e-cigarettes at early ages should be discouraged because the e-vapor ROS might alter cell proliferation [41].

It is worth mentioning that coexisting environmental exposures might further elevate oxidative stress. Particulate matter (PM) from air pollution is a known source of transition metal ion exposure such as iron and copper. In fact, the two transition metal ions were known to induce •OH in simulated epithelial lining fluid [22]. Reactions between redox active components in e-vapor and PM constituents (i.e. transition metal ions) can form •OH through the Fenton reaction. Therefore, the interaction between e-vapor and air pollutants needs to be further studied.

The limitation of this study was that this study included limited number of flavoring agents and chemicals to evaluate the •OH levels. There are more than hundred thousand e-liquid recipes which might contain numerous flavoring chemicals [14]. These flavoring chemicals could affect •OH formation in e-vapor, and induce •OH with ELF components (e.g. ascorbic acid). In this study, we could test the most popular flavoring agents and flavoring chemicals after intensive searching for e-liquid recipes. Future researches need to test the impact of flavoring agents on •OH formation based on their redox potentials and chemical structures. In addition, there is limited information regarding the redox potential of flavoring chemicals and their thermal degradation products of these chemicals at temperature of 100-150 ˚C [13, 28, 29, 42]. The redox potential and the thermal oxidation of the flavoring chemical should be evaluated using comparable heating temperatures of e-cigarette (i.e. 200-300 ˚C).

REFERENCES

[1] Arrazola, R.A., et al., *Tobacco use among middle and high school students-United States, 2011-2014.* MMWR. Morbidity and mortality weekly report, 2015. **64**(14): p. 381-385.

[2] Schoenborn, C.A. and R.M. Gindi, *Electronic cigarette use among adults: United States, 2014.* NCHS data brief, 2015. **217**: p. 1-8.

[3] Goniewicz, M.L., et al., *Levels of selected carcinogens and toxicants in vapour from electronic cigarettes.* Tobacco control, 2014. **23**(2): p. 133-139.

[4] Tierney, P.A., et al., *Flavour chemicals in electronic cigarette fluids.* Tobacco control, 2015: p. tobaccocontrol-2014-052175.

[5] Goel, R., et al., *Highly reactive free radicals in electronic cigarette aerosols.* Chemical Research in Toxicology, 2015. **28**(9): p. 1675-1677.

[6] Lerner, C.A., et al., *Vapors produced by electronic cigarettes and e-juices with flavorings induce toxicity, oxidative stress, and inflammatory response in lung epithelial cells and in mouse lung.* PloS one, 2015. **10**(2).

[7] Pryor, W.A., et al., *Fractionation of aqueous cigarette tar extracts: fractions that contain the tar radical cause DNA damage.* Chemical research in toxicology, 1998. **11**(5): p. 441-448.

[8] Ciencewicki, J., S. Trivedi, and S.R. Kleeberger, *Oxidants and the pathogenesis of lung diseases.* Journal of Allergy and Clinical Immunology, 2008. **122**(3): p. 456-468.

[9] Halliwell, B. and J.M. Gutteridge, *Free radicals in biology and medicine*. Vol. 3. 1999: Oxford university press Oxford.

[10] Zhao, T., et al., *Effects of design parameters and puff topography on heating coil temperature and mainstream aerosols in electronic cigarettes.* Atmospheric Environment, 2016. **134**: p. 61-69.

[11] Ayres, J.G., et al., *Evaluating the toxicity of airborne particulate matter and nanoparticles by measuring oxidative stress potential - A workshop report and consensus statement.* Inhalation Toxicology, 2008. **20**(1): p. 75-99.

[12] Levent, A., Y. Yardim, and Z. Senturk, *Voltammetric behavior of nicotine at pencil graphite electrode and its enhancement determination in the presence of anionic surfactant.* Electrochimica Acta, 2009. **55**(1): p. 190-195.

[13] Mourtzinos, I., et al., *Thermal oxidation of vanillin affects its antioxidant and antimicrobial properties.* Food Chemistry, 2009. **114**(3): p. 791-797.

[14] ELiquidRecipes. *e-Liquid Recipes*. 2017 [cited 2017 May 31]; Available from: http://e-liquid-recipes.com/.

[15] Dautzenberg, B. and D. Bricard, *Real-Time Characterization of E-Cigarettes Use: The 1 Million Puffs Study.* Journal of Addiction Research & Therapy, 2015. **2015**.

[16] Meng, Q., et al., *Has the mist been peered through? Revisiting the building blocks of human health risk assessment for electronic cigarette use.* Human and Ecological Risk Assessment: An International Journal, 2016. **22**(2): p. 558-579.

[17] Norton, K.J., K.M. June, and R.J. O'Connor, *Initial puffing behaviors and subjective responses differ between an electronic nicotine delivery system and traditional cigarettes.* Tobacco induced diseases, 2014. **12**(1): p. 17.

[18] Robinson, R., et al., *Electronic cigarette topography in the natural environment.* PloS one, 2015. **10**(6): p. e0129296.

[19] Spindle, T.R., et al., *Preliminary results of an examination of electronic cigarette user puff topography: The effect of a mouthpiece-based topography measurement device on plasma nicotine and subjective effects.* Nicotine & Tobacco Research, 2014: p. ntu186.

[20] Hua, M. and P. Talbot, *Potential health effects of electronic cigarettes: a systematic review of case reports.* Preventive medicine reports, 2016. **4**: p. 169-178.

[21] Misthub. *Tutorial: Variable Voltage and Vaping Power Chart*. 2013 [cited 2017 Oct 30]; Available from: https://www.misthub.com/blogs/vape-tutorials/76788421-tutorial-variable-voltage-and-vaping-power-chart.

[22] Son, Y., et al., *A Novel High-Throughput Approach to Measure Hydroxyl Radicals Induced by Airborne Particulate Matter.* International journal of environmental research and public health, 2015. **12**(11): p. 13678-13695.

[23] van der Vliet, A., et al., *Determination of low-molecular-mass antioxidant concentrations in human respiratory tract lining fluids.* American Journal of Physiology-Lung Cellular and Molecular Physiology, 1999. **276**(2): p. L289-L296.

[24] Talih, S., et al., *Effects of user puff topography, device voltage, and liquid nicotine concentration on electronic cigarette nicotine yield: measurements and model predictions.* Nicotine & Tobacco Research, 2015. **17**(2): p. 150-157.

[25] Lin, Y.-C., *Catalytic valorization of glycerol to hydrogen and syngas.* international journal of hydrogen energy, 2013. **38**(6): p. 2678-2700.

[26] Jensen, R.P., R.M. Strongin, and D.H. Peyton, *Solvent chemistry in the electronic cigarette reaction vessel.* Scientific Reports, 2017. **7**: p. 42549.

[27] Barker-Hemings, E., et al., *A detailed kinetic study of pyrolysis and oxidation of glycerol (propane-1, 2, 3-triol).* Combustion Science and Technology, 2012. **184**(7-8): p. 1164-1178.

[28] Singh, G., S. Maurya, and C.A. Catalan, *A comparison of chemical, antioxidant and antimicrobial studies of cinnamon leaf and bark volatile oils, oleoresins and their constituents.* Food and chemical toxicology, 2007. **45**(9): p. 1650-1661.

[29] Yaylayan, V., et al., *Oxidative pyrolysis and postpyrolytic derivatization techniques for the total analysis of Maillard model systems: investigation of control parameters of Maillard reaction pathways.* Annals of the New York Academy of Sciences, 2005. **1043**(1): p. 41-54.

[30] Jamal, A., et al., *Current cigarette smoking among adults-United States, 2005–2015.* MMWR. Morbidity and mortality weekly report, 2016. **65**.

[31] Church, D.F. and W.A. Pryor, *Free-radical chemistry of cigarette smoke and its toxicological implications.* Environmental health perspectives, 1985. **64**: p. 111.

[32] Sussan, T.E., et al., *Exposure to Electronic Cigarettes Impairs Pulmonary Anti-Bacterial and Anti-Viral Defenses in a Mouse Model.* PloS one, 2015. **10**(2): p. e0116861.

[33] Anderson, C., et al., *E-cigarette aerosol exposure induces reactive oxygen species, DNA damage, and cell death in vascular endothelial cells.* Toxicological Sciences, 2016: p. kfw166.

[34] Rouabhia, M., et al., *E-Cigarette Vapor Induces an Apoptotic Response in Human Gingival Epithelial Cells Through the Caspase-3 Pathway.* Journal of Cellular Physiology, 2017. **232**(6): p. 1539-1547.

[35] Yu, V., et al., *Electronic cigarettes induce DNA strand breaks and cell death independently of nicotine in cell lines.* Oral oncology, 2016. **52**: p. 58-65.

[36] Pryor, W.A., *Why is the hydroxyl radical the only radical that commonly adds to DNA? Hypothesis: it has a rare combination of high electrophilicity, high thermochemical reactivity, and a mode of production that can occur near DNA.* Free Radical Biology and Medicine, 1988. **4**(4): p. 219-223.

[37] Thorne, D., et al., *The comparative in vitro assessment of e-cigarette and cigarette smoke aerosols using the γH2AX assay and applied dose measurements.* Toxicology Letters, 2017. **265**: p. 170-178.

[38] Taylor, M., et al., *E-cigarette aerosols induce lower oxidative stress in vitro when compared to tobacco smoke.* Toxicology Mechanisms and Methods, 2016. **26**(6): p. 465-476.

[39] Giovenco, D.P., et al., *E-cigarette market trends in traditional US retail channels, 2012–2013.* Nicotine & Tobacco Research, 2015. **17**(10): p. 1279-1283.

[40] Corey, C.G., et al., *Flavored tobacco product use among middle and high school*

students—United States, 2014. MMWR Morb Mortal Wkly Rep, 2015. **64**(38): p. 1066-1070.

[41] Moses, E., et al., *Molecular impact of electronic cigarette aerosol exposure in human bronchial epithelium.* Toxicological Sciences, 2017. **155**(1): p. 248-257.

[42] Jeong, S.-M., et al., *Effect of heat treatment on the antioxidant activity of extracts from citrus peels.* Journal of agricultural and food chemistry, 2004. **52**(11): p. 3389-3393.

CHAPTER 5

CARBONYLS EMITTED FROM THE E-CIGARETTE

5.1. INTRODUCTION

Carbonyl compounds are the most abundant toxic chemicals emitted from electronic cigarettes (e-cigarette) [1-4]. However, factors affecting carbonyl emissions from e-cigarettes are still largely unknown. Most current studies report that higher e-cigarette power outputs significantly increase formaldehyde and acetaldehyde emissions [5-11]. However, there is a 1,000-fold difference across the literature in formaldehyde emission data from e-cigarette at comparable e-cigarette device power outputs [6-8], suggesting that carbonyl emissions are not dependent on e-cigarette power output alone.

Flavoring agents used in e-liquids could be sources of carbonyl emission. Thermal fragmentation of flavoring chemicals has been shown to form carbonyls under the burning temperatures of conventional cigarette [12], but the contribution of flavoring chemicals to carbonyl emission has not been well studied for e-cigarettes. In addition, some toxic flavoring chemicals [e.g. 2,3-Butanedione (diacetyl) and 2,3-Pentanedione (acetylpropionyl)] in e-vapor need to be quantified under real-world e-cigarette use patterns [13-16].

The contribution of e-liquid base materials on carbonyl emissions is also largely unknown. It has been shown that thermal degradation of vegetable glycol (VG) and propylene glycol (PG) generates various carbonyl compounds [9, 17]. However, the thermal degradation of VG and PG has not been studied at a wide range of e-cigarette coil temperatures [8, 10]. This is a problem as coil temperatures are important determinant of e-cigarette carbonyl emission.

E-cigarette vaping topography could also potentially affect carbonyl formation. Vaping topography can affect carbonyl emissions by modifying e-cigarette heating coil temperature [18]. However, most of the previous studies generated e-vapors under the ‘Health Canada Intense (HCI) Regime’ (55 ml puff volume, 2 seconds puff duration, every 30 seconds), which was

developed for conventional cigarette smokers and not e-cigarette vapors [6, 7, 9, 19]. Real-world vaping topography should be used to study carbonyl emissions. In addition, most of the preceding studies only focused on formaldehyde and acetaldehyde emissions. However, other potentially harmful carbonyl compounds, such as acrolein and glyoxal, in e-vapor also need to be evaluated under real-world vaping conditions.

To address the knowledge gaps, this study evaluated the impacts of real-world vaping conditions (i.e. real-world e-cigarette heating power, vaping topography, and e-liquid components) on the emission of six potentially harmful carbonyls (i.e. glyoxal, formaldehyde, acetaldehyde, acrolein, diacetyl, and acetylpropionyl) and thirteen additional carbonyl species.

5.2. MATERIAL AND METHODS

5.2.1. E-cigarettes and E-liquids

The versatile refillable tank type e-cigarette used in this study consisted of an adjustable air hole (1, 1.5, and 2 mm diameters) and replaceable Nichrome heating coils (dual-bottom coils with 0.8, 1.2, and 2.0 Ω), and was obtained from a e-cigarette retailer (The Council of Vapor, Walnut, CA, USA). Two types of battery boxes, an Apollo Valiant battery (Apolo E-cigarette, Concord, CA, USA) and a Sigelei-100W battery (Sigelei US, Pomona, CA, USA), were used to provide a wide range of power output from 3 to 80 watts.

Freshly prepared e-liquids from our lab were used in all experiments for quality control purposes [20]. E-liquids used in our study were composed of vegetable glycol (VG, USP grade, J.T. Baker, Phillipsburg, NJ, USA), propylene glycol (PG, USP grade, Sigma-Aldrich, St. Louis, MO, USA), (-)-nicotine (≥99.0%, Sigma-Aldrich, St. Louis, MO, USA), and flavoring agents (The Perfumer's Apprentice, Scotts Valley, CA, USA). The selected flavoring agents were strawberry, dragon fruit, menthol, sweet cream, Bavarian, cinnamon, bubble gum, and graham cracker flavor. The eight flavoring agents were the most frequently used ones in e-liquid recipes on the market [21].

5.2.2. E-vapor Generation Conditions

We measured vaping topographies from 23 current e-cigarette users using a CReSS Pocket device (Borgwaldt KC Incorporated, North Chesterfield, VA, USA) with the approval of the Rutgers' IRB. Demographics of the study participants are summarized in the supplemental information in Table S2-1. The observed vaping topographies, device settings, and e-liquid compositions were tabulated in the supplemental information in Table S2-2.

Throughout the experiments, the median values of the observed power output (6.4 watts), puff volume (90 ml) and puff duration (3.8 seconds) were used. The selected vaping topography was consistent with the median value of the reported e-cigarette vaping topographies, which was

91 ml puff volume (ranging from 51 to 133 ml) and 3.8 seconds puff duration (ranging from 2.65 to 4.3 seconds) [16, 22-28].

A variety of e-liquids were prepared to assess the impact of e-liquid composition on carbonyl formation. Three base materials, 100% VG, PG:VG mixture (v/v=1:1), and 100% PG e-liquids, containing 12 mg/ml nicotine was tested to evaluate the impact of e-liquid base material on carbonyl formation. Then, eight flavored e-liquids (strawberry, dragon fruit, menthol, sweet cream, Bavarian, cinnamon, bubble gum, and graham cracker) were used to generate e-vapors to evaluate the impact of flavoring agents on carbonyl formation. The flavored e-liquids in the experiments consisted of 10% of flavoring agents (1% for the cinnamon flavor) in VG.

To test the impact of device power output and vaping topography on carbonyl emission, the average and the 95% of the observed device power outputs (14.7 watts and 31.3 watts) and 95% of observed puff volume (170 ml) from the 23 subjects were used for e-vapor generation. The wide ranges of experimental conditions reflected real-world vaping conditions.

5.2.3. Carbonyl Collection and Analysis

The sampling and analytical protocols for carbonyl measurements were developed based on the U.S. EPA compendium method OA-11A [29]. In brief, the sampling system was composed of a LXe1 smoking machine (Borgwaldt KC Incorporated, Hamburg, Germany), a sampling chamber, a 2,4-dinitrophenylhydrazine (DNPH) cartridge (Waters, Milford, MA, USA), and a vacuum pump (Figure S5-1). E-vapors were generated using the smoking machine under the experimental conditions as described above (and specified Table S5-1). The generated e-vapors were directly introduced into the 2 L sampling chamber. The inlet of the DNPH cartridge was connected with the sampling chamber, and 30 puffs of e-vapor were collected using the DNPH cartridge with a sampling flow rate of 200 ml/min. After sampling, both ends of the DNPH cartridge were sealed and the cartridge was stored in an aluminum zip lock at 4 °C until analysis.

The sampled DNPH cartridges were then eluted with 4 mL of acetonitrile (ACN), and 20 μL

of the eluted DNPH-aldehyde derivatives were injected into the HPLC/UV system which was equipped with a Waters Nova-Pak C18 column (Waters, Milford, MA, USA). The mobile phase was programmed as follows: after holding 100% of solvent A (H_2O/ACN/THF (tetrahydrofuran) = 6/3/1) for 4 minutes, the mobile phase changed to 100% solvent B (ACN/H_2O = 6:4) over 20 minutes, then 100% solvent B was held for 10 minutes. The flow rate of the mobile phase was set constant at 1 mL/min and the UV detector was set at an absorbance wavelength of 365 nm.

Calibration curves for the nineteen carbonyls were prepared using purchased DNPH-aldehyde analytical standards (ResTek, Bellefonte, PA, USA) and five standards prepared in our lab (Table 5-1). For preparation of the five carbonyl standard samples, glyoxal (40%) and Vanillin (99%) was obtained from Sigma-Aldrich (St. Louis, MO, USA). Cinnamaldehyde (≥98), diacetyl (99%), and acetylpropionyl (97%) were purchased from Alfa Aesar (Haverhill, MA, USA). Then, the carbonyl standard samples were spiked into the DNPH cartridge. Limits of detection (LOD) and limits of quantification (LOQ) were three and ten times the standard deviations of the standard with the lowest concentration (n=7).

Table 5-1. Retention times, calibration parameters, LODs, and LOQs for the selected carbonyls

Chemical	Time (min)	Range (ng/µl)	Calibration parameter[†]		R^2	LOD (ng/30 puff)[††]	LOQ (ng/30 puff)[††]
			a	b			
Glyoxal	4.4	0.1-10.0	3.712×10^{-6}	0.1127	0.9982	49.6	165.
Formaldehyde	4.9	0.1-20.0	3.417×10^{-6}	0.1052	0.9981	31.1	104.
Acetaldehyde	7.3	0.1-10.0	4.796×10^{-6}	0.1351	0.9990	22.4	74.8
Diacetyl	8.3	0.1-10.0	1.654×10^{-6}	0.0981	0.9981	11.1	36.9
Acetone	10.8	0.1-10.0	6.131×10^{-6}	0.0931	0.9947	25.8	86.1
Vanillin	12.0	0.1-10.0	6.888×10^{-6}	0.2507	0.9967	4.58	15.3
Acrolein	11.5	0.1-10.0	5.276×10^{-6}	0.1753	0.9957	10.9	36.3
Propionaldehyde	12.8	0.1-10.0	4.655×10^{-6}	0.3606	0.9912	4.32	14.4
Acetylpropionyl	13.7	0.1-10.0	1.828×10^{-6}	0.2324	0.9944	8.61	28.7
Crotonaldehyde	15.8	0.1-10.0	6.869×10^{-6}	0.1955	0.9965	5.19	17.3
n-Butylaldehyde	17.7	0.1-10.0	6.744×10^{-6}	0.4268	0.9896	14.9	49.6
Benzaldehyde	20.1	0.1-10.0	1.002×10^{-5}	0.2561	0.9970	8.58	28.6
Isovaleraldehyde	22.0	0.1-10.0	1.045×10^{-5}	0.0960	0.9943	4.77	15.9
n-Valeraldehyde	22.8	0.1-10.0	7.352×10^{-6}	0.5103	0.9833	3.03	10.1
o-Tolualdehyde	24.3	0.1-10.0	1.778×10^{-5}	0.2090	0.9947	5.04	16.8
p-Tolualdehyde	24.9	0.1-10.0	4.480×10^{-6}	0.4780	0.9858	6.32	21.1
Cinnamaldehyde	25.7	0.1-10.0	1.642×10^{-5}	0.1297	0.9960	8.11	27.0
n-Hexaldehyde	28.0	0.1-10.0	1.591×10^{-5}	0.0620	0.9976	16.6	55.2
Dimethylbenzaldehyde	28.8	0.1-10.0	1.248×10^{-5}	0.1502	0.9829	0.36	1.19

[†] a and b indicates slope and intercept of the calibration equation, respectively
[††] LOD and LOQ were three and ten times standard deviation of 0.1 ng/µl sample (n=7), respectively

5.3. RESULTS AND DISCUSSION

5.3.1. The Impact of E-liquid Base Materials and Power Outputs

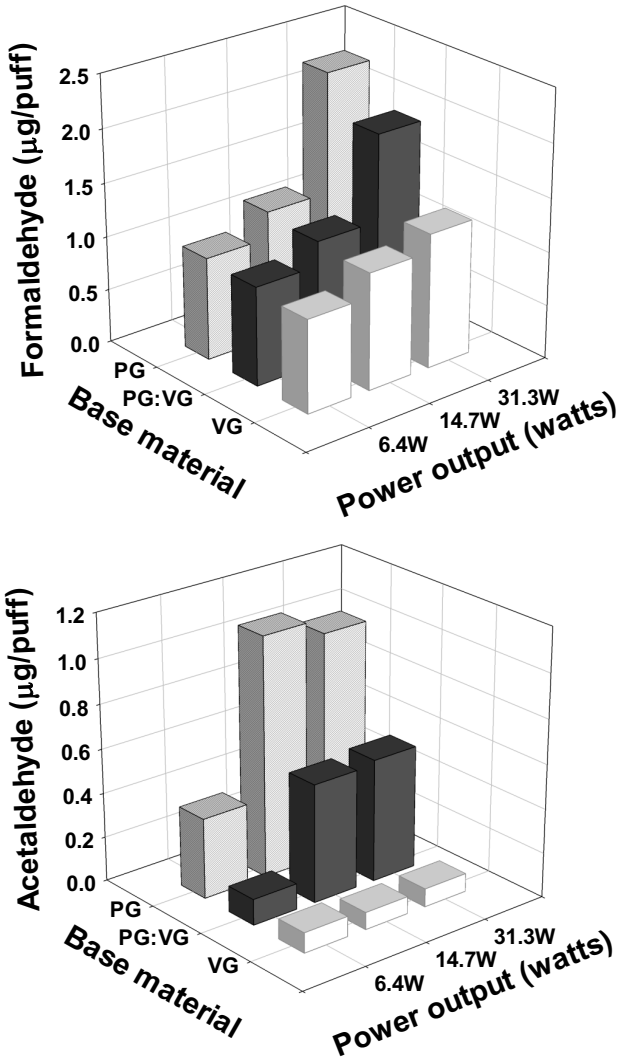

Figure 5-1. Formaldehyde (upper panel) and acetaldehyde (lower panel) concentrations (µg/puff) generated by different base materials (100% PG, PG:VG 1:1 (v/v), and 100% VG) and device power outputs (watt). 90 ml puff volume, 3.8 sec puff duration, and 24 sec puff interval was used as vaping topography, and 12 mg/ml nicotine was added into all e-liquids

Figure 5-1 shows the impact of e-cigarette power output and the base material on the emission of formaldehyde and acetaldehyde, which are carcinogenic carbonyls found in e-vapor. Higher device power outputs increased formaldehyde emissions from all three base materials.

The amount of formaldehyde generated at 31.3 watts were 39.3%, 111.0%, and 142.1% higher than the amounts of formaldehyde generated at 6.4 watts for VG, PG:VG, and PG based e-liquids, respectively. At 31.3 watts e-cigarette power output, PG:VG and PG based e-liquids generated 57.8% and 86.9% more formaldehyde than VG based e-liquids (p-value < 0.003, t-test).

PG-based e-liquids generated significantly higher amounts of acetaldehyde than VG-based e-liquids. PG:VG mixture (v:v=1:1) and PG based e-liquids generated 2.7 and 8.5 times more acetaldehyde than VG based e-liquids at 6.4 watts power output condition (p-value < 0.001, t-test). The increase in e-cigarette power output from 6.4 watts to 31.1 watts increased acetaldehyde formation by a factor of 3.0-4.6 (p-value < 0.001, t-test).

In addition to formaldehyde and acetaldehyde, higher power output also generated other harmful carbonyls (Table 5-2). We observed 240±13.7 ng/puff of glyoxal generated from VG-based e-liquids at 31.3 watts. It has been reported that thermal oxidation of VG leads to the formation of glyoxal [9]. Compared with 6.4 watts conditions, 31.3 watts generated 2 times larger amount of acrolein, n-butylaldehyde and isovaleraldehyde (p-value < 0.001, t-tests).

To the best of our knowledge, this is the first study to present the carbonyl formations using the various combinations of base materials and device power outputs. Thermal decomposition of the VG and PG forms carbonyls during the e-cigarette vaping [17], and increased coil temperatures accelerate the decomposition rates of e-liquid base materials [30]. PG may form higher levels of carbonyl compounds (e.g. formaldehyde, acetaldehyde, butylaldehyde, tolualdehyde) during e-cigarette vaping than VG, because PG is prone to the thermal decomposition. The thermal decomposition of PG starts as low as 127 ˚C [31], while VG requires at least 200 ˚C to begin the reaction [32]. Kosmider and Sobczak [8] also reported that PG-containing e-liquids generated significantly higher amounts of formaldehyde and acetaldehyde than VG based e-liquids.

Table 5-2. Impact of power outputs and base materials on carbonyl concentrations in e-vapor (mean ± standard deviation, n=5)

Carbonyl	Unit	Base material and power output (watts)[†]								
		VG			PG:VG (v:v=1:1)			PG		
		6.4W	14.7W	31.3W	6.4W	14.7W	31.3W	6.4W	14.7W	31.3W
Glyoxal	ng/puff	ND	ND	240.±13.7	ND	ND	ND	ND	ND	ND
Formaldehyde	µg/puff	0.903±0.0562	1.10±0.0920	1.26±0.127	0.927±0.0474	1.15±0.0653	1.96±0.348	0.957±0.0288	1.20±0.0824	2.32±0.0419
Acetaldehyde	µg/puff	0.0917±0.0181	0.0778±0.044	0.0825±0.0360	0.117±0.0104	0.534±0.0584	0.553±0.0853	0.362±0.0742	1.09±0.0883	1.02±0.0611
Acetone	ng/puff	<LOD	ND	<LOD	<LOD	ND	ND	<LOD	ND	<LOD
Acrolein	ng/puff	<LOQ	<LOQ	252.±51.9	42.6±6.55	29.2±7.81	199.±14.8	67.3±14.8	97.5±62.5	209.±89.6
Propionaldehyde	ng/puff	ND	ND	ND	ND	ND	ND	ND	ND	24.0±3.74
Crotonaldehyde	ng/puff	29.8±6.02	ND	17.7±0.08	ND	ND	33.6±4.4	ND	ND	54.0±12.3
n-Butylaldehyde	ng/puff	ND	ND	156.±7.82	ND	93.1±28.1	402.±16.9	25.5±2.2	28.4±2.9	423.±9.34
Benzaldehyde	ng/puff	23.1±12.4	ND	27.7±1.75	ND	ND	31.2±2.69	ND	ND	31.3±2.82
Isovaleraldehyde	ng/puff	ND	ND	68.1±13.5	ND	ND	137.±8.21	ND	ND	86.4±44.3
n-Valeraldehyde	ng/puff	81.1±19.4	ND	70.7±20.0	ND	53.4±13.3	ND	ND	ND	ND
o-Tolualdehyde	ng/puff	ND	ND	ND	ND	ND	198.±15.0	42.0±3.80	ND	329.±68.4
p-Tolualdehyde	ng/puff	18.1±1.63	ND	ND	ND	ND	ND	ND	ND	ND
n-Hexaldehyde	ng/puff	248.±65.1	563.±142.	ND	ND	54.0±4.49	ND	ND	130.±34.8	ND
Dimethyl-benzaldehyde	ng/puff	ND	ND	ND	ND	ND	31.4±4.03	ND	ND	35.8±3.77

[†] 1.5 mm air hole, 12 mg/ml nicotine, and 90 ml puff volume, 3.8 sec puff duration and 24 sec puff interval used

[††] ND indicates non-detected

[†††] <LOD indicates the measurement which is below the detection limit

[††††] <LOQ indicates the measurement which is below the quantification limit

Table 5-3. Impact of flavoring agents on carbonyl concentrations in e-vapor (mean ± standard deviation, n=5)

Carbonyl	Unit	Flavoring agents (10% by volume, 1% for cinnamon flavor in VG-base)†							
		Strawberry	Dragon Fruit	Menthol	Cinnamon	Bavarian cream	Sweet cream	Bubble gum	Grahamcracker
Glyoxal	ng/puff	ND	ND	ND	ND	ND	ND	ND	ND
Formaldehyde	µg/puff	1.26±0.116	1.18±0.035	0.951±0.0501	0.672±0.195	0.624±0.0164	0.607±0.0421	0.703±0.0238	0.486±0.0711
Acetaldehyde	ng/puff	49.0±21.4	30.5±1.24	30.4±1.96	<LOQ	<LOQ	<LOQ	30.2±2.35	<LOQ
Diacetyl	ng/puff	ND	ND	ND	ND	21.1±11.7	86.4±2.89	ND	34.9±16.8
Acetone	ng/puff	<LOD	<LOD	<LOQ	<LOD	ND	ND	ND	<LOD
Acrolein	ng/puff	28.4±8.92	20.9±5.99	20.3±1.81	29.0±5.55	ND	ND	19.5±4.18	131.±21.9
Vanillin	ng/puff	ND	ND	ND	ND	177.±60.1	179.±65.8	45.2±3.15	184.±27.0
Propionaldehyde	ng/puff	ND	ND	ND	ND	ND	ND	ND	ND
Acetylpropionyl	ng/puff	ND	ND	ND	ND	ND	ND	ND	ND
Crotonaldehyde	ng/puff	32.5±1.65	ND	ND	29.8±3.86	ND	19.0±0.41	ND	ND
n-Butylaldehyde	ng/puff	ND	29.4±4.71	28.9±4.01	ND	ND	ND	27.3±4.81	ND
Benzaldehyde	ng/puff	29.2±2.95	31.3±5.48	30.4±5.41	27.8±2.47	26.8±0.58	ND	27.6±2.55	25.0±2.71
Isovaleraldehyde	ng/puff	16.8±1.57	ND	ND	17.3±0.85	33.6±3.73	24.4±6.12	ND	ND
n-Valeraldehyde	ng/puff	24.1±3.65	ND	ND	25.3±6.08	19.7±1.91	17.2±0.14	18.9±1.55	ND
o-Tolualdehyde	ng/puff	ND	29.3±5.37	32.1±4.65	26.1±7.87	ND	60.5±2.34	62.3±13.6	ND
p-Tolualdehyde	ng/puff	18.9±1.74	ND	17.7±0.37	ND	74.2±9.65	51.4±3.22	ND	ND
Cinnamaldehyde	ng/puff	ND	ND	ND	473.±234.	ND	ND	ND	ND
n-Hexaldehyde	ng/puff	206.±7.54	179.±36.9	139.±15.5	160.±35.9	ND	ND	155.±3.28	ND
Dimethyl-benzaldehyde	ng/puff	ND	ND	ND	ND	ND	ND	ND	ND

† 6.4W power output, 1.5 mm air hole, 90 ml puff volume, 3.8 sec puff duration, and 24 sec puff interval used

†† ND indicates non-detected

††† <LOD indicates the measurement which is below the detection limit

†††† <LOQ indicates the measurement which is below the quantification limit

5.3.2. The Impact of E-liquid Flavors

Carbonyl compounds generated from flavored e-liquids are tabulated in Table 5-3. The fruit-flavored e-liquids (i.e. strawberry and dragon fruit) generated 1.7-2.6 times higher amounts of formaldehyde than spicy (cinnamon), and creamy/sweet (Bavarian cream, sweet cream, bubble gum, and graham cracker) flavored e-liquids. Acetaldehyde generated from the flavored e-liquids were below or similar to the quantification limit. The Graham cracker flavor generated the highest amount of acrolein, while other flavored e-liquids generated trace or non-detectable amount of acrolein.

The reasons for the differential carbonyl formation patterns across different flavoring agents are not completely understood, because flavor manufacturers usually do not disclose the ingredients [33]. Based on partially revealed information by the vendor (The Perfumer's Apprentice, Scotts Valley, CA, USA), the flavoring agents consist of PG, water, ethyl alcohol, and natural/artificial flavoring chemicals. PG in flavoring agents might contribute to formaldehyde formation (see results reported in Section 5.3.1). However, further studies of thermal degradation of flavoring chemicals are warranted to better understand the contribution of flavoring agents on carbonyl formation.

Diacetyl and acetylpropionyl are the 'butter' flavoring chemicals and are known to increase airway injury (aka 'popcorn lung') [13]. Three flavored e-vapor samples (i.e. Bavarian cream, sweet cream and graham cracker flavors) contained 21.1-86.4 ng/puff of diacetyl, but acetylpropionyl was not detected in any sample. Diacetyl concentrations observed in our samples are comparable to those reported in previous studies [28, 34]. Based on the diacetyl concentrations we measured, and assuming 200 puffs/day of e-cigarette vaping and 20 m^3/day of air inhalation, the observed diacetyl levels in our study were at least 90-fold lower than the NIOSH reference exposure level (18 $\mu g/m^3$). .

Four flavored e-liquids (i.e. Bavarian cream, sweet cream, bubble gum, and graham cracker flavors) contained 45.2-184.4 ng/puff of vanillin, and cinnamaldehyde (473.1±234.9 ng/puff) was

detected only in the cinnamon flavored e-vapor. An *in vitro* study demonstrated that vanilla and cinnamon flavored e-liquids had three and ten-fold lower no-observable-adverse-effect-level (NOAEL) doses (0.1-0.01% dose) than VG only e-liquid (0.3% in culture media), respectively [15]. The cytotoxicity of cinnamaldehyde (IC_{50}=0.037-0.04 mM) was approximately 100 times higher than vanillin (IC_{50}=2.5-4 mM) [16].

5.3.3. E-cigarette coil settings affect carbonyl formation

The reported e-vapor formaldehyde concentrations have been shown to range from 1.8 µg/puff to 34.5 µg/puff for 9.6-10 watts device power outputs and PG:VG mixed e-liquids [8, 35]. The wide range of formaldehyde concentration might be affected by the coil settings [7].

Figure 5-2 illustrates formaldehyde concentrations for different coil types, device power outputs, and base materials [6-8, 35]. The single-top coils formed 3.5-fold more formaldehyde per puff than conventional cigarette smoking due to the limited e-liquid supply to the heating coil. A top coil is located on the top of the atomizer with long wicks dropping down into the e-liquid tank. A long wick cannot supply enough e-liquid to the coil, and the limited e-liquid supply can easily dry up the heating coil, leading to a rapid coil temperature increase. The dramatic increase of coil temperature is known as ‘dry puff’ or ‘dry hit’, which results in significantly increased amounts of carbonyl formation [35].

In contrast, a bottom coil is located at the bottom of the atomizer, with a short wick contacting with the e-liquid. Bottom-coils, commonly used in the up-to-date generations of e-cigarettes, generally provide consistent hits without ‘dry puffs’. Consequently, a bottom coil generated 10-10,000 times less formaldehyde per puff than conventional cigarettes due to the stable e-liquid supply rate and coil temperature. Gillman and Kistler [7] stated that e-cigarette devices with steady e-liquid supplies to the coil generated the lowest amount of formaldehyde.

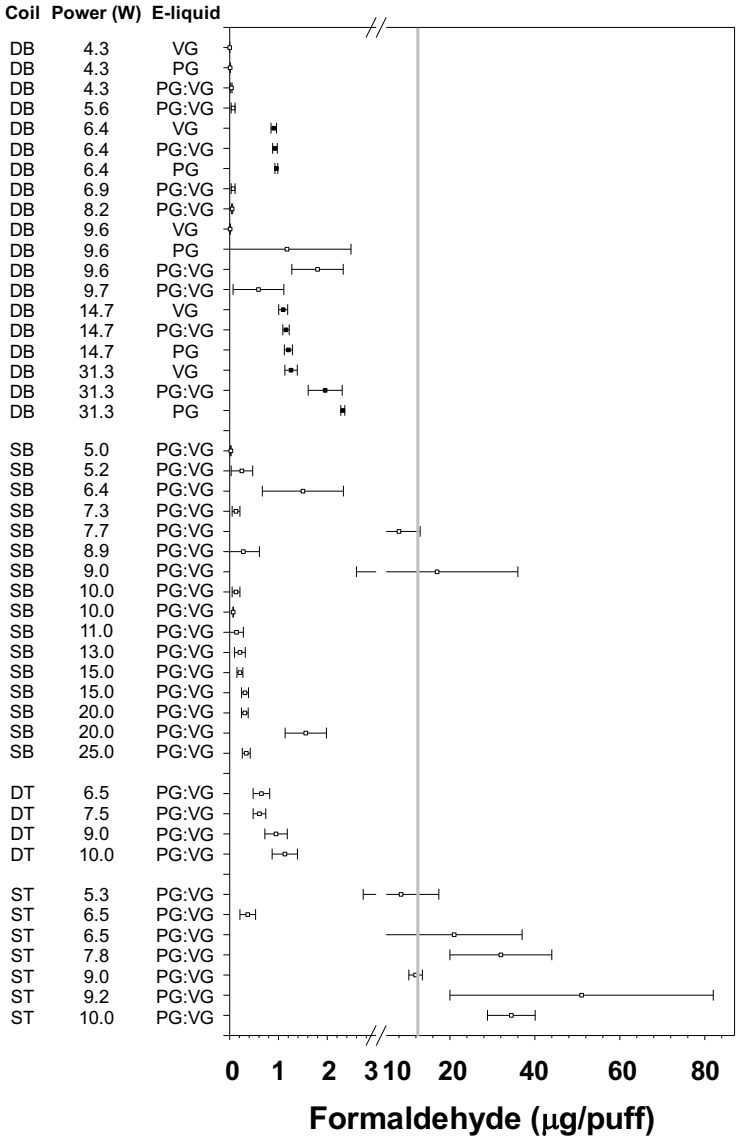

Figure 5-2. Formaldehyde concentrations (mean and standard deviation) for the four different coil types, power outputs (watts), and e-liquid base materials. DB, SB, DT, and ST indicate dual-bottom, single-bottom, dual-top, and single-top coil, respectively. Black squares indicate our results, and white squares are the results obtained from Farsalinos et al. [35], Geiss et al. [6], Gillman et al. [7], and Kosmider et al. [8]. The grey line is the formaldehyde concentration of conventional cigarette smoke (Fujioka and Shibamoto [36]

Table 5-4. Impact of vaping topography on carbonyl concentrations in e-vapor (mean ± standard deviation, ng/puff)

Carbonyl	Puff volume and duration[†]					
	35ml		90ml		170ml	
	2sec	3.8sec	2sec	3.8sec	2sec	3.8sec
	n=3	n=3	n=3	n=5	n=3	n=3
Glyoxal	ND	ND	ND	ND	ND	ND
Formaldehyde	683.±32.3	730.±53.8	790.±32.3	903.±56.2	747.±47.2	867.±32.7
Acetaldehyde	41.0±9.35	39.9±4.35	<LOQ	91.7±18.1	<LOQ	47.1±1.14
Acetone	<LOQ	<LOD	<LOQ	<LOD	<LOQ	<LOD
Acrolein	17.6±1.32	32.0±1.81	32.7±1.27	<LOQ	28.9±0.52	38.1±1.52
Propionaldehyde	ND	ND	ND	ND	ND	ND
Crotonaldehyde	56.4±3.82	34.9±28.9	40.8±0.56	29.8±6.02	42.4±0.67	ND
n-Butylaldehyde	ND	ND	ND	ND	ND	37.9±1.80
Benzaldehyde	45.8±1.41	31.4±4.14	32.5±0.46	23.1±12.4	30.3±2.45	29.5±2.47
Isovaleraldehyde	ND	23.3±5.56	33.4±0.57	ND	ND	34.0±1.55
n-Valeraldehyde	32.9±12.8	ND	30.7±2.18	81.1±19.4	29.4±0.92	ND
o-Tolualdehyde	134.1±4.2	95.3±17.9	196.±4.38	ND	186.±1.11	114.±4.19
p-Tolualdehyde	17.1±0.26	21.6±3.22	17.1±0.18	18.1±1.63	17.8±0.15	20.4±1.89
n-Hexaldehyde	ND	128.±8.06	ND	248.±65.1	ND	413.±4.65
Dimethylbenzaldehyde	33.1±4.33	ND	28.4±1.02	ND	ND	ND

[†]6.4W power output, 1.5 mm air hole, VG based e-liquid containing 12 mg/ml nicotine, and 24 sec puff interval used
[††] ND indicates non-detected
[†††] <LOD indicates the measurement which is below the detection limit
[††††] <LOQ indicates the measurement which is below the quantification limit

5.3.4. The Impact of Vaping Topography

Puff volume and puff duration significantly changed carbonyl concentrations in e-vapor (Table 5-4). An increase in puff volume from 35 ml to 90 ml lead to 15.6% and 23.8% higher amounts of formaldehyde formation for 2 seconds and 3.8 seconds puffs, respectively (p-value < 0.016, t-tests). In general, longer puff durations generated significantly higher amounts of formaldehyde.

The puff volume and puff duration determine the volume of air and the flow rate passing through the e-cigarette heating coil. Increased puff volume with a fixed puff duration were shown not only to increase the amount of e-vapor passing through but also to decrease the heating coil temperatures due to increased flow rate [18]. The significant difference between 35 ml and 90 ml puff volume observed in our study might be due to the increased e-vapor mass, but the carbonyl composition might be affected by coil temperature changes. The lower heating coil temperature under the higher air flow regimes might decrease the thermal degradation of the base materials resulting in the observed differences in carbonyl formation.

The vaping topographies used in most recent e-cigarette studies did not reflect the real-world vaping conditions, as the puff volumes used in previous studies were usually much lower than that of the e-cigarette users as explained in the method section. In addition, the short puff durations used in previous studies (≤ 2 seconds) might be insufficient to heat up the heating coil to evaporate e-liquid [18].

5.3.5. Significant Public Health Implications

For the first time, we systematically evaluated the impact of e-liquid base materials, flavorings, and device settings on e-vapor carbonyl formations. Carbonyl exposures associated with e-cigarette vaping were significantly lower than that associated with conventional cigarette smoking. Formaldehyde, acetaldehyde, acrolein, diacetyl, and glyoxal concentrations of the conventional cigarette smoke were reported to be 14.5±0.738, 176.±3.73, 36.5±1.68, 33.6±1.65,

and 0.32±0.02 μg/puff, respectively [36]. In our study, e-cigarettes generated usually 10, 400, 250, 650, and 1.5-fold lower formaldehyde, acetaldehyde, acrolein, diacetyl, and glyoxal per puff, respectively, than conventional cigarette smoke. However, e-cigarette vaping is still expected to pose potential health risks due to the non-threshold characteristics of carcinogenic carbonyls.

E-vapor and conventional cigarette smoke contain similar levels of glyoxal [9]. Glyoxal has been identified as an occupational allergen among health care workers who use glyoxal containing disinfectants [37]. An *in vitro* study showed that glyoxal depleted glutathione, increased reactive oxygen species (ROS), and induced cell damage to isolated rat hepatocytes [38]. Higher device power output could increase such glyoxal exposures which might induce airway oxidative stress.

Moreover, carbonyl compounds in e-vapor were shown to form secondary harmful chemicals. Autoxidation of acetoin, which is a safer alternative of 'butter' flavoring chemicals (i.e diacetyl and acetopropionyl), could form diacetyl during the e-liquid storage [39]. Acrylamide is a human carcinogen damaging the reproductive and endocrine system [40], and it was formed through the reaction between acrolein in e-vapor and amino acid or ammonia [41]. In addition to acetoin and acrolein, other precursor chemicals may present in e-vapor. Future research needs to study the formation of secondary air toxics induced by e-vapor.

Even though we thoughtfully identified large numbers of carbonyl compounds induced by the various e-cigarette vaping conditions, this study still has several limitations. First, the DNPH cartridges were designed for the gas phase carbonyl sampling rather than particle phase carbonyls [29]. Carbonyl collection efficiencies for the e-vapor using the DNPH cartridge might be less than the labeled efficiency for the gas phase carbonyls because carbonyls in e-vapors are reported to present in both gas and particle phase [9]. Second, our analytical method might underestimate unsaturated aldehydes and ketones. Unsaturated carbonyls, such as acrolein, crotonaldehyde, and cinnamaldehyde, and DNPH adducts could further react with additional DNPH to form side products [42]. Further studies also need to test other carbonyl sampling methods such as N-

Methyl-4-hydrazino-7-nitrobenzofurazan (MNBDH), 4-(2-aminooxyethyl)-morpholin-4-ium chloride (AMAH) or DNPH-hydroquinone methods.

In conclusion, various carbonyl compounds were explored under different vaping conditions, and higher carbonyl levels were expected for PG e-liquid, higher power output, and top coil setting. PG-based e-liquid under 31.3W generated approximately 2.6, 11.2, and 200-fold higher formaldehyde, acetaldehyde, and acrolein than VG e-liquid under 6.4W. High power output generated glyoxal, acrolein, and butylaldehyde. Diacetyl, vanillin, and cinnamaldehyde were identified from the flavored e-liquids. In addition, flavored e-liquids changed the profile of carbonyl formation but the impact of flavoring chemicals could not be well explained due to the limited information. Therefore, future studies need to evaluate the impact of flavoring chemicals on carbonyl formation and the inhalation toxicity of flavoring chemical itself.

REFERENCES

[1] Flora, J.W., et al., *Characterization of potential impurities and degradation products in electronic cigarette formulations and aerosols.* Regulatory Toxicology and Pharmacology, 2016. **74**: p. 1-11.

[2] Goniewicz, M.L., et al., *Levels of selected carcinogens and toxicants in vapour from electronic cigarettes.* Tobacco control, 2014. **23**(2): p. 133-139.

[3] Schripp, T., et al., *Does e-cigarette consumption cause passive vaping?* Indoor air, 2013. **23**(1): p. 25-31.

[4] Uchiyama, S., et al., *Determination of carbonyl compounds generated from the E-cigarette using coupled silica cartridges impregnated with hydroquinone and 2, 4-dinitrophenylhydrazine, followed by high-performance liquid chromatography.* Analytical Sciences, 2013. **29**(12): p. 1219-1222.

[5] Geiss, O., et al., *Characterisation of mainstream and passive vapours emitted by selected electronic cigarettes.* International journal of hygiene and environmental health, 2015. **218**(1): p. 169-180.

[6] Geiss, O., I. Bianchi, and J. Barrero-Moreno, *Correlation of volatile carbonyl yields emitted by e-cigarettes with the temperature of the heating coil and the perceived sensorial quality of the generated vapours.* International journal of hygiene and environmental health, 2016. **219**(3): p. 268-277.

[7] Gillman, I., et al., *Effect of variable power levels on the yield of total aerosol mass and formation of aldehydes in e-cigarette aerosols.* Regulatory Toxicology and Pharmacology, 2016. **75**: p. 58-65.

[8] Kosmider, L., et al., *Carbonyl compounds in electronic cigarette vapors—effects of nicotine solvent and battery output voltage.* Nicotine & Tobacco Research, 2014: p. ntu078.

[9] Uchiyama, S., et al., *Determination of Chemical compounds generated from Second-generation E-cigarettes using a Sorbent Cartridge followed by a Two-step Elution Method.* Analytical Sciences, 2016. **32**(5): p. 549-555.

[10] Wang, P., et al., *A Device-Independent Evaluation of Carbonyl Emissions from Heated Electronic Cigarette Solvents.* PloS one, 2017. **12**(1): p. e0169811.

[11] Ogunwale, M.A., et al., *Aldehyde Detection in Electronic Cigarette Aerosols.* ACS omega, 2017. **2**(3): p. 1207-1214.

[12] Baker, R.R., E.D. Massey, and G. Smith, *An overview of the effects of tobacco ingredients on smoke chemistry and toxicity.* Food and Chemical Toxicology, 2004. **42**:

p. 53-83.

[13] NIOSH, *Criteria for a recommended standard: occupational exposure to diacetyl and 2,3-pentanedione*, N.R. By McKernan LT, Kreiss K, Hubbs A, Park R, Dankovic D, Dunn , P.J. KH, Fedan K, Streicher R, Fedan J, Garcia A, Whittaker C, Gilbert S, Nourian F, Galloway E, , and L.T. Smith R, Hirst D, Topmiller J, Curwin B. Cincinnati,, Editors. 2016, Department of Health and Human Services, Centers for Disease Control and Prevention, National Institute for Occupational Safety and Health, DHHS (NIOSH): OH: U.S.

[14] Patnaik, P., *A comprehensive guide to the hazardous properties of chemical substances*. 2007, Hoboken, NJ: John Wiley & Sons.

[15] Bahl, V., et al., *Comparison of electronic cigarette refill fluid cytotoxicity using embryonic and adult models.* Reproductive toxicology, 2012. **34**(4): p. 529-537.

[16] Behar, R., et al., *Identification of toxicants in cinnamon-flavored electronic cigarette refill fluids.* Toxicology in Vitro, 2014. **28**(2): p. 198-208.

[17] Jensen, R.P., R.M. Strongin, and D.H. Peyton, *Solvent chemistry in the electronic cigarette reaction vessel.* Scientific Reports, 2017. **7**: p. 42549.

[18] Zhao, T., et al., *Effects of design parameters and puff topography on heating coil temperature and mainstream aerosols in electronic cigarettes.* Atmospheric Environment, 2016. **134**: p. 61-69.

[19] Flora, J.W., et al., *Method for the Determination of Carbonyl Compounds in E-Cigarette Aerosols.* Journal of chromatographic science, 2017. **55**(2): p. 142-148.

[20] Etter, J.F., E. Zäther, and S. Svensson, *Analysis of refill liquids for electronic cigarettes.* Addiction, 2013. **108**(9): p. 1671-1679.

[21] ELiquidRecipes. *e-Liquid Recipes*. 2017 [cited 2017 May 31]; Available from: http://e-liquid-recipes.com/.

[22] Dautzenberg, B. and D. Bricard, *Real-Time Characterization of E-Cigarettes Use: The 1 Million Puffs Study.* Journal of Addiction Research & Therapy, 2015. **2015**.

[23] Meng, Q., et al., *Has the mist been peered through? Revisiting the building blocks of human health risk assessment for electronic cigarette use.* Human and Ecological Risk Assessment: An International Journal, 2016. **22**(2): p. 558-579.

[24] Norton, K.J., K.M. June, and R.J. O'Connor, *Initial puffing behaviors and subjective responses differ between an electronic nicotine delivery system and traditional cigarettes.* Tobacco induced diseases, 2014. **12**(1): p. 17.

[25] Robinson, R., et al., *Electronic cigarette topography in the natural environment.* PloS

one, 2015. **10**(6): p. e0129296.

[26] Spindle, T.R., et al., *Preliminary results of an examination of electronic cigarette user puff topography: The effect of a mouthpiece-based topography measurement device on plasma nicotine and subjective effects.* Nicotine & Tobacco Research, 2014: p. ntu186.

[27] Hua, M., H. Yip, and P. Talbot, *Mining data on usage of electronic nicotine delivery systems (ENDS) from YouTube videos.* Tobacco Control, 2013. **22**(2): p. 103-106.

[28] Farsalinos, K.E., et al., *Evaluation of electronic cigarette liquids and aerosol for the presence of selected inhalation toxins.* Nicotine & Tobacco Research, 2014. **17**(2): p. 168-174.

[29] U.S. EPA, *Compendium Method TO-11A: Determination of Formaldehyde in Ambient Air Using Adsorbent Cartridge Followed by High Performance Liquid Chromatography (HPLC) [Active Sampling Methodology], 2nd Edition*. 1999: Cincinnati, OH

[30] Lin, Y.-C., *Catalytic valorization of glycerol to hydrogen and syngas.* international journal of hydrogen energy, 2013. **38**(6): p. 2678-2700.

[31] Díaz, E., M.E. Sad, and E. Iglesia, *Homogeneous oxidation reactions of propanediols at low temperatures.* ChemSusChem, 2010. **3**(9): p. 1063-1070.

[32] Miner, C.S. and N.N. Dalton, *Glycerol*. 1953: Reinhold Pub. Corp.

[33] Tierney, P.A., et al., *Flavour chemicals in electronic cigarette fluids.* Tobacco control, 2015: p. tobaccocontrol-2014-052175.

[34] Allen, J.G., et al., *Flavoring Chemicals in E-Cigarettes: Diacetyl, 2, 3-Pentanedione, and Acetoin in a Sample of 51 Products, Including Fruit-, Candy-, and Cocktail-Flavored E-Cigarettes.* Environ Health Perspect, 2015.

[35] Farsalinos, K.E., V. Voudris, and K. Poulas, *E-cigarettes generate high levels of aldehydes only in 'dry puff'conditions.* Addiction, 2015.

[36] Fujioka, K. and T. Shibamoto, *Determination of toxic carbonyl compounds in cigarette smoke.* Environmental toxicology, 2006. **21**(1): p. 47-54.

[37] Uter, W., et al., *Glyoxal is an important allergen for (medical care) cleaning staff.* International Journal of Hygiene and Environmental Health, 2001. **204**(4): p. 251-253.

[38] Shangari, N. and P.J. O'Brien, *The cytotoxic mechanism of glyoxal involves oxidative stress.* Biochemical pharmacology, 2004. **68**(7): p. 1433-1442.

[39] McAdam, K., et al. *Diacetyl in e-cigarettes: sources, stability and aerosol transfer*. in *SRNT 23rd annual meeting*. 2017. The Society for Research on Nicotine & Tobacco.

[40] EPA, U., *Toxicological review of acrylamide (CAS No. 7906-1) in support of summary information on the Integrated Risk Information System (IRIS)*. 2010, U.S. Environmental

Protection Agency: Washington, DC.

[41] Yasuhara, A., et al., *Gas chromatographic investigation of acrylamide formation in browning model systems.* Journal of Agricultural and Food Chemistry, 2003. **51**(14): p. 3999-4003.

[42] Schulte-Ladbeck, R., et al., *Characterization of chemical interferences in the determination of unsaturated aldehydes using aromatic hydrazine reagents and liquid chromatography.* Journal of Environmental Monitoring, 2001. **3**(3): p. 306-310.

CHAPTER 6

ESTIMATION OF THE HUMAN LUNG CANCER RISKS ASSOCIATED WITH E-CIGARETTE VAPING

6.1. INTRODUCTION

E-cigarettes have been claimed to be a 'safe' or 'safer' product than conventional cigarette products but the e-cigarette vaping is not risk free. Previous reports have shown that e-vapor contains various levels of vegetable glycol (VG), propylene glycol (PG), nicotine, carbonyls, volatile organic compounds (VOCs), polycyclic aromatic hydrocarbons (PAHs), tobacco-specific nitrosamines (TSNAs), and other flavoring chemicals [1-4]. Many of these chemicals are carcinogens. However, the cancer risks associated with e-cigarette vaping have not been quantified in studies appropriately reflecting real-world e-cigarette emissions and use patterns.

Current e-cigarette risk assessments, therefore, need to be improved for several reasons [5, 6]. First, one of the previous risk assessment studies compared e-vapor exposure estimates with workplace exposure standards [threshold limit value (TLV)] [5]. However, occupational exposures are generally much higher than air toxicant exposures in the general population. Moreover, workplace standards do not account for susceptible and vulnerable populations. Second, other studies evaluated the risk of e-cigarette vaping based on air toxic levels and smoking topographies of conventional cigarette smoking, but not based on real-world e-cigarette vaping behaviors [6]. E-cigarette risk assessments need to integrate various exposure patterns and air toxicant emissions. Lastly, previous studies accessed e-vapor air toxic concentrations emitted mainly from first-generation e-cigarette devices. But, the emissions of the second- and third-generation e-cigarettes need to be evaluated because the evolved e-cigarette devices could generate higher levels of e-vapor toxicants [7-9].

To fill the knowledge gaps, in this study, human lung cancer risks associated with e-cigarette vaping were estimated based on air toxic concentrations in e-vapor that were studied under various real-world vaping conditions.

6.2. METHODS

6.2.1. Carcinogen Concentrations

The target carcinogens were selected based on data availability and the target organ, the lungs (Table 6-1). The selected carcinogens included carbonyls (formaldehyde and acetaldehyde), TSNAs [N-nitrosonornicotine (NNN) and 4-(methylnitrosamino)-1-(3-pyridyl)-1-butanone (NNK)], and metal ions [Cd, Ni, and Pb]. The levels of carcinogens in e-vapor were obtained from the measured carcinogenic carbonyl concentration in the Chapter 5 and the references [2-4]. For comparison purposes, the concentrations of carcinogens generated during conventional cigarette smoking were obtained from the International Agency for Research on Cancer (IARC) Monographs 83 [10].

Table 6-1. Carcinogen concentrations for e- vapor and conventional cigarette smoke

Group	Chemical	Concentration	
		E-cigarette	Cigarette*
Carbonyls	Acetaldehyde	0.4±0.4 µg/puff	119.0±61.1 µg/puff
	Formaldehyde	1.3±0.5 µg/puff	6.4±3.9 µg/puff
TSNAs**	NNN	0.02±0.02 ng/puff	12.8±10.8 ng/puff
	NNK	0.10±0.13 ng/puff	13.3±5.9 ng/puff
Metals**	Cd	0.6±0.8 ng/puff	15.4±8.0 ng/puff
	Ni	1.3±0.8 ng/puff	0.9±0.7 ng/puff
	Pb	2.0±2.5 ng/puff	3.6±2.8 ng/puff

*[10], **[2-4]; ***Not detected

Formaldehyde and acetaldehyde were found to be the most abundant carcinogens in e-vapor. Limited number of studies reported trace amount of TSNAs and heavy metals in e-vapor [2-4]. The level of carcinogens found in e-vapor were generally 10^0-10^8-fold lower than the concentrations in the conventional cigarette smoke except for nickel. E-vapor might contain higher concentrations of nickel than conventional cigarette smoke because most e-cigarettes use nickel-alloy coils. E-vapor contains much less acetaldehyde, NNN, NNK, and cadmium (i.e. 10^3-

10^8-fold lower) than cigarette smoke. But, the differences of formaldehyde and lead levels between e-vapor and conventional cigarette smoke were less than 10-fold. Several VOCs (e.g. benzene and toluene) were also reported to be in e-vapor [3, 4], but they were not included in the risk assessment because they are not pulmonary carcinogens and this study focused on the estimation of lung cancer risks [11].

6.2.2. Exposure Assessment

The average lifetime exposure concentrations for individual e-vapor carcinogens [E_i ($\mu g/m^3$)] were estimated using the Equation 6-1.

$$\boldsymbol{E_i = \frac{N \times f \times C_i \times EF \times ED}{V \times AT}} \qquad \text{Equation 6-1}$$

where, N (puffs/day) is the number of e-cigarette puffs per day, which was obtained from the literature [12-17] and the 23 study subjects mentioned in the previous chapters; f (unitless) is the lung deposition fraction of e-vapor particles, estimated from the MPPD model in Chapter 2; C_i is the amount of the i^{th} carcinogen per puff (μg/puff); EF is the exposure frequency (365 days/year); ED is the exposure duration (55 years); V is the average inhalation volume per day (20 m^3) [18]; and AT is the average life time of a person (365 × 75 = 27,375 days). We assume (1) e-cigarette users vape every day, (2) the lifespan is 75 years, and (3) e-cigarette users started vaping at the age of 20 years old.

To propagate uncertainties, probability distributions for the number of puffs (N), deposition fraction (f), and carcinogen concentration (C_i) were generated (Table 6-2). Log-normal distributions were used for the number of puffs per day (N), and normal distribution was applied to the deposition fraction (f), and carcinogen concentration (C_i) variables. The geometric mean and the geometric standard deviation for the number of puffs per day (N) were 5.13 and 1.29,

respectively. Means and standard deviations for lung deposition fractions (*f*) and carcinogen concentrations (C_i) under various vaping conditions were obtained from Chapter 2 and 5. The random samplings were repeated for 10,000 times using a Monte Carlo method.

Table 6-2. Parameters used in the cancer risk assessment

Symbol	Parameter	Unit	Distribution	Input*
N	The number of puffs per day	puff/day	Log-normal	Geo-mean, GSD
f	Lung deposition fraction	unitless	Normal	Mean, SD
C_i	Concentration of the ith carcinogen	μg/m^3	Normal	Mean, SD

*GSD and SD represent geometric standard deviation and standard deviation, respectively.

6.2.3. Human Lung Cancer Risk Estimation

The excess lifetime lung cancer risks associated with e-cigarette vaping and cigarette smoking were estimated using the Equation 6-2.

$$\boldsymbol{CR_t = \sum_i CR_i = E_i \times IUR_i} \qquad \text{Equation 6-2}$$

$$\boldsymbol{CR_n = \sum_i CR_i / C_{nicotine}} \qquad \text{Equation 6-3}$$

where, CR_t (unitless) is the cumulative lung cancer risk; CR_i (unitless) is the estimated excess lifetime lung cancer risks for the ith carcinogen; IUR_i [(μg/m^3)$^{-1}$] is the inhalation unit risks for the ith carcinogen; and E_i (μg/m^3) is the estimated lifetime average exposure concentrations to the ith carcinogen. In addition, cancer risks normalized by nicotine yields (CR_n) were estimated by dividing the estimated cancer risks by nicotine concentrations in e-vapor or cigarette smoke ($\boldsymbol{C_{nicotine}}$). All the parameters used in risk calculations are presented in Table 6-3.

The cumulative lung cancer risks for vapers were estimated using population- weighted-average carcinogen concentrations. The weighing factors were based the frequency distributions of the device power, vaping topography, and the use of e-liquid base materials of the 23 study

subjects. The weighting factors are listed in Table S6-1-S6-4.

Table 6-3. Parameters used in the cancer risk assessment

Parameter	Symbol	Unit	Value
Total cumulative lung cancer risk	CR_t	unitless	To be calculated
Nicotine-normalized lung cancer risk	CR_n	unitless	To be calculated
Lung cancer risk for the i^{th} carcinogen	CR_i	unitless	To be calculated
Inhalation unit risk for the i^{th} carcinogen	URE_i	$(\mu g/m^3)^{-1}$	See Table 6.4
Exposure concentration for the i^{th} carcinogen	E_i	$\mu g/m^3$	To be calculated
Number of puffs per day	N	puffs/day	To be calculated
Lung deposition fraction	f	unitless	To be calculated
Concentration of the i^{th} carcinogen per puff	C_i	µg/puff	To be calculated
Exposure frequency	EF	days	365
Exposure duration	ED	years	55
Average inhalation volume per day	V	m^3	20
Averaging time	AT	days	27,375

Table 6-4. Inhalation unit risks for the selected carcinogens

Group	Chemicals	Carcinogen		Unit risk	Target system
		IRIS	IARC	$(\mu g/m^3)^{-1}$	
Carbonyls	Acetaldehyde	B2	2B	0.0000022	Respiratory
	Formaldehyde	B1	2A	0.000013	Respiratory
TSNAs	NNN		2B	0.0004	Respiratory
	NNK		2B	0.0004**	Respiratory
Metals	Cd	B1	1	0.0018	Respiratory
	Ni	A	1	0.00024	Respiratory
	Pb	B2	2B	0.000012	Respiratory

**Unit risk for NNN was used

Inhalation unit risks are listed in Table 6-4. The carcinogen classification, the inhalation unit risks, and the target organ/systems were obtained from the U.S. EPA's integrated risk information system (IRIS) [11], the California Office of Environmental Health Hazard Assessment (CalEPA) [19] and the International Agency for Research on Cancer (IARC) [10].

6.2.4. Cancer Risk Estimates for Conventional Cigarette Smoking

In order to compare the estimated human cancer risks associated with e-cigarette vaping and the cancer risk induced by conventional cigarette smoking, cancer risk estimates for conventional cigarette smoking were obtained from the literature (Table 6-5). Cumulated cancer risks associated with conventional cigarette smoking were estimated for all types of cancers and ranged from 2.0×10^{-4} to 1.6×10^{-2}.

Table 6-4. Cancer risk estimates for conventional cigarette smoking

Cancer potency factor	Exposure assessment	Mean cancer risk	Reference
Unit risks for 41 carcinogens	Smoke a pack per day for 60 years out of 75 years lifespan	1.6×10^{-2}	Fowles and Dybing [20]
Slope factors estimated for 13 carcinogens	A pack per day, 70 years of smoking, 70 kg body weight	2.0×10^{-4}	Pankow, Watanabe [21]

6.3. RESULTS AND DISCUSSIONS

6.3.1. Cumulated Human Lung Cancer Risk Estimates

The estimated lifetime lung cancer risks for each carcinogen in e-vapor are presented in Table 6-5. The mean of cumulated lung cancer risks associated with e-cigarette vaping was 1.83×10^{-4} and was 26-fold lower than the reported mean cancer risk for conventional cigarette smoking. Although the estimated lung cancer risk associated with e-cigarette vaping was significantly lower than that of conventional cigarette smoking, e-cigarette posed 100-fold higher lung cancer risk than the acceptable cancer risk (i.e. one in a million). Among the e-vapor carcinogens, carbonyls contributed 88.6% of the total cumulated lung cancer risk induced by e-cigarette vaping, followed by heavy metals (11.0%), and TSNAs (0.38%). Formaldehyde was the most abundant carcinogen in e-vapor and contributed 87.0% of the total lung cancer risk associated with e-cigarette vaping.

Table 6-5. Lung cancer risks for each carcinogen emitted from e-cigarette

Group	Chemical	5%	Median	95%	Mean±SD
Carbonyls	Acetaldehyde	2.26×10^{-7}	3.71×10^{-6}	3.93×10^{-5}	$1.05\pm2.46\times10^{-5}$
	Formaldehyde	5.71×10^{-6}	6.47×10^{-5}	5.91×10^{-4}	$1.59\pm3.44\times10^{-4}$
TSNAs	NNN	2.06×10^{-9}	3.46×10^{-8}	3.62×10^{-7}	$0.94\pm2.27\times10^{-7}$
	NNK	1.27×10^{-8}	2.19×10^{-7}	2.41×10^{-6}	$0.63\pm1.51\times10^{-6}$
Metal	Cd	3.81×10^{-7}	5.94×10^{-6}	6.41×10^{-5}	$1.70\pm4.01\times10^{-5}$
	Ni	1.13×10^{-7}	1.46×10^{-6}	1.43×10^{-5}	$3.79\pm8.40\times10^{-6}$
	Pb	7.78×10^{-9}	1.36×10^{-7}	1.49×10^{-6}	$3.88\pm9.01\times10^{-7}$
Total		7.31×10^{-6}	7.58×10^{-5}	6.84×10^{-4}	$1.83\pm3.89\times10^{-4}$

6.3.2. Impact of Vaping Conditions on Lung Cancer Risks

Higher e-cigarette device power outputs and the use of PG based e-liquid resulted in greater lung cancer risks (Figure 6-1). On average, e-vapor generated at 31.3W poses 1.5, 3.2, and 2.7 times higher lung cancer risks than e-vapor generated under 6.4 watts, for VG-, PG&VG-, and

PG-based e-liquids, respectively. PG and PG&VG based e-liquids induced 3.9 and 2.3-fold higher lung cancer risks than VG-based e-liquids. Moreover, the estimated mean lung cancer risks (i.e. dash line in the box plot) of e-vapors, generated from PG- and PG&VG based e-liquids under high power output conditions, overlapped with the reported mean lung cancer risks for conventional cigarette smoking. The results suggest that e-cigarette users should avoid generating e-vapor from PG-based e-liquids under high power output settings.

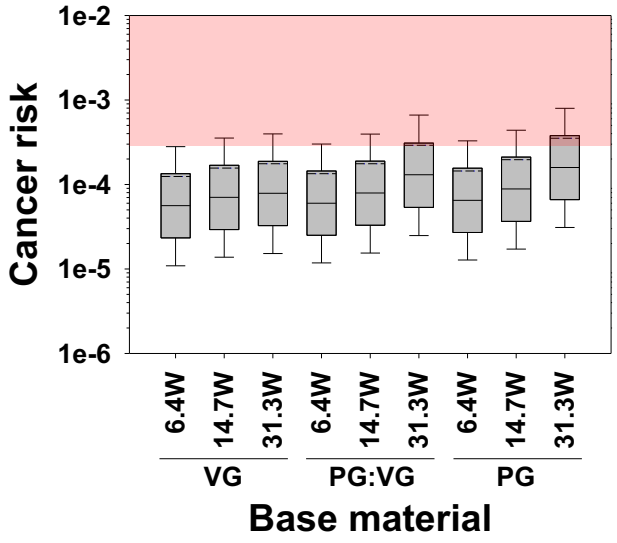

Figure 6-1. Cancer risks induced by the different e-cigarette device power outputs and base materials. 90 ml puff volume, 3.8 seconds puff duration, VG e-liquids containing 12 mg/ml nicotine was used. Red shaded area indicates the ranges of mean cancer risk for the conventional cigarette smoking

Table 6-7 shows e-cigarette cancer risks at different vaping topographies. Both higher puff volume and duration slightly increased cancer risks. However, for VG-based e-liquids, the estimated mean cancer risks for e-cigarette vaping was 42 times smaller than the cancer risks associated with conventional cigarette smoking, even under the vaping conditions of high puff volume and long puff duration.

Table 6-7. Lung cancer risks at different puff volumes (ml) and puff durations (seconds)*

Puff volume	Puff duration	Cancer risk			
		5%	Median	95%	Mean±SD
35 ml	2 seconds	5.31×10^{-6}	4.39×10^{-5}	3.47×10^{-4}	$0.97\pm1.87\times10^{-4}$
	3.8 seconds	5.73×10^{-6}	4.72×10^{-5}	3.69×10^{-4}	$1.04\pm1.96\times10^{-4}$
90 ml	2 seconds	6.05×10^{-6}	5.04×10^{-5}	3.96×10^{-4}	$1.12\pm2.12\times10^{-4}$
	3.8 seconds	7.13×10^{-6}	5.89×10^{-5}	4.59×10^{-4}	$1.30\pm2.47\times10^{-4}$
170 ml	2 seconds	5.75×10^{-6}	4.75×10^{-5}	3.74×10^{-4}	$1.05\pm2.01\times10^{-4}$
	3.8 seconds	6.71×10^{-6}	5.59×10^{-5}	4.37×10^{-4}	$1.24\pm2.35\times10^{-4}$

*6.4 watts power output and VG e-liquids containing 12 mg/ml nicotine was used

Table 6-8. Estimated cancer risks for different flavored e-liquids*

	Cancer risk			
	5%	Median	95%	Mean±SD
VG only	7.13×10^{-6}	5.89×10^{-5}	4.59×10^{-4}	$1.30\pm2.47\times10^{-4}$
Strawberry	9.81×10^{-6}	8.02×10^{-5}	6.38×10^{-4}	$1.80\pm3.40\times10^{-4}$
Dragonfruit	9.09×10^{-6}	7.55×10^{-5}	5.93×10^{-4}	$1.68\pm3.20\times10^{-4}$
Menthol	7.29×10^{-6}	6.10×10^{-5}	4.78×10^{-4}	$1.35\pm2.58\times10^{-4}$
Cinnamon	4.63×10^{-6}	4.10×10^{-5}	3.43×10^{-4}	$0.95\pm1.89\times10^{-4}$
Bubble Gum	5.45×10^{-6}	4.51×10^{-5}	3.52×10^{-4}	$1.00\pm1.91\times10^{-4}$
Bavarian Cream	4.83×10^{-6}	3.98×10^{-5}	3.16×10^{-4}	$0.88\pm1.68\times10^{-4}$
Sweet Cream	4.64×10^{-6}	3.87×10^{-5}	3.06×10^{-4}	$0.86\pm1.64\times10^{-4}$
Graham Cracker	3.71×10^{-6}	3.09×10^{-5}	2.49×10^{-4}	$0.69\pm1.35\times10^{-4}$

*6.4 watts power output, 90 ml puff volume and 3.8 seconds puff duration, and VG e-liquids containing 10% of flavoring agents were used (1% for cinnamon flavor)

Fruit flavored e-liquids (i.e. strawberry and dragonfruit) induced higher cancer risks than non-flavored e-liquids (Table 6-8). The estimated mean cancer risks for strawberry and dragonfruit flavored e-liquids were 32.8% and 17.8% higher than non-flavored e-liquids, while other flavoring agents showed lower cancer risks than VG only e-liquid. The inconsistency of the estimated cancer risks posed by flavored e-liquids cannot be well explained due to the lack of chemical concentrations of the flavoring agents sold on the market. The impact of flavoring agents on the risks associated with e-cigarette vaping needs to be further studied [22].

6.3.2. Nicotine-Normalized Lung Cancer Risks

Nicotine-normalized lung cancer risks were estimated by dividing lung cancer risks with nicotine concentrations in e-vapor . Nicotine-normalized lung cancer risks represent lung cancer risks per unit nicotine intake. Interestingly, increased e-cigarette device power output decreased nicotine-normalized cancer risks (CRn) (Figure 6-2). The nicotine-normalized cancer risks for e-vapors generated under 14.7W and 31.3W were 7 and 10-fold smaller than the risks of e-vapors generated under 6.4W. Our nicotine and carbonyl measurements presented in Chapter 3 and Chapter 5 suggest that both nicotine and carbonyl concentrations increased with the increase in e-cigarette power output, however, nicotine levels increased faster than carbonyl compounds in e-vapor, leading to the observed pattern of nicotine-normalized cancer risks presented in Figure 6-2.

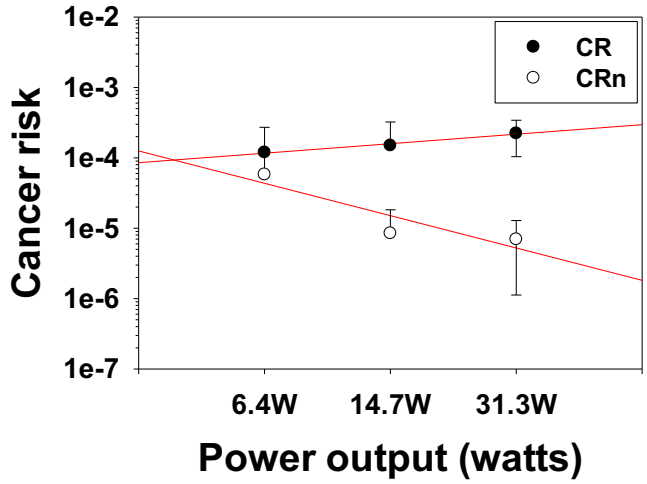

Figure 6-2. Mean cancer risks (CR) and normalized cancer risks by the nicotine concentrations (CRn) under different device power outputs. 90 ml puff volume, 3.8 seconds puff duration, VG e-liquids containing 12 mg/ml nicotine was used. Red lines indicate the trend lines for CR and CRn

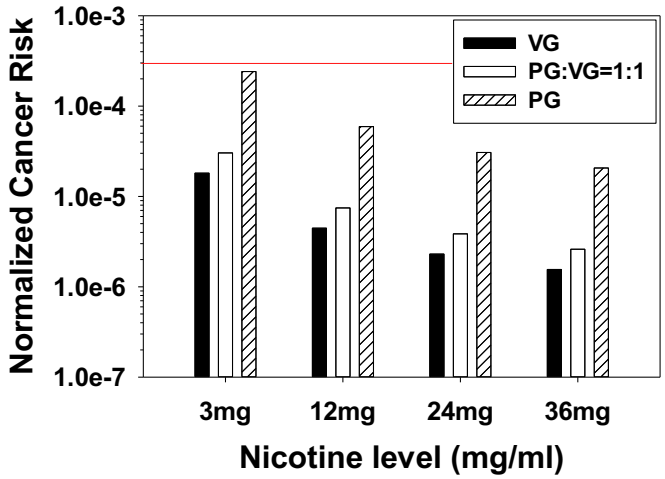

Figure 6-3. Normalized cancer risk by nicotine yield (CRn) associated with the base materials and the e-liquid nicotine levels. Red line indicates lowest cancer risk estimates for conventional cigarette smoking

Higher e-liquid nicotine level posed lower nicotine-normalized cancer risks (Figure 6-3). E-liquids containing 36 mg/ml nicotine posed 89-95% lower nicotine-normalized cancer risks than e-liquids with 3 mg/ml nicotine. The cancer risks normalized by e-vapor nicotine levels might reflect the 'real-world' cancer risks experienced by e-cigarette users. As shown, e-cigarette users adjust their vaping patterns to inhale a desired level of nicotine [23]. Also, e-cigarette users, using low nicotine level e-liquids, tend to vape more to reach the desired plasma nicotine level. Indeed, experienced e-cigarette users, who tested low nicotine e-liquids, increased their puff number and puff duration by 1.5 and 1.4-fold, and consumed 1.9 times more e-liquids than the e-cigarette users testing high nicotine e-liquids [23]. As a result, low nicotine concentration in e-vapor actually increased potentially harmful chemical exposures and resulted in higher cancer risks.

REFERENCES

[1] Flora, J.W., et al., *Characterization of potential impurities and degradation products in electronic cigarette formulations and aerosols.* Regulatory Toxicology and Pharmacology, 2016. **74**: p. 1-11.

[2] Goniewicz, M.L., et al., *Levels of selected carcinogens and toxicants in vapour from electronic cigarettes.* Tobacco control, 2014. **23**(2): p. 133-139.

[3] Marco, E. and J.O. Grimalt, *A rapid method for the chromatographic analysis of volatile organic compounds in exhaled breath of tobacco cigarette and electronic cigarette smokers.* Journal of Chromatography A, 2015. **1410**: p. 51-59.

[4] McAuley, T.R., et al., *Comparison of the effects of e-cigarette vapor and cigarette smoke on indoor air quality.* Inhalation toxicology, 2012. **24**(12): p. 850-857.

[5] Burstyn, I., *Peering through the mist: systematic review of what the chemistry of contaminants in electronic cigarettes tells us about health risks.* BMC public health, 2014. **14**(1): p. 18.

[6] Farsalinos, K.E. and R. Polosa, *Safety evaluation and risk assessment of electronic cigarettes as tobacco cigarette substitutes: a systematic review.* Therapeutic advances in drug safety, 2014. **5**(2): p. 67-86.

[7] Kosmider, L., et al., *Carbonyl compounds in electronic cigarette vapors—effects of nicotine solvent and battery output voltage.* Nicotine & Tobacco Research, 2014: p. ntu078.

[8] Geiss, O., I. Bianchi, and J. Barrero-Moreno, *Correlation of volatile carbonyl yields emitted by e-cigarettes with the temperature of the heating coil and the perceived sensorial quality of the generated vapours.* International journal of hygiene and environmental health, 2016. **219**(3): p. 268-277.

[9] Gillman, I., et al., *Effect of variable power levels on the yield of total aerosol mass and formation of aldehydes in e-cigarette aerosols.* Regulatory Toxicology and Pharmacology, 2016. **75**: p. 58-65.

[10] IARC, *Tobacco smoke and involuntary smoking*, ed. W.G.o.t.E.o.C.R.t. Humans, W.H. Organization, and I.A.f.R.o. Cancer. Vol. 83. 2004: IARC.

[11] EPA, U. *Integrated Risk Information System*. 2017 [cited 2017 July 21].

[12] Dautzenberg, B. and D. Bricard, *Real-Time Characterization of E-Cigarettes Use: The 1 Million Puffs Study.* Journal of Addiction Research & Therapy, 2015. **2015**.

[13] Etter, J.-F., *Electronic cigarettes: a survey of users.* BMC public health, 2010. **10**(1): p. 231.

[14] Etter, J.F., *Levels of saliva cotinine in electronic cigarette users.* Addiction, 2014. **109**(5): p. 825-829.

[15] Etter, J.F. and C. Bullen, *Electronic cigarette: users profile, utilization, satisfaction and perceived efficacy.* Addiction, 2011. **106**(11): p. 2017-2028.

[16] Robinson, R., et al., *Electronic cigarette topography in the natural environment.* PloS one, 2015. **10**(6): p. e0129296.

[17] Meng, Q., et al., *Has the mist been peered through? Revisiting the building blocks of human health risk assessment for electronic cigarette use.* Human and Ecological Risk Assessment: An International Journal, 2015(just-accepted): p. 00-00.

[18] EPA, U., *Exposure Factors Handbook 2011 Edition (Final)*. EPA/600/R-09/052F. 2011, Washington, DC: U.S. Environmental Protection Agency.

[19] CalEPA. *Toxicity criteria on chemicals evaluated by OEHHA*. 2017 [cited 2017 July 21].

[20] Fowles, J. and E. Dybing, *Application of toxicological risk assessment principles to the chemical constituents of cigarette smoke.* Tobacco Control, 2003. **12**(4): p. 424-430.

[21] Pankow, J.F., et al., *Calculated cancer risks for conventional and "potentially reduced exposure product" cigarettes.* Cancer Epidemiology and Prevention Biomarkers, 2007. **16**(3): p. 584-592.

[22] Khlystov, A. and V. Samburova, *Flavoring compounds dominate toxic aldehyde production during e-cigarette vaping.* Environmental science & technology, 2016. **50**(23): p. 13080-13085.

[23] Dawkins, L.E., et al., *Self-titration by experienced e-cigarette users: blood nicotine delivery and subjective effects.* Psychopharmacology, 2016: p. 1-9.

CHAPTER 7

OVERALL CONCLUSION AND FUTURE DIRECTIONS

7.1. OVERALL CONCLUSIONS

The overall aim of this dissertation was to evaluate the impact of e-cigarette user's vaping patterns on air toxic emissions from e-cigarettes, and to quantify human cancer risks associated with e-cigarette vaping. This study included a wide range of e-cigarette device power output, vaping topography, and e-liquid compositions, reflecting real-world vaping conditions.

The most important conclusions are summarized below:

1) E-cigarettes generated less amount of harmful chemicals per puff than conventional cigarettes, but nicotine-normalized chemical concentrations and cancer risks for vaping could exceed those for cigarette smoking.
2) E-cigarette device power output was the dominant factor affecting all air toxic emissions. The higher device power output generated higher levels of air toxicants (particles, nicotine and nicotyrine, carbonyls and OH radicals) in e-vapor.
3) Larger puff volume and/or longer puff duration also lead to higher levels of air toxicants in e-vapor.
4) The impacts of e-liquids composition on air toxicant emission was complicated, and competing exposures were observed. For example, PG-based e-liquid generated lower levels of OH radical but increased levels of formaldehyde. E-cigarette users select base materials based on their preferences (e.g. PG for indoor use and cost; and VG for flavor, cloud, and smooth vaping); thus there is no simple way to regulate e-liquid composition to minimize exposures to all potentially harmful carcinogens.
5) Flavored e-liquids generated more air toxics, such as aldehyde and OH radical, than non-flavored e-liquids, indicating that flavored e-liquids should be regulated.
6) The cancer risk estimates indicate that long-term e-cigarette vaping poses similar lung cancer risks as conventional cigarette smoking.

7.2. SIGNIFICANCE OF THIS STUDY

Despite the fact that e-cigarettes are believed to be safer than conventional cigarettes and the number of e-cigarette users has been rapidly increasing, they are not risk-free products. For the first time, this dissertation characterized e-cigarette emissions and estimates human cancer risks under 'real-world' conditions.

The study results will help inform the Federal and state governments regulation of e-cigarette, i.e. regulating e-cigarette device and e-liquid, because the FDA regulation over e-cigarettes requires testing air toxic emissions from e-cigarette under conditions reflecting 'real-world' use patterns (i.e. under various wattage and use conditions by light, typical and heavy users). In addition, the study results can be used to inform the government how to design potential product testing methodology, because e-cigarette vaping topography were found to change e-vapor particle sizes and chemical emissions. Currently, a large number of published reports used conventional cigarette topographies (e.g. 35-55 mL and 2 sec puffs), which do not reflect how people use e-cigarette.

In addition, since vaping behavior and e-cigarette product choice can affect e-cigarette emissions, the study results can also be used to identity vulnerable populations with high exposures to air toxics (e.g. the recreational e-cigarette users). The study results can be used as the scientific bases for developing education messages for public health protection.

7.3. STRENGTHS AND LIMITAIONS

Strengths of this study include: (1) E-cigarette emissions were tested at a wide range of 'real-world' vaping conditions; (2) For the first time, the impact of measurement conditions on e-cigarette particle size distribution and nicotyrine concentrations were evaluated, and all the final results were generated in carefully controlled experimental settings; (3) Cancer risk estimates integrated a wide range of real-world exposure patterns (e.g. vaping frequency) and measured e-vapor chemical concentrations; and (4) The study results are presented in comparison with traditional cigarette smoking, so that the risk of e-cigarette vaping can be better understood in a broader FDA's tobacco regulation context.

Limitations of this study lie in the following aspects. First, while eight of the most common flavoring agents were evaluated, only a limited number of flavored e-liquids of the more than hundred thousand e-liquid recipes on the market. Second, exposure patterns of different e-cigarette user subgroups were not well considered, such as dual cigarette and e-cigarette users vs. sole e-cigarette users, and cloud chasers vs. e-cigarette users for smoking cessation purposes. We expect the vaping patterns and the resulting risks associated with vaping are different for these subgroups.

7.4. FUTURE RESEARCH QUESTIONS

The following research questions need to be studied in the future.

- Because e-cigarette devices and e-liquids are rapidly evolving, the impact of emerging e-cigarette devices (e.g. silicon coil, braided coil) and e-liquid ingredients (e.g. flavoring enhancers, polyethylene glycol, cannabidiol, tetrahydrocannabinol) on e-vapor emission needs to be further studied.
- The impact of e-cigarette coil material (e.g. nichrome, kanthal, nickel, titanium, stainless steel), e-liquid water content, and oxygen supply rate on e-liquid decomposition needs to be studied because thermal degradation of VG can be accelerated by metal catalyzer (i.e. nickel, copper, lead, cobalt, and aluminum), water, and oxygen at above 400 ˚C.
- Thermal degradation of flavoring chemicals and their inhalation toxicity needs to be studied.
- Studies need to be conducted to better understand e-vapor exposure and risks for different e-cigarette user subgroups (e.g. dual cigarette and e-cigarette users vs. sole e-cigarette users, and cloud chasers vs. e-cigarette users for smoking cessation purposes).

APPENDICIES

Appendix 1

Summary tables for literature review

Table S1-1. Summary of human *in vivo* studies associated with the e-cigarette vaping

Study	Subjects	Study design	Outcome measurement	Major Findings
Carnevale et al. [1]	40 healthy subjects (20 smokes and 20 non-smokers, matched for age and sex)	First, all participants smoked a cigarette (0.6 mg nicotine). A week after, the same subjects vaped a tobacco-flavored e-cigarette (9 puffs, 16 mg/ml nicotine). For each phase, blood sample and ultrasound were performed	NOX2-derived peptide (sNOX2-dp), 8-iso-prostaglandin F2α (8-iso-PGF2α), serum NO, α-tocopherol/serum cholesterol ratio and flow-mediated dilation (FMD)	Both cigarette smoke and e-cigarette vaping acutely increased oxidative stress markers and reduced FMD
Dawkins et al. [2]	11 current, experienced e-cigarette users (11 white male adults)	Two e-liquids with 6 and 24 mg/ml nicotine were randomly assigned to the e-cigarette users, then took the blood samples at 10, 30, and 60 minutes after start vaping	Plasma nicotine, craving/withdrawal symptom	High nicotine group showed significantly higher plasma nicotine concentration, while craving/withdrawals were not. Puff number, duration, and consumed e-liquid for low nicotine group were 1.5, 1.4, and 1.9 folds higher
Hecht et al. [3]	35 healthy E-cigarette vapers, who did not smoke tobacco at least 2 months, use E-cigarette at least 1 month and 4 days per week.	E-cigarette vapers visited a clinic to complete a questionnaire and a spot urine sample was collected. Results were compared to previous studies of cigarette smokers.	Urine biomarkers were measured: 1-HOP, total NNAL, 3-HPMA, 2-HPMA, HMPMA, SPMA, total nicotine and total cotinine.	All metabolite levels were significantly lower than conventional cigarette smokers, but nicotine and cotinine levels were comparable in one study.
Farsalinos et al. [4]	Regular smokers, 18-70 years old with good general health were recruited.	"Categoria" E-cigarette was provided to group A (2.4% nicotine for 12 weeks), B (2.4% and 1.8% nicotine for 6 weeks each) and C (0% nicotine for 12 weeks).	Exhaled CO, blood pressure and heart rate was measured in 0, 2, 4, 6, 8, 10, 12, 24 and 52 weeks; 0 week indicated cigarette smoking and 52 weeks were E-cigarette vaping condition	Significant but slight decrease in systolic blood pressure (from 128.0±15.3 mmHg to 123.1±13.8 mmHg) was observed; no significant difference between group A, B and C.
Flouris et al. [5]	30 healthy subjects (15 smokers vs. 15 non-smokers)	Control, active and passive cigarette smoking or E-cigarette vaping sessions were assigned	Cotinine level was measured after 30 minutes of each session	Serum cotinine levels for active E-cigarette vapers (60.6 ng/mL) and traditional tobacco smokers (61.3 ng/mL) were similar.

Table S1-1. Summary of human *in vivo* studies associated with the e-cigarette vaping (continue)

Study	Subjects	Study design	Outcome measurement	Major Findings
Ramôa et al. [6]	16 E-cig users who vaped more than 3 months, used e-liquid higher than 12 mg/ml nicotine.	Participants used 3.3 V eGo battery and 1.5 ohm dual coil 510-style cartomizer with 1 ml of a E-liquid (0 to 36 mg/ml nicotine). In each session, participants complete two, 10 puff vaping.	Plasma nicotine level was measured using blood samples. 10 blood samples were taken 10 minute before vaping and up to 55 minutes after start vaping.	Plasma nicotine level could be increased up to 30.2 ng/ml for the e-liquid containing 36 mg/ml nicotine. It is compatible to conventional tobacco (~15 ng/ml).
Rosbrook et al. [7]	32 adult smokers, 18-42 years of age	V2 Standard E-cigarette with 0-24 mg/ml nicotine and 0.0%-3.5% l-menthol in a 7:3 PG:VG was tested.	General Labeled Magnitude Scale (gLMS) and the Labeled Hedonic Scale (LHS) were used for rating sensation intensity and rating flavor.	High l-menthol concentration increased sensory irritation and harshness at low nicotine level, but it was similar in high nicotine level.
Spindle et al. [8]	13 healthy E-cigarette users who vaped more than 3 months.	Participants visited laboratory to complete 10 puff vaping session and physiology measurement.	Blood was sampled before and after 10^{th} puff. Another blood sample was taken after 10 minutes and nicotine level was analyzed. Heart rate was also measured before and after Vaping session.	Plasma nicotine level increased from 2.4±0.2 ng/ml to 19.2±2.3 ng/ml, and it decreased to 10.2±1.1 ng/ml after 10 minutes. Heart rate was significantly increased from 65.7±1.5 to 74.2±1.6.
Wang et al. [9]	45,128 student, 12-17 years old, was recruited from the Global Youth Tobacco Survey.	Smoking status and additional information were collected using questionnaire.	Respiratory symptoms for 3 consecutive months in the past 12 months were asked.	Adjusted OR was 1.28 (1.06-1.56) for all study subject and 2.06 (1.24-3.42) for never-smoker group who used E-cigarette without nicotine.

Table S1-2. Summary of animal *in vivo* studies associated with the e-cigarette vaping

Study	Animal	Exposure Material	Exposure Condition	Major Findings
Glynos et al. [10]	C57BL/6 mice	E-vapor from humectant (PG:VG), 1% tobacco flavored and 1.8% nicotine	Mice were exposed to e-vapor for 3 days or 4 weeks	BALF cellularity increased in e-vapor and cigarette smoke group; oxidative stress and inflammation was observed only in cigarette smoke group
Golli et al. [11]	Male Wistar rats (160 ± 20 g body weight)	E-liquid containing 50% PG, 40% VG, 5-10% water, 1-5% flavoring and 0-1.8% nicotine	Physiological serum (Group 1), 0.5 mg nicotine/kg/day (Group 2), E-liquid without nicotine (Group 3) or E-liquid with 0.5 mg nicotine/kg/day (Group 4) were injected intra-peritoneally.	E-liquid with and without nicotine resulted in abnormal metabolism and impaired glucose and cholesterol homeostasis.
Lerner et al. [12]	C57BL/6J mice (8 weeks old)	E-vapor generated from Blu (Classic tobacco flavor, 16 mg nicotine)	Approximately 200 mg/m^3 TPM aerosols were generated using smoking machine. Mice received 5 h whole body e-vapor exposures per day for 3 successive days.	E-vapor exposure significantly increased IL-1α, IL-13, IL-16, and MCP-1 secretion compare to air breathing condition; Lung glutathione level was depleted
Lim et al. [13]	5 weeks old, female BALB/c mice	E-liquid containing 16 mg/ml nicotine (Z-company, Korea)	100 µl of 50-time diluted E-liquid was intratracheally instilled to Ovalbumin-sensitized (OVA-S) mice two times a week for 10 weeks.	Long-term exposure increased airway eosinophil accumulation and influx of inflammatory cells; stimulated the production of Th2 cytokines, including IL-4, IL-5 and IL-13, and OVA-specific IgE production. The results indicate that E-vapor exposure can exacerbate asthmatic symptoms and allergic responses.
McGrath-Morrow et al. [14]	Neonatal C57BL/6J mice (0-10 days)	Vapor generated from Joyetech 510-T e-cigarette and Johnson Creek e-liquid (0 and 1.8% nicotine)	Neonatal mice were exposed to room air (control) or 0% nicotine in PG or 1.8% nicotine in PG once a day for days 1 and 2 of life then twice a day from days 3 to 9 of life. E-vapor was generated every 15 sec with 6 sec puff duration.	E-vapor exposure during the neonatal period reduced weight gain and cell proliferation in alveoli region, increased plasma and urinary cotinine level.

Table S1-2. Summary of animal *in vivo* studies associated with the e-cigarette vaping (continue)

Study	Animal	Exposure Material	Exposure Condition	Major Findings
Palpant et al. [15]	Cleavage stage zebrafish (*Danio rerio*) embryos	E-vapor extract was prepared using one South Beach Smoke E-cig (tobacco classic flavor, 16 mg nicotine/ml)	The embryos continuously exposed to purified nicotine, e-cigarette or tobacco extracts for 3 days.	E-vapor extract showed significantly increased mild heart defects, while tobacco extract markedly caused severe heart defects.
Ponzoni et al. [16]	BALB/cJ mice (183 month old)	21 commercial cigarettes containing 0.8 mg nicotine/cig, 10 mg tar and 10 mg CO; E-cig vapor containing 5.6 mg nicotine per session	Cigarette smoke or E-vapor was provided three 30 minute sessions/day for seven weeks. 25 puffs were introduced per a minute and the puff volume was 8 ml. Nicotine dose for cigarette and E-cigarette group was same (16.8 mg nicotine/day).	Both cigarette and e-cigarette group showed similar brain nicotine and cotinine level compare with control group, and nicotinic acetylcholine receptors up-regulation.
Sussan et al. [17]	Male C57BL/6 (8 weeks old)	E-vapor generated from NJOY menthol bold, 1.8% nicotine or traditional bold 1.8% nicotine	Mice were exposed in a whole body exposure system for 1.5 h, twice per day for two weeks. Vaping topography was 35 ml puff volume, 2 sec duration and 10 sec interval. Each E-cigarette was vaped every 1 min using rotary system.	E-vapor exposure increased lipid peroxidation and macrophage inflammation, and significantly decreased IL-6 release. E-vapor exposure also impaired bacterial clearance rate in mice.
Werley et al. [18]	Crl:CD(SD) rats	MarkTen protorype E-cigarette, PG:VG mix , 2% nicotine with and without flavoring ingredients	3.2, 9.6 or 32.0 mg/kg of E-vapor were introduced using nose-only exposure system per day.	High nicotine level resulted in decreased body, organ and tissue weight of rats; there was no difference between formulations. High nicotine group showed decreased appetite and perturbations in total protein and albumin level.

Table S1-3. Summary of *in vitro* studies associated with the e-cigarette vaping

Study	Cells	Exposure Material	Exposure Condition	Major Findings
Alexander et al. [19]	Fresh human neutrophils; mouse alveolar macrophages; human airway epithelial cells (HaCaT and A549)	30 puffs of E-vapor were drawn into 60 mL syringe containing 10 ml of culture medium to prepare E-vapor extract.	Neutrophils and macrophages were incubated (30-120 min) with the E-vapor extract; HaCaT and A549 cells were exposed to E-vapor for 15 min, directly.	E-vapor exposure resulted in reduced cellular antimicrobial function and increased cell death.
Anderson et al. [20]	Human umbilical vein endothelial cells (HUVECs)	Blu, Vuse, Green Smoke, and NJoy	E-cigarette aerosol (55ml, 2 sec puff every 30 sec) was trapped using mid-jet impinge containing culture media, then cell culture with e-vapor extract was incubated for 4, 24, and 72 hr	Cells incubated with e-vapor for showed increased cytotoxicity (neutral red assay), DNA damage (TUNEL assay), apoptotic/necrotic cell death (TUNEL assay, caspase-3 and phosphorylated MLKL antibody), and cellular ROS level (ROS-ID assay); Adding antioxidants (α-tocopherol or n-acetyl-l-cysteine) could prevent cell death
Anthérieu et al. [21]	Human bronchial epithelial cell line (BEAS-2Bs)	Unflavored, tobacco flavor and chlorophyll mint flavored e-liquid with 0 or 16 mg/ml nicotine in PG:VG 65:35 (4.63W power)	Single exposure (up to 576 puffs over 288 min) or continuous exposure (6 exposures of 16 puffs e-vapor) were performed using a Vitrocell VC-1 system (55 ml, 3 sec puff every 30 sec), and then incubated up to 24 hr	No significant cytotoxic effect (ATP assay) and oxidative stress (GSH/GSSG assay), e-vapor exposure stimulated IL-6 secretion, RNA microarray data showed too few deregulated genes
Bahl et al. [22]	Human embryonic stem cells; mouse neural stem cells; and human pulmonary fibroblasts	36 Flavored E-liquids with nicotine concentrations 0 - 24 mg/mL and VG, PG, nicotine	E-liquid (0.001%-1% w/v) was added into cell culture medium directly, and cells were exposed for up to 48 h.	Embryonic or neural stem cells were more sensitive to e-liquid than fibroblasts; cinnamon, coffee, caramel, chocolate and fruit flavors were highly cytotoxic than other flavors.
Behar et al. [23]	Human embryonic stem cells; and human pulmonary fibroblasts	8 cinnamon flavored E-liquids and flavoring chemicals (cinnamaldehyde, 2-methoxycinnamaldehyde and vanillin)	E-liquid (0.001%-1% w/v) and flavoring chemical (1 μM-1 mM) was added into cell culture medium directly, and cells were exposed for up to 48 h.	Cinnamon flavoring agents (cinnamaldehyde and 2-methoxycinnamaldehyde) showed high cytotoxic responses.

Table S1-3. Summary of *in vitro* studies associated with the e-cigarette vaping (continue)

Study	Cells	Exposure Material	Exposure Condition	Major Findings
Cervellati et al. [24]	HaCaT (keratinocyte) and A549 (lung epithelial) cells	E-vapor generated from Balsamic flavored E-liquid with (amount not reported) or without nicotine	Cells were exposed to E-vapor in an air-liquid interface chamber for 50 mins.	E-vapor containing nicotine showed high cytotoxicity; more significant effects were caused by E-vapor with balsamic flavor; an increase in vacuolization and alteration of cytoplasmic membranes was observed.
Davies et al. [25]	Simulated surfactant monolayer (DPPC:POPG:PA = 69:20:11) using a Langmuir trough	Blu classic and Eleaf iStick 50W with Eleaf GS Air Tank atomiser	E-cigarette aerosol (55ml, 2 sec puff every 30 sec) was collected in a round bottom flask, then collected e-vapor was introduced into the lung biosimulator	E-vapor condensed surfactant layer, and lower the surface tension (nicotine insertion, lipid peroxidation, or hydrolysis)
Lerner et al. [12]	Human fetal lung fibroblasts (HFL1) and human bronchial airway epithelial cells (H292)	Tobacco, cinnamon, and grape flavored e-liquid with 0 or 24 mg /ml nicotine; e-vapor generated from Blu (classic tobacco flavor) containing 16 mg nicotine	Cell culture with PG, VG and E-liquid (10% - 0.5% w/v) was incubated for 24 hr; E-vapor from Blu was directly introduced (4 sec puff duration every 30 sec) to cell culture for 5, 10 and 15 mins, then incubate 16 hr	E-liquid decreased viability of HFL1 (acridine orange/propidium iodide staning); cinnamon flavor significantly stimulated IL-8 secretion of HFL1 cells; H292 increased IL-6 and IL-8 secretion
Maina et al. [26]	Human cryopreserved skin from 2 donors (3.29 cm^2 area, 0.7 mm thickness)	E-liquid containing 2.7 mg nicotine/mL	2.7 mg nicotine was introduced to 1 cm^2 skin using static Franz diffusion cells; physiological solution in the receptor chamber was collected after 1, 2, 3, 4, 8, 16 and 24 hours.	Nicotine skin permeation flux was 4.82±1.05 $\mu g/cm^2/h$ and lag time was 3.90±0.1 hours.
Moses et al. [27]	Primary human bronchial epithelium cells (pHBECs) cultured using the EpiAirway ALI culture system	Blu e-cigarette (menthol or tobacco flavor with 0 or 24 mg/ml nicotine)	Up to 400 puffs of e-vapor were introduced (80 ml, 3 sec puff every 30 sec) using a Vitrocell VC-1 system, exposure time was up to 200 min, and then incubated 22-24 hr	No cytotoxicity was observed (LDH assay, transepithelial electrical resistance), RNA microarray data for both e-cig and cigarette showed downregulated cilium assembly/movement genes and upregulated genes related with P450 pathway, apoptosis, xenobiotic stress, oxidative stress, DNA damage, cell cycle regulation (e-cig only), and cell division (e-cig only)

Table S1-3. Summary of *in vitro* studies associated with the e-cigarette vaping (continue)

Study	Cells	Exposure Material	Exposure Condition	Major Findings
Meng et al. [28]	Human peripheral blood mononuclear cells (PBMC) and A549 (lung epithelial) cells	E-vapor generated from Blu E-cigarette (classic tobacco, 2.4% nicotine) using LX1e smoking machine (80.4 ml for 3.3 s, 27 s interval)	E-vapor was introduced BAT air-liquid exposure chamber (100-400 puffs).	Cell viability of PBMC increased at low dose, but 60% decreased at high dose (400 puffs) after 24 hours. A549 showed 20% and 60% decreased viability at 200 puffs and 400 puffs, respectively.
Noerager et al. [29]	Human neutrophils	E-vapor extracts (VG, PG and e-liquid from the Johnson Creek original tobacco flavor)	Neutrophils were exposed to E-vapor extract .	E-vapor exposure inhibited leukotriene A_4 hydrolase peptidase activity.
Romagna et al. [30]	Mouse BALB/3T3 fibroblasts derived from Swiss albino mouse embryos	1% (w/v) E-vapor extract was prepared generated from flavored E-liquid (12 of tobacco like flavor and fruit or sweet flavor), with 0.8% nicotine level	Cells were exposed to the culture medium containing undiluted and diluted E-vapor extract for 24 hours.	E-vapor showed higher cell viability compared to conventional cigarette smoke; only coffee flavor E-liquid showed significant cytotoxic effect.
Rouabhia et al. [31]	Primary human gingival epithelial cells	EMOW e-cigarette (12 mg/ml)	2 puffs of e-vapor were introduced (5 sec puffing every 30 sec) into the exposure chamber containing cell culture plate, incubate 1 hr, and change media, and then incubate 1, 2, and 3 days	E-vapor increased cytotoxicity (LDH assay), apoptotic/necrotic cell death (annexin V-fluorescein isothiocyanate binding assay, TUNEL assay, and caspase-3 analysis), and DNA damage (TUNEL assay)
Rubenstein et al. [32]	Immortalized Kupffer cells from Sprague-Dawley Rats	E-vapor extract for OneJoy (NJoy) and eGo desert sands flavor (0-1.8% nicotine)	E-vapor extract (1 E-cigarette/5 L of culture medium) was added to Kupffer cells for 38 hours.	E-vapor extract activated innate immune responses of the Kupffer cell; C1q, C3b, C4d and C5b-9 protein deposition was 2-3 times higher than control. Pro-inflammatory cytokine (IL1α, IL1β, IL2, IL4 and IL6) release was 2-5 times increased.

Table S1-3. Summary of *in vitro* studies associated with the e-cigarette vaping (continue)

Study	Cells	Exposure Material	Exposure Condition	Major Findings
Sancilio et al. [33]	Human gingival fibroblasts (HGFs)	Two e-liquids (0 and 24 mg/ml nicotine) containing PG, VG, and flavorings	E-liquids (raw and warmed up) were diluted 4.8 to 48 times, and administered to the cell culture up to 72 hr	E-liquid exposure increased cytotoxicity (MTT assay), cellular ROS (CM-H_2DCFDA assay), and apoptotic cell death (annexin V-FITC/PI assay)
Scheffler et al. [34]	Normal human bronchial epithelial cells (NHBE), immortalized human bronchial epithelial cells (CL1548) and A549 (lung epithelial) cells	E-vapor generated by Reevo Mini-S E-cigarette (2.2 ohm, 3.3 V) and Tennessee Cured flavored e-liquid containing 0% or 2.4% nicotine	200 puffs (35 ml for 2 s, 10 s interval) of E-vapor were taken and diluted with clean air (1L/min) and it was introduced to CULTEX® RFS air-liquid exposure chamber.	All three cells showed decreased cell viability; NHBE showed most sensitive response to the E-vapor exposure and less sensitive response was observed from CL1548. A549 showed lest sensitivity to E-vapor exposure.
Scheffler et al. [35]	Normal human bronchial epithelial cells (NHBE)	Tennessee Cured flavored e-liquid containing 0 or 2.4 mg/ml nicotine in PG (4.95W)	200 puffs of e-vapor (35 ml, 2 sec puff, and unclear puff interval) were introduced to CULTEX® RFS air-liquid exposure chamber	E-vapor exposure significantly decreased cell viability (cellTiter-Blue assay) and increased oxidative stress level (ROS-Glo H_2O_2 assay); difference between e-vapor and cigarette smoke exposure was about 6 times for both viability and oxidative stress level.
Schweitzer et al. [36]	Primary rat lung endothelial cell (RLEC), primary mouse lung endothelial cells (MLEC), primary human microvascular cells-lung derived (HMVEC-LB1) and human bronchial epithelial cell line (Beas-2B)	A total of 125 µl of E-vapor condensate was collected from 600 µl of E-liquid over 30 minutes.	E-vapor condensate was added in cell culture medium: 1% to 20% (vol:vol) concentration	15 mM Nicotine and E-vapor condensate with same amount nicotine decreased 40% in Transcellular electrical resistance (TER) of RLEC cell after 5 hours incubation. E-vapor condensate containing 5 mM nicotine showed 60% and 80% decreased in TER of HMVEC-LB1 cell after 5 hours and 10 hours, respectively. CCK8 activity (cell proliferation marker) was reduced ~60% by E-vapor condensate.

Table S1-3. Summary of *in vitro* studies associated with the e-cigarette vaping (continue)

Study	Cells	Exposure Material	Exposure Condition	Major Findings
Taylor et al. [37]	Human bronchial epithelial cells (NCI-H292)	Tobacco flavored variant (36 mg/ml, 3.7V) and modular device (18 mg/ml, 4.0V)	E-vapor was collected (55ml, 3 sec puff every 30 sec) using mid-jet impinger containing culture media (0.5 puff/ml), cell culture with extract incubated for 1, 4, and 6 hr	E-vapor didn't induce cell death and apoptotic cell death (duplex assay), cellular ROS formation (DCFH-DA assay), and glutathione consumption (GSH/GSSG-Glo assay)
Thorne et al. [38]	Human bronchial epithelial cell line (BEAS-2Bs)	Cigalike device (eStick, 36 mg/ml nicotine, classic flavor) and closed modular system (ePen, 18 mg/ml, tobacco flavor)	E-vapor was introduced (55 ml, 3 sec puff every 30 sec) using a Vitrocell VC 10 aerosol exposure system, exposure time was up to 3 hr	E-vapor didn't increased DNA damage (γH2AX assay), while cigarette smoke showed significantly higher DNA damage intensity and cytotoxicity
Willershausen et al. [39]	Clonetics® HPdLF (Human Periodontal Ligament Fibroblasts)	Flavored E-liquids (hazelnuts 2% nicotine, lime 2% nicotine, menthol 2.2% nicotine) from eSmokerShop was diluted with cell culture medium to make 10 ug/mL nicotine concentration	Cells were exposed for up to 96 h with the diluted E-liquids	Menthol flavored E-liquid showed three, two and five times reduced cell proliferation, ATP and migration rate of fibroblasts, respectively.
Williams et al. [40]	Human pulmonary fibroblast (hPF)	E-liquid with and without particles	Fibroblasts were incubated with 0-1% E-liquid for 48 hours	E-liquid inhibited proliferation and cell attachment dose dependently; this effect of E-liquid with particle was stronger than without particles.

Table S1-3. Summary of *in vitro* studies associated with the e-cigarette vaping (continue)

Study	Cells	Exposure Material	Exposure Condition	Major Findings
Wu et al. [41]	Normal human tracheobronchial epithelial (hTBE) cells from the tracheas and bronchi of 8–10 years old organ donors	Medium, tobacco-flavored E-liquids with nicotine concentrations 0 and 18 mg/mL	E-liquid (0% - 0.3% v/v) was added into cell culture medium directly, and cells were exposed for 24 and 48 h.	With or without nicotine, e-liquid promoted IL-6 production (about 2 times higher than control) and HRV infection through inhibiting SPLUNC1 mRNA expression in hTBE cells.
Yu et al. [42]	Normal lung epithelial cells (HaCat) and neck squamous cell carcinoma cell line (NH30 and UMSCC10B)	V2 (red American Tobacco flavor) and VaporFi (Classic Tobacco flavor) containing 0 or 12 mg/mL nicotine in PG:VG 7:3	1% e-vapor extract was prepared in a culture medium was prepared, and cells were incubated with e-vapor extract for 48 hr-8 weeks (replaced every 3 days)	E-vapor extract increased DNA damage (neutral comet assay, γH2AX assay), cell death (trypan blu exclusion assay), apoptosis/necrosis (annexin V-FITC apoptosis detection assay), and altered cell cycle (cell cycle analysis), and decreased cell survival (clonogenic assay)

Table S1-4. Vaping topographies of e-cigarette users

Study	Number of subjects	E-cigarette	Method	Number of Puffs / Day	Puff Duration (s)	Puff Volume (ml)	Puff interval (s)
Behar et al. [43]	20	Blu (16 mg/ml nicotine) and V2 (18 mg/ml)	CReSS Pocket	NA	2.65 ± 0.98	51 ± 21	17.9 ± 7.5
Dautzenberg et al. [44]	185	Smokio (3.7 V, 1.5-2.0 ohms)	SMOKiO	163 (1 - 1,265)	3.79 ± 1.89	NA[a]	16.56 ± 13.50
Etter [45]	81	NA[a]	Questionnaire	175 (10 - 600)	NA[a]	NA[a]	NA[a]
Etter [46]	71	NA[a]	Questionnaire	150 (169 - 271)	NA[a]	NA[a]	NA[a]
Etter et al. [47]	31	NA[a]	Questionnaire	120 (80 - 200)	NA[a]	NA[a]	NA[a]
Farsalinos et al. [48]	45	Epsilon atomizer, eGo-T battery with 9 mg nicotine/ml E-liquid	Video recording	NA[a]	4.2 ± 0.7	NA[a]	20-30
Hua et al. [49]	64	Various E-cigarettes from the users	Video sampling from YouTube	NA[a]	4.3 ± 1.5	NA[a]	NA[a]
Meng et al. [28]	10	Subject's own e-cigarette	CReSS Pocket	Simulated	3.3 ± 1.4	80.4 ± 51.4	NA[a]
Norton et al. [50]	18	Smoke 51 TRIO with 11 mg/ml nicotine cartridge	CReSS Pocket	NA[a]	3 ± 1.6	118.2 ± 13.3	29.6 ± 11.7
Robinson et al. [51]	22	Blu rechargeable E-cig (16 mg nicotine/ml)	RIT wPUM	225 (24 - 1000)	3.5 ± 0.39	133 ± 20	18.4 - 48.7
Spindle et al. [8]	13	12 participants used tank type E-cigarettes.	Manufactured instrument	NA[a]	4.16 ± 1.06	101.37 ± 50.01	NA[a]

[a]Not reported.

Table S1-5. Summary of the e-vapor particle characteristics

Study	E-cigarette	Topography (volume; duration; interval)	E-liquid (flavor; nicotine; humectant)	Method	Dilution	Particle size	Concentration
Fuoco et al. [52]	Two tank type and a cig-like e-cigarette	1 L/min (33.3, 50.0, and 66.7 ml); 2, 3, and 4 sec; 30 sec	Selene, strawberry, menthol, tobacco; 0-18 mg /ml; unknown base material	Condensation particle counter (CPC), fast mobility particle sizer (FMPS), and scanning mobility particle sizer (SMPS)	880 and 1,000 for CPC and FMPS under 37 °C using rotating disk thermodiluter; e-vapor shown much higher volatility than cigarette smoke under 100, 150 °C dilution condition	Mode was 120-150 nm ;type of e-liquid did not show difference	3.26-5.52×10^9 #/cm^3; type of e-cigarette and flavor did not show difference; longer puff duration and higher nicotine increased concentration
Ingebrethsen et al. [53]	A tank type and a cig-like e-cigarette	55 ml; 2, 3, 4 sec; 30 sec	NA[a]	Differential mobility spectrometer (DMS); and transmitted light intensity method	3,400-5,500 using rotating disk dilutor of DMS; and no dilution for the transmission method	CMD was 14-34 nm for the DMS and 238-386 nm for the transmission; longer puff duration increased CMD for both method	4.10-11.8×10^9 #/cm^3 for the DMS and 1.56-5.94×10^9 #/cm^3 for the transmission; longer puff duration increased number concentration using the transmission method only
Laugesen [54]	Ruyan V8	35 ml, 2 sec, 60 sec	16 mg/ml nicotine, unknown flavor and base material	FMPS and cascade impactor,	NA[a]	40 nm CMD; it was confirmed using cascade impactor	NA[a]
Lerner et al. [55]	Blu	52 ml (unclear), 4 sec, 30 sec	NA[a]	Cascade particle impactor	No dilurion	1.03 μm MMAD 1.71 μm GSD	NA[a]

[a]Not reported.

Table S1-5. Summary of the e-vapor particle characteristics (continue)

Study	E-cigarette	Topography (volume; duration; interval)	E-liquid (flavor; nicotine; humectant)	Method	Dilution	Particle size	Concentration
Manigrasso et al. [56]	Tank type e-cigarette	Puff volume is unclear, 2 sec, 30 sec	Selene, strawberry, menthol, tobacco; 0-18 mg /ml; unknown base material	Condensation particle counter (CPC), fast mobility particle sizer (FMPS)	880 and 1,000 for CPC and FMPS under 37 °C using rotating disk thermodiluter	CMD was 107-165 nm; GSD was 1.48-1.68; data might be adopted from Fuoco et al.	3.26-5.29×10^9 #/cm^3; data might be adopted from Fuoco et al.
Manigrasso et al. [57]	Tank type e-cigarette	Puff volume is unclear, 2 sec, 30 sec	14 mg/ml nicotine level; unknown flavor and base material	Condensation particle counter (CPC), fast mobility particle sizer (FMPS)	880 and 1,000 for CPC and FMPS under 37 °C using rotating disk thermodiluter	Mode was 130 nm; data might be adopted from Fuoco et al.	5.3±0.58×10^9 #/cm^3; data might be adopted from Fuoco et al.
Mikheev et al. [58]	5 commercial e-cigarette	75 or 100 ml depending on the e-cig; 5 sec; 60 sec	Tabaco, menthol, mint; 0-24 mg/ml; unknown base material	Differential mobility spectrometer (DMS)	30-3000 dilution (method not mentioned); possibility of CMD change under high dilution ratio was mentioned	CMD was 96-175 nm; impact of nicotine concentration was inconsistent	10^7-10^8 #/cm^3
Schripp et al. [59]	Tank type e-cigarette	3 sec puff duration; unknown puff volume and interval	NA[a]	Fast mobility particle sizer (FMPS)	10 L dilution chamber was used; but dilution ratio was not provided	Mode decreased depending on the dilution temperature increment	concentration decreased depending on the dilution temperature increment

[a]Not reported.

Table S1-5. Summary of the e-vapor particle characteristics (continue)

Study	E-cigarette	Topography (volume; duration; interval)	E-liquid (flavor; nicotine; humectant)	Method	Dilution	Particle size	Concentration
Sosnowski et al. [60]	eGO-CE5 and eGO-W	NA[a]	18 mg/ml; 55-65% PG, 30-35% VG,	Laser diffraction spectrometry	No dilurion	CMD and GSD were 187-219 nm and 1.55-1.67, respectively.	NA[a]
Sundahl et al. [61]	13 commercial e-cigarettes	46 ml; 2.7 sec; 11.8 sec	NA[a]	Next generation pharmaceutical impactor with 60 L/min flow rate	No dilurion	MMAD was 0.53-0.96; GSD was 1.51-1.78	0.35-1.31 mg/20 puffs
Talih et al. [62]	Vape 4 Life CoolCart; 3.0 and 7.5 watt	66-264 ml, 2-8 sec, unknown puff interval	8.53 and 15.73 mg nicotine/ml; 80:20 PG:VG	NA[a] (gravitational method)	No dilurion	NA[a]	E-vapor mass was ranged from 29.4 to 152.7 mg per 15 puffs; mass increased depending on device power, puff volume, and puff duration
Zhang et al. [63]	Bloog MaxX Fusion, 3.5V battery	25 ml, unclear puff duration, 30 sec	16 mg/mL nicotine in PG or VG	Scanning mobility particle sizer (SMPS)	2 times dilution: e-vapor was introduced to 50 ml chamber	VMAD of PG base E-liquid was 250 nm and VG base was 440 nm	PG particle volume was 30% greater than VG aerosol
Zhao et al. [64]	Rechargeable e-cigarettes	0.5-2 L/min flow rate; 2-5 sec; 30 sec interval	Tobacco flavor; no nicotine; unknown base material	Scanning mobility particle sizer (SMPS).	3,200-12,800 dilution using 320L stainless-steel chamber, 30±10% and 24±1 °C	CMD was 18-29 nm; smaller puff volume and longer puff duration increased CMD	$0.58\text{-}1.64\times10^{9}$ #/cm^{3}; Larger puff volume and longer puff duration increased concentration

[a]Not reported.

Table S1-6. Chemical compositions of e-liquids

Study	E-liquid	Analytical method	Chemical composition
Beauval et al. [65]	27 e-liquids from the French NHOSS brand	Trace elements in e-liquid was analyzed using ICP-MS after diluted with nitric acid	All samples contained Al (12.9 ppb), Cr (7.16 ppb), and Sb 7.21 ppb. Some samples had As (57%, 1.57 ppb), Cu (4%, 27.0 ppb), and Hg (6%, 4.38 ppb)
Etter et al. [66]	20 e-liquids of 10 different brands	E-liquid was diluted with 1 M ammonia solution and nicotine and nicotine-related substances were analyzed using UPLC with a combination of UV and photodiode array detector, GC/MS	Nicotine impurities ranged from 0 to 4.4% of total nicotine contents; most common impurities were Cis- and Trans-N-oxide, anatabine, myosmine and anabasine
Farsalinos et al. [67]	159 e-liquids from 36 manufacturers	E-liquid was mixed with DNPH solution and allowed to derivatize for 20 min, then measured using HPLC/UV	69.2% and 33.3% of e-liquid samples contained diacetyl (10-170 µg/ml) and acetylpropionyl (7-172 µg/ml)
Goniewicz et al. [68]	20 cartridges, 15 nicotine refill solutions	E-liquid was diluted with methanol and analyzed using GC/TSD	Relative difference in nicotine level ranged from -89 % to 28%
Hess et al. [69]	48 e-liquid cartridges from 5 brands	A pad of the e-liquid cartridge was centrifuges for 10 min, and two aliquots were diluted with HNO_3/HCl micture, then analyzed using ICP-MS	Cd, Cr, Pb, Mn, and Ni concentrations were 0.204-12.40, 56.7-726, 4.98-1630, 26.1-918, and 58.1-15400, respectively
Kavvalakis et al. [70]	263 e-liquids from 13 different companies	Humectants (PG, VG, linalool, diethy-lene glycol) and PAHs were analyzed using GC/MS; nicotine, nitrosamines and flavoring ingredients were analyzed using LC/MS	Labeled and measured nicotine concentration was well correlated; No PAHs and nitrosamines were detected; methyl cyclopentenolone and ethyl maltol was most frequently detected flavoring ingredients
Kim et al. [71]	A total of 105 e-liquids from 11 companies	E-liquid was analyzed using LC/MS/MS system after solid and liquid extraction	LOQs of TSNAs were 0.04-0.06 µg/L; TSNAs ranged from 0.33 µg/L to 86.92 µg/L. Mean and standard deviation was 12.99 µg/L and 18.23 µg/L

[a]Not reported.

Table S1-6. Chemical compositions of e-liquids (continue)

Study	E-liquid	Analytical method	Chemical composition
Kubica et al. [72]	37 E-liquids	Sucrose level of E-liquid was measured using HPLC/MS/MS system	Sucrose level ranged from 0.56 μg/g to 72.9 μg/g; there is no clear relationship between the sucrose level and the manufacturer or flavor
Lim et al. [73]	225 E-liquids	Aldehyde levels of E-liquids were analyzed using headspace solid-phase micro extraction and GC/MS	Formaldehyde and acetaldehyde were detected in the concentration rage of 0.02-10.09 mg/L and 0.10-15.63 mg/L, respectively; acrolein was not detected
Lisko et al. [74]	A total of 36 different e-liquids	Nicotine, alkaloids and flavors were measured using GC/MS/MS. pH of e-liquid was measured using pH meter	Nicotine levels in E-liquid were consistently lower (6%-42% lower) than labeled amount. The pH ranged from 5.1 to 9.1. Some of the products exceeded tobacco alkaloids concentration criteria
Tierney et al. [75]	30 different flavored e-liquids	The level of flavoring chemicals were measured using GC/MS	Total flavoring chemicals were found to be in 10-40 mg/ml range. Most of them were aldehydes
Varlet et al. [76]	A total of 42 different e-liquids from 14 brands	Microbial concentration (colony forming unite method), hydrocarbons (GC/MS), aldehyde-DNPH (LC/UV/MS) and TSNAs (LC/MS/MS) were analyzed from E-liquids	There were no microbial contaminations. E-liquids contained formaldehyde (0.06-9.00 μg/g), acetaldehyde (0.03-10.2 μg/g), acetone (9-20 μg/g) and ethyl acetate (8-253 μg/g)

[a]Not reported.

Table S1-7. Nicotine and nicotine related compounds in e-vapor

Study	E-cigarette	Topography (volume, duration, interval)	E-liquid	Analytical method	Chemical composition
Farsalinos et al. [77]	Three cigarette type and four tank type e-cigarettes with 7-25W power	60 ml, 3-4 sec, 30 sec	PG: VG: water: nicotine = 45:45:8:2	20 puffs of E-vapor were collected using 44 mm diameter glass fiber filter pad and analyzed using GC/NPD	Nicotine levels were ranged from 1.88 mg/20 puffs to 9.45 mg/20puffs depending on the device; tank type device showed lower variability; nicotine level increased according to the device power setting
Farsalinos et al. [78]	Novacco Epsilon 1100 e-cigarette	55 ml, 4 sec, 30 sec	E-liquid containing 18 mg/ml nicotine	Spiked sample was prepared to contain NNN, NAT, NAB and NNK of 46.9, 53.9 45.6 and 42.0 mg/g, respectively. 100 puffs of e-vapor was collected on a glass fiber filter and analyzed using UPLC-MS/MS	TSNAs exposure was strongly associated with, and similar to, the liquid TSNAs content
Goniewicz et al. [68]	16 E-cigarettes	70 ml, 1.8 sec, 10 sec	20 cartridges and 15 nicotine refill solutions	150-300 puffs of e-vapor collected using impinger containing 50 ml methanol was analyzed using GC/TSD	Nicotine level of 150 puffs e-vapor ranged from 0.3 mg to 8.7 mg and 300 puffs of e-vapor ranged from 1.1 mg to 14 mg
Goniewicz et al. [79]	12 E-cigarettes	70 ml, 1.8 sec, 10 sec	12 E-liquids containing 4-18 mg/ml nicotine, tobacco and menthol flavor	150 puffs of e-vapor was extracted using two gas-washing bottles with 100 ml of methanol for tobacco specific nitrosamines (TSNAs), and then analyzed using UPLC/MS	N'-nitrosonornicotine (NNN) and 4-(methylnitrosoamino)-1-(3-pyridyl)-1-butanone (NNK) was 0.08-0.43 ng/15 puffs and 0.11-2.83 ng/15 puffs, respectively
Martinez et al. [80]	Viva Nova, 9.8 watt power (4.2 V, 1.8 ohm)	25 ml, 1 sec, no puff duration	18 mg nicotine/ ml in PG and PG:VG	E-vapor was trapped using chemically passivated collection thermal desorption cell, then analyzed using GC/MS	Nicotine and nicotyrine ratio was 0.19 and 0.09 for PG and PG:VG, respectively; Longer puff duration decreased NNR

[a]Not reported.

Table S1-7. Nicotine and nicotine related compounds in e-vapor (continue)

Study	E-cigarette	Topography (volume, duration, interval)	E-liquid	Analytical method	Chemical composition
Talih et al. [62]	Vape 4 Life CoolCart, 3.0-7.5 watt power	66-264 ml, 2-8 sec, no puff interval	8.53 and 15.73 mg nicotine/ml in 80:20 PG:VG	15 puffs of E-vapor were collected on the glass fiver filter. Nicotine yield was measured using GC/MS.	Nicotine concentration was ranged from 0.29 mg nicotine/15 puffs to 1.50 mg nicotine/15 puffs. Higher device power and nicotine content of e-liquid resulted in higher nicotine yield.
Trehy et al. [81]	NJOY, Smoking Everywhere and CIXI	100 ml, unclear puff duration, 60 sec	NA[a]	30 puffs of E-vapor was collected using impinge containing 50 ml extraction solution (10% acetonitrile in water); nicotine and impurities were measured using HPLC/UV	Nicotine delivery was ranged from 0 to 43.2 µg nicotine/100 ml puff; nicotine related impurities were not observed

[a]Not reported.

Table S1-8. Summary of the chemical components found in e-vapor

Study	E-cigarette	Topography (volume, duration, interval)	E-liquid	Analytical method	Chemical composition
Allen et al. [82]	E-cigarette devices from 9 brands	Unclear puff volume,8 sec, 15-30 sec	51 flavored e-liquids	Three flavoring chemicals were collected using OSHA method 1012 (dry silica bed method).	Fruit flavor generated high chemical concentrations; ≤ 239 μg diacetyl/e-cigarette, ≤ 64 μg 2,3-pentanedione/e-cigarette, ≤ 529 μg acetoin/e-cigarette
Farsalinos et al. [83]	Kayfun Lite plus	50 ml, 4 sec, 30 sec	PG: VG: water: nicotine = 45:45:8:2	60 puffs of E-vapor were collected using impinger containing DNPH in acetonitrile and analyzed using HPLC/UV	Normal puff (10W) generated 1.13 μg formaldehyde/puff, 0.45 μg acetaldehyde/puff, 0.10 μg acrolein/puff and dry puff (10W) generated 34.5, 206, 2.25, and 210 μg /puff of formaldehyde, acetaldehyde, acetone, and acrolein, respectively
Flora et al. [84]	Four cig-like e-cigarettes (MarkTen brand)	55 ml, 4 sec, 30 sec	1.5% nicotine	Approximately five sets (20 puffs/set, up to battery exhaustion) of e-vapor was collected using impinger containing DNPH in acetonitrile and analyzed using UPLC/UV	Formaldehyde was 0.090-0.33 ng/puff. Acetaldehyde level was below LOQ
Flora et al. [85]	6 commercial e-cigarettes	55 ml, 4 sec, 30 sec	NA[a]	20 puffs of e-vapor were collected using 44 mm CFP and impinger containing DNPH, then analyzed using UPLC/MS	Formaldehyde and acetaldehyde in e-vapor were 0.07-14.1 μg/puff and 0.03-13.61 μg/puff; ~70% was particle phase and ~30% was gas phase; High formaldehyde concentration was observed above 350 ˚C
Geiss et al. [86]	An atomizer and a cartomizer type e-cigarette	35 ml, 4 sec, 30 sec (bell shape puff profile)	PG:VG mixed e-liquids with tobacco-like flavor	13 puffs of e-vapor was collected in a 2L Tedlar gas-sampling bag connected with Sep-Pak DNPH-silica cartridge (100 ml/min sampling rate). DNPH-aldehyde adducts were analyzed using HPLC/UV	Formaldehyde, acetaldehyde, acetone and acrolein concentrations were 19.6-23.5, 8.1-39.9, 2.7-8.8, and 0.5-13.5 ng/puff, respectively.

[a]Not reported.

Table S1-8. Summary of the chemical components found in e-vapor (continue)

Study	E-cigarette	Topography (volume, duration, interval)	E-liquid	Analytical method	Chemical composition
Geiss et al. [87]	3rd generation e-cig with battery pack (5-20W), 1.6 ohm Nichrome coil	50 ml, 3 sec, 20 sec	50% VG, 40% PG, 6% water, 0.9% nicotine, and tobacco flavor	10 puffs of e-vapor were generated using 5, 10, 15, and 20W power output, and then collected using DNPH cartridge. Aldehyde concentrations were analyzed using HPLC/UV. Coil temperature was measured using thermographic infrared camera	Formaldehyde and acetaldehyde concentrations were 24.2-1559.9 and 13.2-348.4 ng/puff, respectively. 2.5 ng/puff acrolein was observed only under 20W condition. Formaldehyde and acetaldehyde levels for PG only e-liquid were 16.5-143.7 and 56.9-119.2 ng/puff, respectively, and VG:Water (8:2) were 68.2-1000 and 0-53 ng/puff, respectively.
Gillman et al. [88]	Five tank type E-cigarettes with 5.2-25 W power	55 ml, 4 sec, 30 sec	48% PG, 2% nicotine and VG	25 puffs were collected using 35 ml of DNPH trapping solution using an impinger. A 5 ml of aliquot was quenched with 0.250 ml of pyridine, and then analyzed using HPLC/UV	Aldehyde concentrations were 0.13-51 µg formaldehyde/puff, 0.05-41 µg acetaldehyde/puff and 0.02-5.5 µg acrolein/puff
Goniewicz et al. [79]	12 E-cigarettes	70 ml, 1.8 sec, 10 sec	12 E-liquids containing 4-18 mg/ml nicotine, tobacco and menthol flavor	150 puffs of E-vapor was collected using DNPH cartridge, Anasorb CSC tube for aldehydes and VOCs. Aldehydes and VOCs were analyzed using HPLC/DAD and GC/MS, respectively.	Formaldehyde, acetaldehyde, acrolein and toluene concentrations were 0.20-5.61 µg/15 puffs, 0.11-1.36 µg/15 puffs, 0.07-4.19 µg/15 puffs and 0.02-0.63 µg/15 puffs, respectively. Measured concentrations were 9-450 times lower than cigarette smoke.
Herrington et al. [89]	Four 1st generation E-cigarette	40 ml, 4 sec, no puff interval	NA[a]	1 puff of e-vapor was collected using adsorption-thermal desorption tube (Tenax TA, Carbograph 1TD, Carboxen 1003) and analyzed using GC/MS	3-15 ng acrolein/mL was quantified ;chemical component profile was generated using single puff sampling
Jensen et al. [90]	"tank system" e-cigarette with various voltage	50 ml, 3-4 sec, unclear puff interval	NA[a]	10 puffs of e-vapor were collected and detected using a nuclear magnetic resonance (NMR) spectroscopy.	380±90 µg formaldehyde-containing hemiacetal/10 puff was observed at high voltage (5.0V); it was not detected at low voltage (3.3V)

[a]Not reported.

Table S1-8. Summary of the chemical components found in e-vapor (continue)

Study	E-cigarette	Topography (volume, duration, interval)	E-liquid	Analytical method	Chemical composition
Khlystov et al. [91]	Kangertech eVod Glass (10.7W), V2 Standard (5.2W), E-Cig CE4 (4.9W)	40 ml, 4 sec, 30 sec	Flavored e-liquids in 6:4 or 8:2 PG:VG e-liquids	Two puffs of e-vapor were sampled using DNPH cartridges and analyzed using HPLC equipped with a photodiode array detector	Flavored e-liquids formed significantly higher carbonyls (0.37-49.5 µg/puff formaldehyde) than non-flavored e-liquids (0.64 µg/puff formaldehyde)
Kosmider et al. [92]	Crystal 2 clearomizer (3.2-4,8V, 2.4 ohm)	70 ml, 1.8 sec, 17 sec	18 to 24 mg/ml nicotine content in VG, VG:PG or PG base	E-vapor was collected using DNPH cartridge and aldehydes were analyzed using HPLC equipped with a diode array detector	Formaldehyde in VG. VG:PG and PG base e-liquid generated 0.02, 0.13 and 0.53 µg/15 puffs, respectively; increasing voltage from 3.2 V to 4.8 V resulted in 4 to 200 times higher formaldehyde, acetaldehyde and acetone level.
Marco et al. [93]	Disposable and rechargeable e-cigarettes	NA[a]	NA[a]	150 ml of e-vapor samples were collected using Bio-VOC cylinder, then the Bio-VOC output was connected to the sorbent cartridge (Tenax TA 35/60 mesh) to collect the VOCs. Samples were analyzed using the GC/MS system coupled with the thermal desorption system	Benzene, toluene, o- and p-xylene concentrations were 0-0.6, 0-4, 0-0.6, and 0-0.4 µg/m^3, respectively
McAuley et al. [94]	NA[a]	50 ml, 4 sec, 30 sec	Tobacco flavor, extra high or high nicotine Nicotine and humectant level is not clear	Nicotine, PG and PAHs were collected using filter cassettes, XAD-4 treated quartz filter and DNPH cartridge, respectively. Carbonyls and VOCs were collected using thermal desorption tubes. GC/NPD was used for nicotine; GC/MS for TSNAs, PAHs, PG and DEG; HS-GC/MS for VOCs; and carbonyls for HPLC/MS.	Chemical components were 0-28.2 ng benzene/L, 17.9-606.6 ng toluene/L, 0-152.8 ng xylene/L, 0.48-1.12 mg formaldehyde/L, 0.43-1.32 mg acetaldehyde/L, 0.72-4.73 mg acetone/L and 0.53-5.90 mg nicotine/L

[a]Not reported.

Table S1-8. Summary of the chemical components found in e-vapor (continue)

Study	E-cigarette	Topography (volume, duration, interval)	E-liquid	Analytical method	Chemical composition
Ogunwale et al. [95]	Blu (4.6W) and EVOD2 e-cigarette (9.1-16.6W)	91 ml, 4 sec, 30 sec	16 mg nicotine for Blu, 6 mg/ml for EVOD2 e-liquids	E-vapors were introduced into the microreactor functionalized with 4-(2-Aminooxyethyl)-morpholin-4-ium chloride (AMAH) to capture aldehydes. AMAH-aldehyde adducts were analyzed using GC/MS	Formaldehyde level were 0.018-0.062 µg/puff (4.6W) and 0.82-7.40 µg/puff (9.1W). Formaldehyde level increased from 2.01 to 81.98 µg/puff by increasing power output from 9.1W to 16.6W
Sleiman et al. [96]	eGO CE4 (2.6 ohms) and Kangertech Aerotank Mini (2.0 ohms) with 3.3-4.8 V	50 ml, 5 sec, 25 sec	3 e-liquids (tobacco, bubblicious, and mojito mix) with 18 or 24 mg/ml nicotine	Volatile constituents, carbonyls, and VOCs were analyzed using head space-GC/MS, HPLC/UV, and TD-GC/MS methods	Higher power output (4.8V) generated 3 folds higher carbonyls than 3.3V (from 53 to 165 µg/puff)
Tayyarah et al. [97]	Blu and SKYCIG	35 ml, 2 sec, 30 sec (ISO regime)	16-24 mg nicotine/ml	99 puffs or 200 mg of E-vapor were collected using glass fiber filter (VG, nicotine) and impinger (aldehydes, VOCs, PAHs); analyzed using GC/FID, GC/MS (VG, nicotine, amines and VOCs), HPLC/UV (aldehyde), UPLC/fluorescence detection (phenolics)	Detected concentrations were 8-33 µg nicotine/puff, 0.7-0.9 µg carbonyls/puff, 4-80 ng VOCs/puff, 0.04-0.14 ng PAHs/puff; detected concentrations were 100 times lower than cigarette smoke
Uchiyama et al. [98]	NA[a]	35 ml, 2 sec, 60 sec	NA[a]	E-vapor was collected using DNPH or DNPH-hydroquinone cartridge and analyzed using HPLC/UV	Formaldehyde, acetaldehyde, acetone, and acrolein concentrations were 8.3, 11, 2.9, and 9.3 mg/m^3, respectively
Uchiyama et al. [99]	13 brands of e-cigarette	55 ml, 2 sec, 30 sec, 10 puffs	NA[a]	Hydroquinone cartridge and DNPH cartridge were connected, and e-vapor was collected. The extract of coupled cartridges were analyzed using HPLC/UV	Formaldehyde, acetaldehyde, acrolein, and glyoxal concentrations were 1.3-61, 0.3-48, 1.1-36, and 1.3-29 mg/m^3, respectively

[a]Not reported.

Table S1-8. Summary of the chemical components found in e-vapor (continue)

Study	E-cigarette	Topography (volume, duration, interval)	E-liquid	Analytical method	Chemical composition
Uchiyama et al. [100]	10 e-cigarettes, 5.1-14W	55 ml, 2 sec, 30 sec	Apple and other flavors (base material and nicotine level is unknown)	Particle and gas phase e-vapor were collected using CFP and Carboxen-572 sorbent tube, respectively. CFP and sorbent was extracted using DNPH and analyzed using HPLC/UV for aldehyde analysis. Nicotine and VOCs were measured using GC/MS after solvent extraction	Formaldehyde, acetaldehyde, acetone, acrolein, and glyoxal concentrations were 0-12.0, 0-7.3, 0-1.5, 0-2.4, 0-4.3 µg/puff respectively
Wang et al. [101]	Heat reactor with 50-300 ˚C temperature	200 ml/min, 2.9 sec	PG, VG, PG:VG 1:1, and two commercial e-liquid	E-vapor was collected using DNPH cartridge and analyzed using HPLC/UV	Formaldehyde and acetaldehyde were formed above 200 ˚C. VG based e-liquid formed higher aldehyde than PG (7.97 µg/mg-VG vs. 0.29 µg/mg-PG): the impact of heating material (stainless steel)

[a]Not reported.

Table S1-9. Heavy metals found in e-vapor

Study	E-cigarette	Topography (volume, duration, interval)	E-liquid	Analytical method	Chemical composition
Goniewicz et al. [79]	12 E-cigarettes	70 ml, 1.8 sec, 10 sec	12 E-liquids containing 4-18 mg/ml nicotine, tobacco and menthol flavor	150 puffs of e-vapor were extracted using two gas-washing bottles with 100 ml of methanol for heavy metal analysis using the ICP/MS	Cd, Ni and Pb concentration was 0.01-0.17 µg/150 puffs, 0.11-0.29 µg/150 puffs, 0.03-0.57 µg/150 puffs, respectively
Lerner et al. [55]	Blu e-cigarette	35 ml, 2 sec, 60 sec	NA	4 puffs of aerosols were collected on a methyl-cellulose filter and analyzed using atomic absorption spectrometer	Cu concentration was 116.79±85.59 ng/puff (24.3-224.7 ng/puff)
Williams et al. [40]	NA[a]	4.3 sec puff duration, unclear puff volume and interval	NA[a]	60 puffs of E-vapor was generated and fully dissolved in a solution of 10 % nitric acid, 3 % hydrochloric acid and 87 % of DI water. Elemental analysis was done using ICP-OES.	Na, Br, Si, Ca, Fe, and Al concentration was 4.18, 3.83, 2.24, 1.03, 0.52 and 0.39 µg/10 puffs, respectively.

[a]Not reported.

Table S1-10. Reactive oxidative species formed by the e-cigarettes

Study	E-cigarette	Topography (volume, duration, interval)	E-liquid	Method	ROS formation
Goel et al. [102]	SmokTech cartomizer (1.5 ohms) with eGo-ce4 (3.3 V) and Tesla (3-6 V) battery	500 ml/min, 5 sec, 20 sec	NA[a]	E-vapor was passed through impingers containing spin trap (PBN). PBN-radical adducts were analyzed using EPR	Radical product ranged from 2.2×10^{13} to 10.3×10^{13} radicals per puff; radical concentration was 100 to 1000 times lower than cigarette smoke
Lerner et al. [12]	Blu e-cigarette and Anyvape clearomizer + eGO Vision Spinner battery	Puff volume is not clear, 4-5 sec, 30 sec	PG, VG, PG:VG 5:5, classic tobacco flavor containing 0 or 24 mg nicotine	E-vapor was introduced through DCFH solution in the impinge for 10 minutes	ROS concentrations as H_2O_2 equivalents (μM) were 125.7±2.5 μM, 255.9±33.6 μM and 306.6±81.3 μM for PG, VG and PG:VG, respectively; less nicotine concentration and non-tobacco flavored e-liquid showed higher ROS formation
Lerner et al. [55]	Blu e-cigarette, Anyvape clearomizer; 3R4F, Marlboro 100s	33.3 ml, 4 sec, 30 sec	NA[a]	E-vapor or cigarette smoke was introduced through DCFH solution in the impinge for 10 minutes	E-vapor and cigarette smoke formed 33.3 μM H_2O_2 and 11.8 μM H_2O_2, respectively.

REFERENCES

[1] R. Carnevale, S. Sciarretta, F. Violi, C. Nocella, L. Loffredo, L. Perri, M. Peruzzi, A.G. Marullo, E. De Falco, and I. Chimenti, Acute Impact of Tobacco vs Electronic Cigarette Smoking on Oxidative Stress and Vascular Function. CHEST Journal, (2016). **150**(3): p. 606-612.

[2] L.E. Dawkins, C.F. Kimber, M. Doig, C. Feyerabend, and O. Corcoran, Self-titration by experienced e-cigarette users: blood nicotine delivery and subjective effects. Psychopharmacology, (2016): p. 1-9.

[3] S.S. Hecht, S.G. Carmella, D. Kotandeniya, M.E. Pillsbury, M. Chen, B.W. Ransom, R.I. Vogel, E. Thompson, S.E. Murphy, and D.K. Hatsukami, Evaluation of toxicant and carcinogen metabolites in the urine of e-cigarette users versus cigarette smokers. Nicotine & Tobacco Research, (2015). **17**(6): p. 704-709.

[4] K. Farsalinos, F. Cibella, P. Caponnetto, D. Campagna, J.B. Morjaria, E. Battaglia, M. Caruso, C. Russo, and R. Polosa, Effect of continuous smoking reduction and abstinence on blood pressure and heart rate in smokers switching to electronic cigarettes. Internal and emergency medicine, (2016): p. 1-10.

[5] A.D. Flouris, M.S. Chorti, K.P. Poulianiti, A.Z. Jamurtas, K. Kostikas, M.N. Tzatzarakis, A. Wallace Hayes, A.M. Tsatsakis, and Y. Koutedakis, Acute impact of active and passive electronic cigarette smoking on serum cotinine and lung function. Inhalation toxicology, (2013). **25**(2): p. 91-101.

[6] C.P. Ramôa, M.M. Hiler, T.R. Spindle, A.A. Lopez, N. Karaoghlanian, T. Lipato, A.B. Breland, A. Shihadeh, and T. Eissenberg, Electronic cigarette nicotine delivery can exceed that of combustible cigarettes: a preliminary report. Tobacco control, (2015): p. tobaccocontrol-2015-052447.

[7] K. Rosbrook and B.G. Green, Sensory effects of menthol and nicotine in an E-cigarette. Nicotine & Tobacco Research, (2016): p. ntw019.

[8] T.R. Spindle, A.B. Breland, N.V. Karaoghlanian, A.L. Shihadeh, and T. Eissenberg, Preliminary results of an examination of electronic cigarette user puff topography: The effect of a mouthpiece-based topography measurement device on plasma nicotine and subjective effects. Nicotine & Tobacco Research, (2014): p. ntu186.

[9] M.P. Wang, S.Y. Ho, L.T. Leung, and T.H. Lam, Electronic Cigarette Use and Respiratory Symptoms in Chinese Adolescents in Hong Kong. JAMA pediatrics, (2016): p. 1-2.

[10] C. Glynos, S.-I. Bibli, A. Pavlidou, P. Katsaounou, I. Kalomenidis, S. Zakynthinos, and

A. Papapetropoulos, Comparison of the effects of e-cigarette vapor vs cigarette smoke on lung function and inflammation in mice. European Respiratory Journal, (2015). **46**(suppl 59): p. OA279.

[11] N.E. Golli, H. Dkhili, Y. Dallagi, D. Rahali, M. Lasram, I. Bini-Dhouib, M. Lebret, J.-P. Rosa, S. El Fazaa, and M. Allal-El Asmi, Comparison between electronic cigarette refill liquid and nicotine on metabolic parameters in rats. Life sciences, (2016). **146**: p. 131-138.

[12] C.A. Lerner, I.K. Sundar, H. Yao, J. Gerloff, D.J. Ossip, S. McIntosh, R. Robinson, and I. Rahman, Vapors produced by electronic cigarettes and e-juices with flavorings induce toxicity, oxidative stress, and inflammatory response in lung epithelial cells and in mouse lung. PloS one, (2015). **10**(2).

[13] H.B. Lim and S.H. Kim, Inhallation of e-Cigarette Cartridge Solution Aggravates Allergen-induced Airway Inflammation and Hyper-responsiveness in Mice. Toxicological research, (2014). **30**(1): p. 13.

[14] S.A. McGrath-Morrow, M. Hayashi, A. Aherrera, A. Lopez, A. Malinina, J.M. Collaco, E. Neptune, J.D. Klein, J.P. Winickoff, and P. Breysse, The effects of electronic cigarette emissions on systemic cotinine levels, weight and postnatal lung growth in neonatal mice. PloS one, (2015). **10**(2): p. e0118344.

[15] N.J. Palpant, P. Hofsteen, L. Pabon, H. Reinecke, and C.E. Murry, Cardiac development in zebrafish and human embryonic stem cells is inhibited by exposure to tobacco cigarettes and e-cigarettes. PloS one, (2015). **10**(5): p. e0126259.

[16] L. Ponzoni, M. Moretti, M. Sala, F. Fasoli, V. Mucchietto, V. Lucini, G. Cannazza, G. Gallesi, C. Castellana, and F. Clementi, Different physiological and behavioural effects of e-cigarette vapour and cigarette smoke in mice. European Neuropsychopharmacology, (2015). **25**(10): p. 1775-1786.

[17] T.E. Sussan, S. Gajghate, R.K. Thimmulappa, J. Ma, J.-H. Kim, K. Sudini, N. Consolini, S.A. Cormier, S. Lomnicki, and F. Hasan, Exposure to Electronic Cigarettes Impairs Pulmonary Anti-Bacterial and Anti-Viral Defenses in a Mouse Model. PloS one, (2015). **10**(2): p. e0116861.

[18] M.S. Werley, D.J. Kirkpatrick, M.J. Oldham, A.M. Jerome, T.B. Langston, P.D. Lilly, D.C. Smith, and W.J. Mckinney Jr, Toxicological assessment of a prototype e-cigaret device and three flavor formulations: a 90-day inhalation study in rats. Inhalation Toxicology, (2016): p. 1-17.

[19] L.C. Alexander, J. Hwang, M. Lyes, and A. Moshensky, E-Cigarette Vapor Decreases

Antimicrobial Function Of Macrophages, Neutrophils And Airway Epithelial Cells. Am J Respir Crit Care Med, (2015). **191**: p. A3680.

[20] C. Anderson, A. Majeste, J. Hanus, and S. Wang, E-cigarette aerosol exposure induces reactive oxygen species, DNA damage, and cell death in vascular endothelial cells. Toxicological Sciences, (2016): p. kfw166.

[21] S. Anthérieu, A. Garat, N. Beauval, M. Soyez, D. Allorge, G. Garçon, and J.-M. Lo-Guidice, Comparison of cellular and transcriptomic effects between electronic cigarette vapor and cigarette smoke in human bronchial epithelial cells. Toxicology in Vitro, (2017).

[22] V. Bahl, S. Lin, N. Xu, B. Davis, Y.-h. Wang, and P. Talbot, Comparison of electronic cigarette refill fluid cytotoxicity using embryonic and adult models. Reproductive toxicology, (2012). **34**(4): p. 529-537.

[23] R. Behar, B. Davis, Y. Wang, V. Bahl, S. Lin, and P. Talbot, Identification of toxicants in cinnamon-flavored electronic cigarette refill fluids. Toxicology in Vitro, (2014). **28**(2): p. 198-208.

[24] F. Cervellati, X. Muresan, C. Sticozzi, R. Gambari, G. Montagner, H. Forman, C. Torricelli, E. Maioli, and G. Valacchi, Comparative effects between electronic and cigarette smoke in human keratinocytes and epithelial lung cells. Toxicology in Vitro, (2014). **28**(5): p. 999-1005.

[25] M.J. Davies, J.W. Birkett, M. Kotwa, L. Tomlinson, and R. Woldetinsae, The impact of cigarette/e-cigarette vapour on simulated pulmonary surfactant monolayers under physiologically relevant conditions. Surface and Interface Analysis, (2017).

[26] G. Maina, C. Castagnoli, V. Passini, M. Crosera, G. Adami, M. Mauro, and F.L. Filon, Transdermal nicotine absorption handling e-cigarette refill liquids. Regulatory toxicology and pharmacology, (2016). **74**: p. 31-33.

[27] E. Moses, T. Wang, S. Corbett, G.R. Jackson, E. Drizik, C. Perdomo, C. Perdomo, E. Kleerup, D. Brooks, and G. O'Connor, Molecular impact of electronic cigarette aerosol exposure in human bronchial epithelium. Toxicological Sciences, (2017). **155**(1): p. 248-257.

[28] Q. Meng, S. Schwander, Y. Son, C. Rivas, C. Delveno, J. Graber, D. Giovenco, U. Bruen, R. Mathew, and M. Robson, Has the mist been peered through? Revisiting the building blocks of human health risk assessment for electronic cigarette use. Human and Ecological Risk Assessment: An International Journal, (2015)(just-accepted): p. 00-00.

[29] B. Noerager, J. Wells, J. Blalock, W. Bailey, P. Jackson, and D. Sullivan, Mechanical

And Chemical Components Of Electronic Cigarettes Affect Combustion Product Formation And Biological Pathways Of Inflammation. Am J Respir Crit Care Med, (2015). **191**: p. A2712.

[30] G. Romagna, E. Allifranchini, E. Bocchietto, S. Todeschi, M. Esposito, and K.E. Farsalinos, Cytotoxicity evaluation of electronic cigarette vapor extract on cultured mammalian fibroblasts (ClearStream-LIFE): comparison with tobacco cigarette smoke extract. Inhalation toxicology, (2013). **25**(6): p. 354-361.

[31] M. Rouabhia, H.J. Park, A. Semlali, A. Zakrzewski, W. Chmielewski, and J. Chakir, E-Cigarette Vapor Induces an Apoptotic Response in Human Gingival Epithelial Cells Through the Caspase-3 Pathway. Journal of Cellular Physiology, (2017). **232**(6): p. 1539-1547.

[32] D.A. Rubenstein, S. Hom, B. Ghebrehiwet, and W. Yin, Tobacco and e-cigarette products initiate Kupffer cell inflammatory responses. Molecular immunology, (2015). **67**(2): p. 652-660.

[33] S. Sancilio, M. Gallorini, A. Cataldi, and V. di Giacomo, Cytotoxicity and apoptosis induction by e-cigarette fluids in human gingival fibroblasts. Clinical oral investigations, (2016). **20**(3): p. 477-483.

[34] S. Scheffler, H. Dieken, O. Krischenowski, and M. Aufderheide, Cytotoxic evaluation of e-liquid aerosol using different lung-derived cell models. International journal of environmental research and public health, (2015). **12**(10): p. 12466-12474.

[35] S. Scheffler, H. Dieken, O. Krischenowski, C. Förster, D. Branscheid, and M. Aufderheide, Evaluation of E-Cigarette Liquid Vapor and Mainstream Cigarette Smoke after Direct Exposure of Primary Human Bronchial Epithelial Cells. International journal of environmental research and public health, (2015). **12**(4): p. 3915-3925.

[36] K.S. Schweitzer, S.X. Chen, S. Law, M.J. Van Demark, C. Poirier, M.J. Justice, W.C. Hubbard, E.S. Kim, X. Lai, and M. Wang, Endothelial disruptive pro-inflammatory effects of nicotine and e-cigarette vapor exposures. American Journal of Physiology-Lung Cellular and Molecular Physiology, (2015): p. ajplung. 00411.2015.

[37] M. Taylor, T. Carr, O. Oke, T. Jaunky, D. Breheny, F. Lowe, and M. Gaça, E-cigarette aerosols induce lower oxidative stress in vitro when compared to tobacco smoke. Toxicology Mechanisms and Methods, (2016). **26**(6): p. 465-476.

[38] D. Thorne, S. Larard, A. Baxter, C. Meredith, and M. Gaça, The comparative in vitro assessment of e-cigarette and cigarette smoke aerosols using the γH2AX assay and applied dose measurements. Toxicology Letters, (2017). **265**: p. 170-178.

[39] I. Willershausen, T. Wolf, V. Weyer, R. Sader, S. Ghanaati, and B. Willershausen, Influence of E-smoking liquids on human periodontal ligament fibroblasts. Head & face medicine, (2014). **10**(1): p. 39.

[40] M. Williams, A. Villarreal, K. Bozhilov, S. Lin, and P. Talbot, Metal and silicate particles including nanoparticles are present in electronic cigarette cartomizer fluid and aerosol. (2013).

[41] Q. Wu, D. Jiang, M. Minor, and H.W. Chu, Electronic cigarette liquid increases inflammation and virus infection in primary human airway epithelial cells. (2014).

[42] V. Yu, M. Rahimy, A. Korrapati, Y. Xuan, A.E. Zou, A.R. Krishnan, T. Tsui, J.A. Aguilera, S. Advani, and L.E.C. Alexander, Electronic cigarettes induce DNA strand breaks and cell death independently of nicotine in cell lines. Oral oncology, (2016). **52**: p. 58-65.

[43] R.Z. Behar, M. Hua, and P. Talbot, Puffing Topography and Nicotine Intake of Electronic Cigarette Users. PloS one, (2015). **10**(2): p. e0117222.

[44] B. Dautzenberg and D. Bricard, Real-Time Characterization of E-Cigarettes Use: The 1 Million Puffs Study. Journal of Addiction Research & Therapy, (2015). **2015**.

[45] J.-F. Etter, Electronic cigarettes: a survey of users. BMC public health, (2010). **10**(1): p. 231.

[46] J.F. Etter, Levels of saliva cotinine in electronic cigarette users. Addiction, (2014). **109**(5): p. 825-829.

[47] J.F. Etter and C. Bullen, Electronic cigarette: users profile, utilization, satisfaction and perceived efficacy. Addiction, (2011). **106**(11): p. 2017-2028.

[48] K.E. Farsalinos, G. Romagna, D. Tsiapras, S. Kyrzopoulos, and V. Voudris, Evaluation of electronic cigarette use (vaping) topography and estimation of liquid consumption: implications for research protocol standards definition and for public health authorities' regulation. International journal of environmental research and public health, (2013). **10**(6): p. 2500-2514.

[49] M. Hua, H. Yip, and P. Talbot, Mining data on usage of electronic nicotine delivery systems (ENDS) from YouTube videos. Tobacco Control, (2013). **22**(2): p. 103-106.

[50] K.J. Norton, K.M. June, and R.J. O'Connor, Initial puffing behaviors and subjective responses differ between an electronic nicotine delivery system and traditional cigarettes. Tobacco induced diseases, (2014). **12**(1): p. 17.

[51] R. Robinson, E. Hensel, P. Morabito, and K. Roundtree, Electronic cigarette topography in the natural environment. PloS one, (2015). **10**(6): p. e0129296.

[52] F. Fuoco, G. Buonanno, L. Stabile, and P. Vigo, Influential parameters on particle concentration and size distribution in the mainstream of e-cigarettes. Environmental Pollution, (2014). **184**: p. 523-529.

[53] B.J. Ingebrethsen, S.K. Cole, and S.L. Alderman, Electronic cigarette aerosol particle size distribution measurements. Inhalation toxicology, (2012). **24**(14): p. 976-984.

[54] M. Laugesen. *Ruyan e-cigarette bench-top tests*. in *Poster presented to the joint conference of the Society for Research on Nicotine and Tobacco and Society for Research on Nicotine and Tobacco-Europe*. 2009.

[55] C.A. Lerner, I.K. Sundar, R.M. Watson, A. Elder, R. Jones, D. Done, R. Kurtzman, D.J. Ossip, R. Robinson, and S. McIntosh, Environmental health hazards of e-cigarettes and their components: Oxidants and copper in e-cigarette aerosols. Environmental Pollution, (2015). **198**: p. 100-107.

[56] M. Manigrasso, G. Buonanno, F.C. Fuoco, L. Stabile, and P. Avino, Aerosol deposition doses in the human respiratory tree of electronic cigarette smokers. Environmental Pollution, (2015). **196**: p. 257-267.

[57] M. Manigrasso, G. Buonanno, L. Stabile, L. Morawska, and P. Avino, Particle doses in the pulmonary lobes of electronic and conventional cigarette users. Environmental Pollution, (2015). **202**: p. 24-31.

[58] V.B. Mikheev, M.C. Brinkman, C.A. Granville, S.M. Gordon, and P.I. Clark, Real-time measurement of electronic cigarette aerosol size distribution and metals content analysis. Nicotine & Tobacco Research, (2016): p. ntw128.

[59] T. Schripp, D. Markewitz, E. Uhde, and T. Salthammer, Does e-cigarette consumption cause passive vaping? Indoor air, (2013). **23**(1): p. 25-31.

[60] T.R. Sosnowski and K. Kramek-Romanowska, Predicted Deposition of E-Cigarette Aerosol in the Human Lungs. Journal of aerosol medicine and pulmonary drug delivery, (2016).

[61] M. Sundahl, E. Berg, and M. Svensson, Aerodynamic particle size distribution and dynamic properties in aerosols from electronic cigarettes. Journal of Aerosol Science, (2017). **103**: p. 141-150.

[62] S. Talih, Z. Balhas, T. Eissenberg, R. Salman, N. Karaoghlanian, A. El Hellani, R. Baalbaki, N. Saliba, and A. Shihadeh, Effects of user puff topography, device voltage, and liquid nicotine concentration on electronic cigarette nicotine yield: measurements and model predictions. Nicotine & Tobacco Research, (2015). **17**(2): p. 150-157.

[63] Y. Zhang, W. Sumner, and D.-R. Chen, In vitro particle size distributions in electronic

and conventional cigarette aerosols suggest comparable deposition patterns. Nicotine & tobacco research, (2013). **15**(2): p. 501-508.

[64] T. Zhao, S. Shu, Q. Guo, and Y. Zhu, Effects of design parameters and puff topography on heating coil temperature and mainstream aerosols in electronic cigarettes. Atmospheric Environment, (2016). **134**: p. 61-69.

[65] N. Beauval, M. Howsam, S. Antherieu, D. Allorge, M. Soyez, G. Garçon, J. Goossens, J. Lo-Guidice, and A. Garat, Trace elements in e-liquids-Development and validation of an ICP-MS method for the analysis of electronic cigarette refills. Regulatory Toxicology and Pharmacology, (2016). **79**: p. 144-148.

[66] J.F. Etter, E. Zäther, and S. Svensson, Analysis of refill liquids for electronic cigarettes. Addiction, (2013). **108**(9): p. 1671-1679.

[67] K.E. Farsalinos, K.A. Kistler, G. Gillman, and V. Voudris, Evaluation of electronic cigarette liquids and aerosol for the presence of selected inhalation toxins. Nicotine & Tobacco Research, (2014). **17**(2): p. 168-174.

[68] M.L. Goniewicz, T. Kuma, M. Gawron, J. Knysak, and L. Kosmider, Nicotine levels in electronic cigarettes. Nicotine & Tobacco Research, (2012): p. nts103.

[69] C.A. Hess, P. Olmedo, A. Navas-Acien, W. Goessler, J.E. Cohen, and A.M. Rule, E-cigarettes as a source of toxic and potentially carcinogenic metals. Environmental Research, (2017). **152**: p. 221-225.

[70] M.P. Kavvalakis, P.D. Stivaktakis, M.N. Tzatzarakis, D. Kouretas, J. Liesivuori, A.K. Alegakis, D. Vynias, and A.M. Tsatsakis, Multicomponent analysis of replacement liquids of electronic cigarettes using chromatographic techniques. Journal of analytical toxicology, (2015). **39**(4): p. 262-269.

[71] H.-J. Kim and H.-S. Shin, Determination of tobacco-specific nitrosamines in replacement liquids of electronic cigarettes by liquid chromatography–tandem mass spectrometry. Journal of Chromatography A, (2013). **1291**: p. 48-55.

[72] P. Kubica, A. Wasik, A. Kot-Wasik, and J. Namieśnik, An evaluation of sucrose as a possible contaminant in e-liquids for electronic cigarettes by hydrophilic interaction liquid chromatography–tandem mass spectrometry. Analytical and bioanalytical chemistry, (2014). **406**(13): p. 3013-3018.

[73] H.-H. Lim and H.-S. Shin, Measurement of aldehydes in replacement liquids of electronic cigarettes by headspace gas chromatography-mass spectrometry. B Kor Chem Soc, (2013). **34**(9): p. 2691-2696.

[74] J.G. Lisko, H. Tran, S.B. Stanfill, B.C. Blount, and C.H. Watson, Chemical composition

and evaluation of nicotine, tobacco alkaloids, pH, and selected flavors in e-cigarette cartridges and refill solutions. Nicotine & Tobacco Research, (2015). **17**(10): p. 1270-1278.

[75] P.A. Tierney, C.D. Karpinski, J.E. Brown, W. Luo, and J.F. Pankow, Flavour chemicals in electronic cigarette fluids. Tobacco control, (2015): p. tobaccocontrol-2014-052175.

[76] V. Varlet, K. Farsalinos, M. Augsburger, A. Thomas, and J.-F. Etter, Toxicity assessment of refill liquids for electronic cigarettes. International journal of environmental research and public health, (2015). **12**(5): p. 4796-4815.

[77] K.E. Farsalinos, N. Yannovits, T. Sarri, V. Voudris, and K. Poulas, Protocol proposal for, and evaluation of, consistency in nicotine delivery from the liquid to the aerosol of electronic cigarettes atomizers: regulatory implications. Addiction, (2016).

[78] K.E. Farsalinos, G. Gillman, K. Poulas, and V. Voudris, Tobacco-Specific Nitrosamines in Electronic Cigarettes: Comparison between Liquid and Aerosol Levels. International journal of environmental research and public health, (2015). **12**(8): p. 9046-9053.

[79] M.L. Goniewicz, J. Knysak, M. Gawron, L. Kosmider, A. Sobczak, J. Kurek, A. Prokopowicz, M. Jablonska-Czapla, C. Rosik-Dulewska, and C. Havel, Levels of selected carcinogens and toxicants in vapour from electronic cigarettes. Tobacco control, (2014). **23**(2): p. 133-139.

[80] R.E. Martinez, S. Dhawan, W. Sumner, and B.J. Williams, On-line chemical composition analysis of refillable electronic cigarette aerosol—measurement of nicotine and nicotyrine. Nicotine & Tobacco Research, (2015). **17**(10): p. 1263-1269.

[81] M.L. Trehy, W. Ye, M.E. Hadwiger, T.W. Moore, J.F. Allgire, J.T. Woodruff, S.S. Ahadi, J.C. Black, and B.J. Westenberger, Analysis of electronic cigarette cartridges, refill solutions, and smoke for nicotine and nicotine related impurities. Journal of Liquid Chromatography & Related Technologies, (2011). **34**(14): p. 1442-1458.

[82] J.G. Allen, S.S. Flanigan, M. LeBlanc, J. Vallarino, P. MacNaughton, J.H. Stewart, and D.C. Christiani, Flavoring Chemicals in E-Cigarettes: Diacetyl, 2, 3-Pentanedione, and Acetoin in a Sample of 51 Products, Including Fruit-, Candy-, and Cocktail-Flavored E-Cigarettes. Environ Health Perspect, (2015).

[83] K.E. Farsalinos, V. Voudris, and K. Poulas, E-cigarettes generate high levels of aldehydes only in 'dry puff'conditions. Addiction, (2015).

[84] J.W. Flora, N. Meruva, C.B. Huang, C.T. Wilkinson, R. Ballentine, D.C. Smith, M.S. Werley, and W.J. McKinney, Characterization of potential impurities and degradation products in electronic cigarette formulations and aerosols. Regulatory Toxicology and

Pharmacology, (2016). **74**: p. 1-11.

[85] J.W. Flora, C.T. Wilkinson, J.W. Wilkinson, P.J. Lipowicz, J.A. Skapars, A. Anderson, and J.H. Miller, Method for the Determination of Carbonyl Compounds in E-Cigarette Aerosols. Journal of chromatographic science, (2017). **55**(2): p. 142-148.

[86] O. Geiss, I. Bianchi, F. Barahona, and J. Barrero-Moreno, Characterisation of mainstream and passive vapours emitted by selected electronic cigarettes. International journal of hygiene and environmental health, (2015). **218**(1): p. 169-180.

[87] O. Geiss, I. Bianchi, and J. Barrero-Moreno, Correlation of volatile carbonyl yields emitted by e-cigarettes with the temperature of the heating coil and the perceived sensorial quality of the generated vapours. International journal of hygiene and environmental health, (2016). **219**(3): p. 268-277.

[88] I. Gillman, K. Kistler, E. Stewart, and A. Paolantonio, Effect of variable power levels on the yield of total aerosol mass and formation of aldehydes in e-cigarette aerosols. Regulatory Toxicology and Pharmacology, (2016). **75**: p. 58-65.

[89] J.S. Herrington and C. Myers, Electronic cigarette solutions and resultant aerosol profiles. Journal of Chromatography A, (2015). **1418**: p. 192-199.

[90] R.P. Jensen, W. Luo, J.F. Pankow, R.M. Strongin, and D.H. Peyton, Hidden formaldehyde in e-cigarette aerosols. New England Journal of Medicine, (2015). **372**(4): p. 392-394.

[91] A. Khlystov and V. Samburova, Flavoring compounds dominate toxic aldehyde production during e-cigarette vaping. Environmental science & technology, (2016). **50**(23): p. 13080-13085.

[92] L. Kosmider, A. Sobczak, M. Fik, J. Knysak, M. Zaciera, J. Kurek, and M.L. Goniewicz, Carbonyl compounds in electronic cigarette vapors—effects of nicotine solvent and battery output voltage. Nicotine & Tobacco Research, (2014): p. ntu078.

[93] E. Marco and J.O. Grimalt, A rapid method for the chromatographic analysis of volatile organic compounds in exhaled breath of tobacco cigarette and electronic cigarette smokers. Journal of Chromatography A, (2015). **1410**: p. 51-59.

[94] T.R. McAuley, P. Hopke, J. Zhao, and S. Babaian, Comparison of the effects of e-cigarette vapor and cigarette smoke on indoor air quality. Inhalation toxicology, (2012). **24**(12): p. 850-857.

[95] M.A. Ogunwale, M. Li, M.V. Ramakrishnam Raju, Y. Chen, M.H. Nantz, D.J. Conklin, and X.-A. Fu, Aldehyde Detection in Electronic Cigarette Aerosols. ACS omega, (2017). **2**(3): p. 1207-1214.

[96] M. Sleiman, J.M. Logue, V.N. Montesinos, M.L. Russell, M.I. Litter, L.A. Gundel, and H. Destaillats, Emissions from electronic cigarettes: key parameters affecting the release of harmful chemicals. Environmental science & technology, (2016). **50**(17): p. 9644-9651.

[97] R. Tayyarah and G.A. Long, Comparison of select analytes in aerosol from e-cigarettes with smoke from conventional cigarettes and with ambient air. Regulatory Toxicology and Pharmacology, (2014). **70**(3): p. 704-710.

[98] S. Uchiyama, Y. Inaba, and N. Kunugita, Determination of acrolein and other carbonyls in cigarette smoke using coupled silica cartridges impregnated with hydroquinone and 2, 4-dinitrophenylhydrazine. Journal of Chromatography A, (2010). **1217**(26): p. 4383-4388.

[99] S. Uchiyama, K. Ohta, Y. Inaba, and N. Kunugita, Determination of carbonyl compounds generated from the E-cigarette using coupled silica cartridges impregnated with hydroquinone and 2, 4-dinitrophenylhydrazine, followed by high-performance liquid chromatography. Analytical Sciences, (2013). **29**(12): p. 1219-1222.

[100] S. Uchiyama, Y. Senoo, H. Hayashida, Y. Inaba, H. Nakagome, and N. Kunugita, Determination of Chemical compounds generated from Second-generation E-cigarettes using a Sorbent Cartridge followed by a Two-step Elution Method. Analytical Sciences, (2016). **32**(5): p. 549-555.

[101] P. Wang, W. Chen, J. Liao, T. Matsuo, K. Ito, J. Fowles, D. Shusterman, M. Mendell, and K. Kumagai, A Device-Independent Evaluation of Carbonyl Emissions from Heated Electronic Cigarette Solvents. PloS one, (2017). **12**(1): p. e0169811.

[102] R. Goel, E. Durand, N. Trushin, B. Prokopczyk, J. Foulds, R.J. Elias, and J.P. Richie Jr, Highly reactive free radicals in electronic cigarette aerosols. Chemical Research in Toxicology, (2015). **28**(9): p. 1675-1677.

Appendix 2

Particles generated from e-cigarette vaping

I. Chemical components of flavoring ingredients used in e-liquids

II. Vaping topography measurements

III. The experimental settings for e-cigarette particle generation

IV. Merging the particle size distributions obtained from SMPS and OPC

V. Mass median diameter (MMD) calculation

VI. The impact of dilution on the sizes and number concentrations of e-cigarette particles

VII. MPPD model assumptions and the deposition of e-cigarette particles

I. Chemical components of flavoring ingredients used in e-liquids (provided by the vendor/manufacturer)

The chemical components of the flavoring ingredients were only partially released by the vendors/manufactures. The strawberry (ripe), dragonfruit, menthol, and sweet cream flavors consist of natural/artificial flavors in propylene glycol (PG). The Bavarian cream flavor consists of natural/artificial flavors, PG, and water. The cinnamon flavor is composed of artificial flavors in ethyl alcohol. The bubblegum (fruity) flavor consists of natural/artificial flavors in PG and ethyl alcohol. The graham cracker flavor is composed of natural/artificial flavor in PG and water, with caramel color, corn syrup, ethyl alcohol, and salt.

II. Vaping topography measurements

The demographics of the study participants are summarized in Table S2-1.

Table S2-1. Summary of the study participants

Number of subject	23
Age	25 ± 10 (18-52) years
Gender	21 men and 2 women
Ethnicity	16 White; 1 Black; 3 Asian; 6 others
Duration of e-cigarette use	1.4 ± 0.9 (0.4-4.0) years

Table S2-2 shows the mean, the standard deviation, and the range of e-cigarette vaping topography, device power output, and nicotine contents of the 23 study participants in our study. E-cigarette device power output ranged from 5 watts to 59.7 watts, with an average power output of 13.7 watts. The average nicotine content in e-liquids was 11.9 ± 10.0 mg/mL, with a maximum nicotine level of 36 mg/mL. Most subjects used vegetable glycerin (VG) based e-liquids (14 participants), followed by PG:VG mixed e-liquids (7 participants), and PG-based e-liquids (2 participants).

Table S2-2. Vaping topographies, e-cigarette device power settings, and nicotine contents in e-liquids across the 23 study participants

Parameters	**Mean**	**SD**	**Percentiles**						
			Min	**10**	**25**	**50**	**75**	**90**	**Max**
Puff volume (mL)	100.17	55.57	9.99	38.39	63.58	90.04	135.6	160.5	251.1
Puff duration (sec)	3.69	1.16	1.26	2.08	3.24	3.85	4.24	5.06	5.77
Puff interval (sec)	24.30	17.30	8.01	11.90	13.86	18.67	26.35	67.91	69.39
Power (W)	13.70	15.14	5.00	5.48	6.26	7.61	12.96	27.38	59.67
Nicotine (mg/mL)	11.92	10.04	0.00	3.00	3.00	12.00	19.50	24.00	36.00

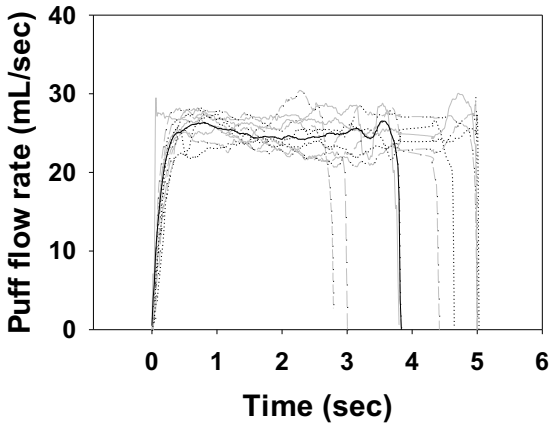

Figure S2-1. Observed e-cigarette puff patterns using the Cress pocket device for the study participants

Figure S2-1 shows Observed e-cigarette puff patterns using the Cress pocket device for the study participants.

III. The experimental settings for e-cigarette particle generation

E-cigarette particles were generated under the following conditions specified in Table S2-3.

Table S2-3. The experimental settings for e-cigarette particle generation

Experiments	Factors	Settings	Other Settings
Device setting	Device power (watt)	6.4, 14.7, 31.3	90 mL puff volume, 3.8 sec puff duration, 12 mg/ml nicotine in VG
	Air hole size (mm)	1, 1.5, 2	
Vaping topography	Puff volume (ml)	35, 90, 170	6.4 W, 2 mm air hole and 12 mg/ml nicotine in VG;
	Puff duration (sec)	2, 3.8	
E-liquid bulk material	Base material	PG, VG, PG&VG (v:v = 1:1)	6.4 W, 2 mm air hole, 90 mL puff volume, 3.8 sec puff duration
	Nicotine (mg/ml)	0, 3, 12, 24, 36	
E-liquid flavoring agents	Flavor	8 flavors*	6.4 W, 2 mm air hole, 90 mL puff volume, 3.8 sec puff duration
	Flavoring level (%)	1, 10**	

***Strawberry (Ripe), dragonfruit, menthol, cinnamon, bubblegum, bavarian cream, sweet cream, and graham cracker; **0.1% and 1% for the cinnamon flavor**

IV. Merging the particle size distributions obtained from SMPS and OPC

The particle size distributions obtained from SMPS and OPC were combined using weighted averages (Figure S2-2). In brief, particle number concentration for 0.434-1.0 μm size bin was obtained from the portable SMPS, and 0.3-0.5 μm, 0.5-1.0 μm size bins were obtained from the OPC. Then, two size bins (0.434-0.5 μm, 0.5-1.0 μm) were reconstructed using the weighted averaging method based on the width of the size bins. In addition, particle number concentrations for the size ranges of 10-434 nm and 1.0-5.0 μm were directly obtained and used from the SMPS and OPC, respectively.

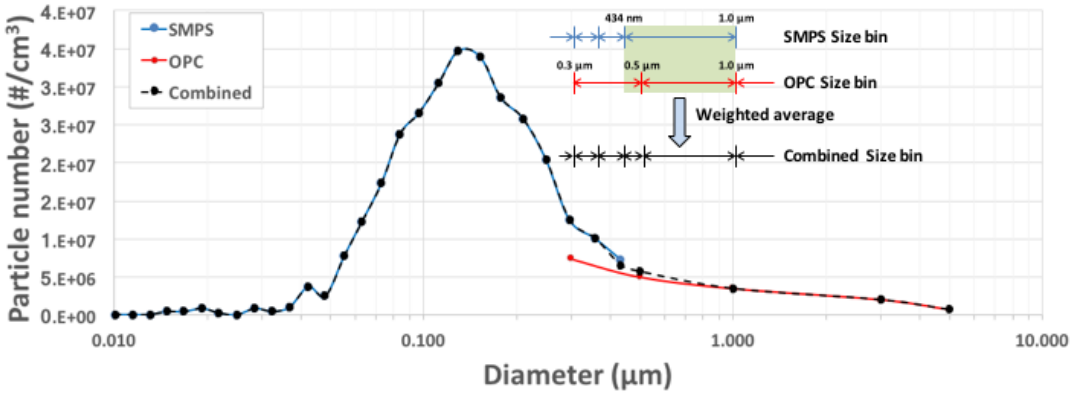

Figure S2-2. Merging particle size distributions obtained from the portable SMPS and the OPC

V. Mass median diameter (MMD) calculation

The MMDs were calculated based on the measured particle count distribution and the density of e-liquids used for e-vapor generation. Briefly, density of the eight flavoring agents were measured in our lab and listed in Table S4. Then, particle mass distributions were generated based on the measured particle count distribution and the densities of e-liquids estimated using the ratio of e-liquid components (e.g. density of VG:PG=1:1 (v/v) is 1.15 g/ml). Finally, MMDs were calculated using the particle mass distribution.

Table S2-4. Density of PG, VG, and flavoring agents

Components	Density (g/ml)
PG	1.040
VG	1.260
Strawberry	1.030
Dragonfruit	1.040
Menthol	0.910
Cinnamon	0.950
Bubble gum	0.975
Bavarian	1.044
Sweet cream	1.072
Graham cracker	1.062

VI. The impact of dilution on the sizes and number concentrations of e-cigarette particles

The measured CMD, GSD and particle number concentration under each dilution condition are presented in Tables S2-5-S2-9. Data presented in Tables S2-5-S2-9 were used to develop the relationship between dilution ratios and CMDs. First, the measured CMDs were regressed on pre-determined dilution ratios using polynomial regressions, and the intercept of the polynomial regression (i.e. the dilution ratio = 0) was regarded as CMD_o. Then, the association between dilution ratios and CMDs were quantified using a non-linear regression (Equation S2-1):

$$\frac{CMD_m}{CMD_o} = ae^{-Db} + c \qquad \textbf{Equation S2-1}$$

where D is the pre-determined dilution ratio; CMD_o is the estimated undiluted CMD with the polynomial regression; CMD_m is the measured CMD; and a, b, and c are the regression coefficients for the exponential decaying curve. The regression parameters are summarized in Table S2-10 for each particle generation condition.

Table S2-5. The impact of dilution on CMD (nm), GSD, and particle number concentration (NC, number of particles per cm^3) of e-cigarette particles generated under different power settings (mean ± sd; N=5)

Dilution ratio	Parameter	Device power		
		6.4W	14.7W	31.3W
548	CMD	202 ± 21	221 ± 15	-
	GSD	1.83 ± 0.13	1.58 ± 0.06	-
	NC	$(1.79 \pm 0.16) \times 10^8$	$(4.04 \pm 0.61) \times 10^8$	-
1068	CMD	164 ± 4	167 ± 15	169 ± 15
	GSD	1.89 ± 0.09	1.89 ± 0.05	1.74 ± 0.05
	NC	$(1.61 \pm 0.11) \times 10^8$	$(4.43 \pm 0.82) \times 10^8$	$(7.00 \pm 0.28) \times 10^8$
2012	CMD	152 ± 26	165 ± 10	158 ± 6
	GSD	2.42 ± 0.18	1.75 ± 0.04	1.76 ± 0.21
	NC	$(1.38 \pm 0.48) \times 10^8$	$(3.19 \pm 0.87) \times 10^8$	$(6.79 \pm 0.65) \times 10^8$
4179	CMD	143 ± 17	170 ± 11	154 ± 2
	GSD	2.70 ± 0.23	1.77±0.15	1.72 ± 0.10
	NC	$(2.35 \pm 0.89) \times 10^8$	$(2.04 \pm 0.86) \times 10^8$	$(5.20 \pm 1.06) \times 10^8$
8087	CMD	136 ± 13	164 ± 10	166 ± 5
	GSD	2.67 ± 0.12	1.79 ± 0.10	1.92 ± 0.09
	NC	$(2.47 \pm 0.67) \times 10^8$	$(2.54 \pm 0.71) \times 10^8$	$(6.03 \pm 0.71) \times 10^8$
15907	CMD	-	-	156 ± 3
	GSD	-	-	1.85 ± 0.10
	NC	-	-	$(5.70 \pm 1.12) \times 10^8$

Table S2-6. The impact of dilution on CMD (nm), GSD, and particle number concentration (NC, number of particles per cm^3) of e-cigarette particles for 35 mL puffs (mean ± sd; N=5)

Dilution ratio	Parameter	Vaping topography (puff volume, puff duration)	
		35mL, 2sec	35mL, 3.8sec
396	CMD	159 ± 6	194 ± 9
	GSD	1.64 ± 0.20	1.50 ± 0.04
	NC	$(1.94 \pm 0.52) \times 10^7$	$(7.07 \pm 0.70) \times 10^7$
1405	CMD	151 ± 14	173 ± 9
	GSD	1.80 ± 0.33	1.60 ± 0.06
	NC	$(1.80 \pm 0.38) \times 10^7$	$(4.66 \pm 1.56) \times 10^7$
2097	CMD	128 ± 28	137 ± 13
	GSD	1.86 ± 0.90	1.55 ± 0.17
	NC	$(1.82 \pm 0.94) \times 10^7$	$(3.28 \pm 1.15) \times 10^7$
4047	CMD	116 ± 23	117 ± 8
	GSD	1.87 ± 0.92	1.44±0.03
	NC	$(1.51 \pm 0.70) \times 10^7$	$(4.45 \pm 0.99) \times 10^7$
8106	CMD	120 ± 16	120 ± 9
	GSD	1.75 ± 0.60	1.47 ± 0.04
	NC	$(1.22 \pm 0.35) \times 10^7$	$(3.29 \pm 0.24) \times 10^7$

Table S2-7. The impact of dilution on CMD (nm), GSD, and particle number concentration (NC, number of particles per cm^3) of e-cigarette particles for 90 mL puffs (mean ± sd; N=5)

Dilution ratio	Parameter	Vaping topography (puff volume, puff duration)	
		90mL, 2sec	90mL, 3.8sec
548	CMD	145 ± 5	202 ± 21
	GSD	2.50 ± 0.05	1.83 ± 0.13
	NC	$(6.10 \pm 0.70) \times 10^7$	$(1.79 \pm 0.16) \times 10^8$
1068	CMD	126 ± 14	164 ± 4
	GSD	2.79 ± 0.30	1.89 ± 0.09
	NC	$(6.66 \pm 1.32) \times 10^7$	$(1.61 \pm 0.11) \times 10^8$
2012	CMD	117 ± 7	152 ± 26
	GSD	3.60 ± 0.13	2.42 ± 0.18
	NC	$(5.23 \pm 0.34) \times 10^7$	$(1.38 \pm 0.48) \times 10^8$
4179	CMD	124 ± 6	143 ± 17
	GSD	3.64 ± 0.15	2.70 ± 0.23
	NC	$(7.95 \pm 1.16) \times 10^7$	$(2.35 \pm 0.89) \times 10^8$
8087	CMD	115 ± 8	136 ± 13
	GSD	3.78 ± 0.18	2.67 ± 0.12
	NC	$(5.07 \pm 0.82) \times 10^7$	$(2.47 \pm 0.67) \times 10^8$

Table S2-8. The impact of dilution on CMD (nm), GSD, and particle number concentration (NC, number of particles per cm^3) of e-cigarette particles for 170 mL puffs (mean ± sd; N=5)

Dilution ratio	Parameter	Vaping topography (puff volume, puff duration)	
		170mL, 2sec	170mL, 3.8sec
548	CMD	135 ± 9	-
	GSD	3.15 ± 0.22	-
	NC	$(8.72 \pm 0.56) \times 10^7$	-
1068	CMD	112 ± 10	183 ± 7
	GSD	3.16 ± 0.23	2.04 ± 0.05
	NC	$(8.47 \pm 0.20) \times 10^7$	$(6.04 \pm 0.37) \times 10^8$
2012	CMD	94 ± 8	146 ± 12
	GSD	3.21 ± 0.14	2.28 ± 0.12
	NC	$(7.86 \pm 0.70) \times 10^7$	$(6.88 \pm 0.45) \times 10^8$
4179	CMD	87 ± 12	120 ± 6
	GSD	2.82 ± 0.32	2.44 ± 0.08
	NC	$(8.45 \pm 1.12) \times 10^7$	$(6.69 \pm 1.15) \times 10^8$
8087	CMD	84 ± 6	115 ± 9
	GSD	2.61 ± 0.11	2.30 ± 0.28
	NC	$(6.82 \pm 3.02) \times 10^7$	$(4.18 \pm 0.45) \times 10^8$
15907	CMD	-	102 ± 6
	GSD	-	2.22 ± 0.22
	NC	-	$(5.26 \pm 0.35) \times 10^8$

Table S2-9. The impact of dilution on CMD (nm), GSD, and particle number concentration (NC, number of particles per cm^3) of e-cigarette particles generated from different e-liquids (mean ± sd; N=5)

Dilution ratio	Parameter	E-liquid (base material with 12 mg/mL nicotine)		
		PG	PG:VG=1:1 (v/v)	VG
548	CMD	146 ± 12	166 ± 16	202 ± 21
	GSD	2.17 ± 0.09	2.06 ± 0.12	1.83 ± 0.13
	NC	$(8.72 \pm 0.85) \times 10^7$	$(2.48 \pm 0.08) \times 10^8$	$(1.79 \pm 0.16) \times 10^8$
1068	CMD	139 ± 6	148 ± 12	164 ± 4
	GSD	2.39 ± 0.09	2.27 ± 0.10	1.89 ± 0.09
	NC	$(8.62 \pm 0.67) \times 10^7$	$(1.60 \pm 0.24) \times 10^8$	$(1.61 \pm 0.11) \times 10^8$
2012	CMD	118 ± 3	136 ± 12	152 ± 26
	GSD	2.71 ± 0.09	2.45 ± 0.13	2.42 ± 0.18
	NC	$(9.25 \pm 0.44) \times 10^7$	$(2.00 \pm 0.27) \times 10^8$	$(1.38 \pm 0.48) \times 10^8$
4179	CMD	120 ± 9	128 ± 10	143 ± 17
	GSD	2.48 ± 0.09	2.53 ± 0.09	2.70 ± 0.23
	NC	$(8.34 \pm 0.99) \times 10^7$	$(2.09 \pm 0.09) \times 10^8$	$(2.35 \pm 0.89) \times 10^8$
8087	CMD	128 ± 6	120 ± 10	136 ± 13
	GSD	2.62 ± 0.14	2.22 ± 0.11	2.67 ± 0.12
	NC	$(7.75 \pm 0.68) \times 10^7$	$(2.34 \pm 0.27) \times 10^8$	$(2.47 \pm 0.67) \times 10^8$

Table S2-10. The regression coefficients of Equation S4 under various particle generation conditions

Category	Conditions	Parameters				R^2
		CMD_o	a	b	c	
Device setting	6.4W*	232	0.414	-0.001	0.586	0.68
	14.7W	256	0.350	-0.001	0.650	0.57
	31.3W	259	0.384	-0.001	0.616	0.74
Topography	35mL, 2sec	168	0.297	0.000	0.703	0.44
	35mL, 3.8sec	211	0.440	-0.001	0.560	0.84
	90mL, 2sec	166	0.278	-0.001	0.722	0.50
	90mL, 3.8sec*	232	0.414	-0.001	0.586	0.68
	170mL,2sec	162	0.473	-0.001	0.527	0.83
	170mL, 3.8sec	223	0.511	0.000	0.489	0.30
E-liquid	VG*	232	0.414	-0.001	0.586	0.68
	PG:VG	184	0.327	-0.001	0.673	0.64
	PG	167	0.258	-0.001	0.742	0.52

***E-cigarette particles were generated under the same setting.**

VII. MPPD model assumptions and the deposition of e-cigarette particles in the human respiratory system

The input parameters for the MPPD model are specified in Table S2-11. In brief, the Yeh/Schum symmetric lung model was used in dosimetry modeling. The functional reserve capacity, the upper respiratory tract volume, the total inhalation volume, and the breathing periods were adopted from the ICRP (International Commission on Radiological Protection) model for human respiratory track deposition [1]. The aerosol density was set as the density of VG, PG, or the averaged density of VG and PG. Input parameters informed directly from our study include smoking topographies which are specified in Table S2-11, and the CMDs and GSDs of e-cigarette particles measured in our study.

Table S2-11. The input parameters for the MPPD model

Parameter	Value	Reference
Model type	Yeh/Schum symmetric lung	ICRP [1]
Functional reserve capacity	3,300 ml	ICRP [1]
Upper respiratory tract volume	50 ml	ICRP [1]
Total inhalation volume	500 ml	ICRP [1]
Breathing period	5 seconds	ICRP [1]
Puff volume	Obtained from this study	This study
Inhalation time	Obtained from this study	This study
Aerosol concentration	Obtained from this study	This study
Aerosol density	VG: 1.26 g/ml, PG: 1.04 g/ml, PG:VG: 1.15 g/ml	This study
Count median diameter	Obtained from this study	This study
Geometric standard deviation	Obtained from this study	This study

Since a single particle in a particle cloud is confined within the cloud and moves with the cloud, the settling velocity of the single particle equals the settling velocity of the cloud. Therefore, a cloud-equivalent particle diameter (D_c) was calculated (Equations S2-2, -3, and -4), so that a free particle with a diameter of D_c has the same settling velocity of a cloud, and acts like the particle cloud in terms of deposition in the upper respiratory airways.

The normalized settling velocity of a particle cloud is defined as:

$$V_c = \frac{\emptyset R^3}{F_c C_c(a)} \qquad \textbf{Equation S2-2}$$

where V_c is the normalized settling velocity of a particle cloud, φ is the volume fraction of particles in the cloud, R is the ratio of the cloud diameter and particle diameter, *a* is the half of the measured CMD, F_c is the drag force of the cloud, and C_c is the Cunningham's slip correction factor [2].

The normalized settling velocity of a particle is defined as:

$$V_p = \frac{a_c{}^2 \rho_p g C_c}{18\mu} \qquad \textbf{Equation S2-3}$$

where V_p is the settling velocity of an individual particle with the cloud-equivalent particle diameter of D_c, a_c is the half of the cloud effect equivalent diameter, ρ_p is the particle density (1.26 mg/cm^3 for VG, 1.06 mg/cm^3 for PG, and 1.15 mg/cm^3 for the PG&VG mixture (PG:VG=1:1)), g is the gravity acceleration (9.8 m/s^2), and μ is the fluid viscosity [3].

When the setting velocity of the particle cloud equals the particle with the cloud-equivalent particle diameter (i.e. $V_c = V_p$), D_c can be calculated as:

$$D_c = 2\sqrt{\frac{8\mu\emptyset R^3}{\rho_p g F_c C_c{}^2(a)}} \qquad \textbf{Equation S2-4}$$

Finally, the measured e-cigarette particle diameter, D_p, was used to estimate the deposition of e-cigarette particles in the bronchoalveolar regions (E_{pul}); and the calculated cloud effect

equivalent diameter, D_c, was employed to estimate the deposition of e-cigarette particles in the TB region (E_{TB}).

We estimated the deposition of cigarette smoke particles in the human respiratory system using the approach we proposed above, and our results was consistent with previous studies [2, 4]. Broday and Robinson [2] reported that the deposition fractions for cigarette smoke (D_p=0.25 μm, GSD=1.3, ρ=1 g/ml, N=10^9 /mL) in the TB and the bronchoalveolar regions were 0.400 and 0.220, respectively. Asgharian et al [4] reported deposition fractions of 0.600 and 0.112, respectively, in the TB and the bronchoalveolar regions for cigarette smoke (D_p=0.20μm, GSD=1.3, ρ=1 g/ml, N=10^9 /ml). Based on the particle properties reported in Broday and Robinson [2] and Asgharian et al [4], we calculated the cloud-equivalent particle diameters using Equations S2-2-S2-4, and we estimated that the deposition fractions of cigarette particles in the TB region were 0.502 and 0.509, similar to the values reported by Broday and Robinson [2] and Asgharian et al [4], respectively.

Figure S2-3 illustrates the calculated e-cigarette particle deposition in human airways with and without cloud effects and Tables S2-12-S2-15 present modeled deposition fractions of e-cigarette particles in the TB and the bronchoalveolar regions in human airways. Similar deposition fractions in the TB and the bronchoalveolar regions were observed across different e-cigarette power outputs: 0.528 in the TB region and 0.265 in the bronchoalveolar regions, respectively, at 6.4 watts; and 0.506 in the TB region and 0.346 in the bronchoalveolar regions, respectively, at 31.3 watts. In contrast, larger puff volumes were associated with higher TB region depositions, which were 0.516, 0.528, and 0.541 for 35 ml, 90 ml, and 170 ml puffs, respectively. Deposition fractions of e-cigarette particles were similar across different e-liquids with various components.

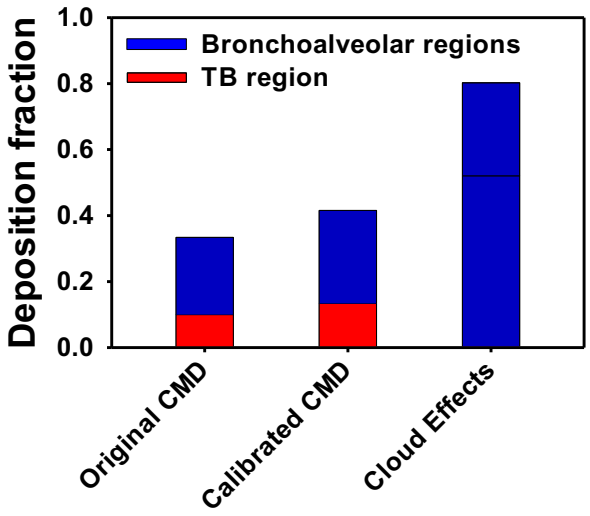

Figure S2-3. The deposition fractions of e-cigarette particles in the bronchoalveolar regions and the TB region, calculated with 1) the originally measured e-cigarette particle size, 2) e-cigarette particle size corrected for dilution, and 3) e-cigarette particle size corrected for both dilution and cloud effects. E-cigarette particles were generated from VG-based non-flavored e-liquids containing 12 mg/ml nicotine, under 6.4 watts, and 90 mL and 3.8 sec puffs

Table S2-12. The deposition fraction of e-cigarette particles, generated under different e-cigarette device power in the tracheal bronchus (TB) region and the bronchoalveolar regions of human airways

Region	Power output		
	6.4W	14.7W	31.3W
TB	0.541	0.532	0.517
Bronchoalveolar	0.269	0.290	0.306

Table S2-13. The deposition fraction of e-cigarette particles in the tracheal bronchus (TB) region and the bronchoalveolar regions of human airways under different vaping topographies

Deposition Region	Puff Volume and Puff Duration					
	35 ml		90 ml		170 ml	
	2 sec	3.8 sec	2 sec	3.8 sec	2 sec	3.8 sec
TB	0.511	0.504	0.534	0.520	0.529	0.542
Bronchoalveolar	0.137	0.159	0.260	0.251	0.073	0.228

Table S2-14. The deposition fraction of e-cigarette particles, generated from e-liquid with different base material and nicotine contents, in the tracheal bronchus (TB) region and the bronchoalveolar regions of human airways

Region	Power output		
	VG	PG:VG (v:v=1:1)	PG
TB	0.530	0.538	0.539
Bronchoalveolar	0.289	0.174	0.156

Table S2-15. The deposition fraction of e-cigarette particles, generated from different flavored e-liquid, in the tracheal bronchus (TB) region and the bronchoalveolar regions of human airways

Flavoring Agent Content*	Deposition Region	Flavoring Agents							
		Straw-berry	Dragon -fruit	Men-thol	Cinna-mon	Bubble -gum	Bavar-ian	Sweet-cream	Gra-ham
Low	**TB**	0.523	0.526	0.534	0.531	0.526	0.532	0.534	0.533
	Broncho-alveolar	0.265	0.273	0.283	0.284	0.284	0.281	0.283	0.282
High	**TB**	0.549	0.530	0.529	0.527	0.538	0.539	0.531	0.534
	Broncho-alveolar	0.290	0.273	0.287	0.278	0.288	0.286	0.284	0.281

***Low level and high level flavoring agents indicate 1% and 10% of flavoring agents in e-liquids, except for the cinnamon flavor (0.1% and 1% in e-liquids for low and high contents, respectively).**

REFERENCES

[1] ICRP, *ICRP Publication 66: Human Respiratory Tract Model for Radiological Protection*. 1994: International Commission on Radiological Protection.

[2] Broday, D.M. and R. Robinson, *Application of cloud dynamics to dosimetry of cigarette smoke particles in the lungs.* Aerosol Science & Technology, 2003. **37**(6): p. 510-527.

[3] Hinds, W.C., *Aerosol technology: properties, behavior, and measurement of airborne particles*. 2012: John Wiley & Sons.

[4] Asgharian, B., et al., *Component-specific, cigarette particle deposition modeling in the human respiratory tract.* Inhalation toxicology, 2014. **26**(1): p. 36-47.

Appendix 3

Nicotine and nicotyrine concentrations of e-vapor

I. The experimental settings for e-vapor generation

II. The calibration curves for nicotine and nicotyrine

III. Nicotine and nicotyrine analysis using GC/MS/MS method

IV. Calibration factors for the measurement artifacts

V. Nicotine, nicotyrine and e-vapor mass under different experimental conditions

I. The experimental settings for e-cigarette particle generation

E-cigarette particles were generated under the following conditions specified in Table S3-1.

Table S3-1. The experimental settings for e-cigarette particle generation

Experiments	Factors	Settings	Other Settings
E-liquid bulk material	Base material	PG, VG, PG&VG (v:v = 1:1)	6.4 W, 2 mm air hole, 90 mL puff volume, 3.8 sec puff duration
	Nicotine (mg/mL)	0, 3, 12, 24, 36	
Device setting	Device power (watt)	6.4, 14.7, 31.3	6.4 W, 2 mm air hole and 12 mg/ml nicotine in VG
Vaping topography	Puff volume (mL)	35, 90, 170	6.4 W, 2 mm air hole and 12 mg/ml nicotine in VG
	Puff duration (sec)	2, 3.8	

***Strawberry (Ripe), dragonfruit, menthol, cinnamon, bubblegum, bavarian cream, sweet cream, and graham cracker; **0.1% and 1% for the cinnamon flavor**

II. The calibration curves for nicotine and nicotyrine

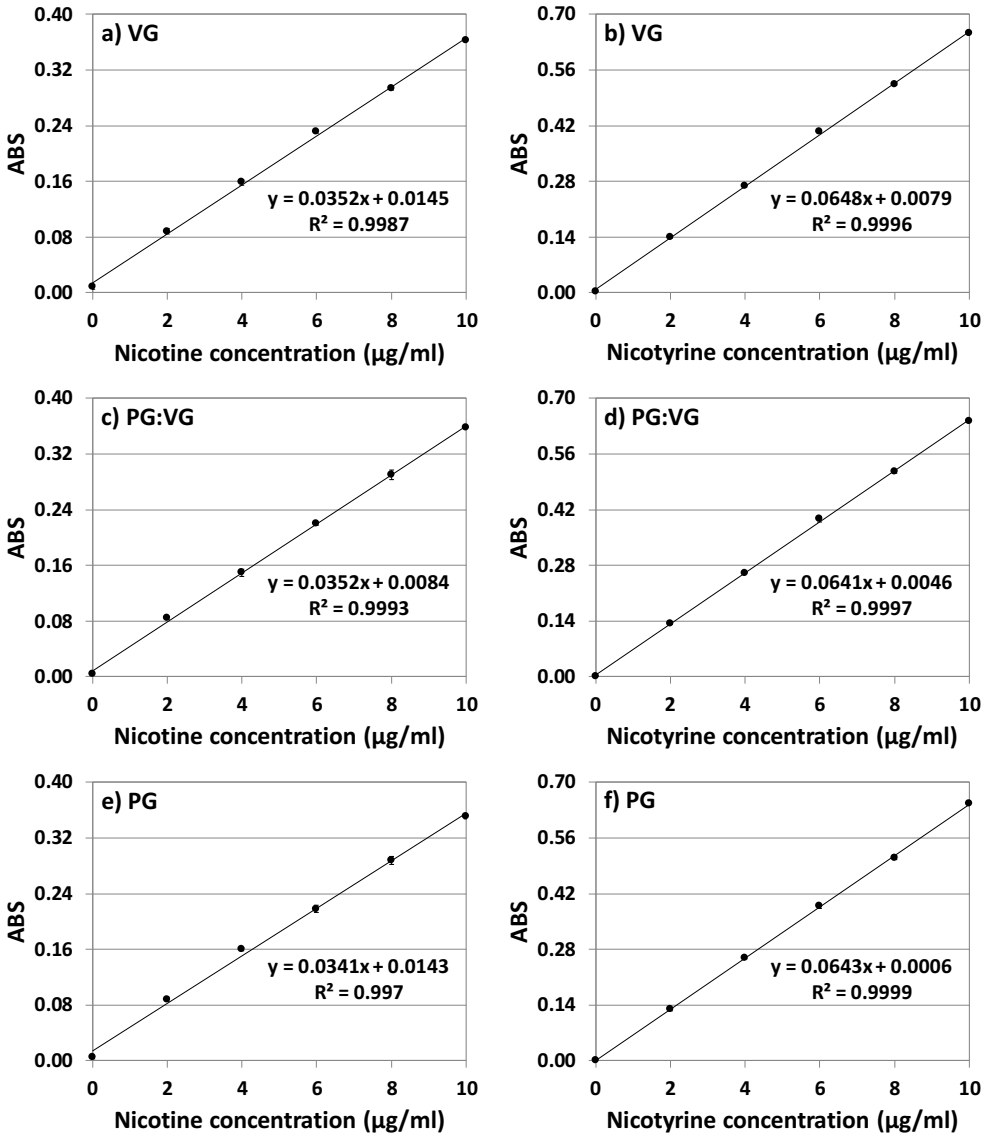

Figure S3-1. Nicotine and nicotyrine calibration curves prepared using 100% VG (a, b), 50% of PG and 50% of VG mixture (c, d), and 100% PG based e-liquid (e,f)

III. Nicotine and nicotyrine analysis using GC/MS/MS method

Table S3-2. GC/MS/MS parameters

Compound	Retention time (min)	Parent (m/z)	Daughter (m/z)	Collision energy (V)
Quinoline	8.59	129	77	35
		129	103	25
Nicotine	12.36	162	84	11
Nicotyrine	17.71	158	130	28

In order to measure nicotine and nicotyrine concentration of e-vapor using GC/MS/MS, 20 puffs of e-vapor were generated using VG based e-liquid containing 12 mg/ml nicotine under the two different power output conditions (6.4W and 31.3W). Vaping topography was 90 ml puff volume, 3.8-sec puff duration, and 24-sec puff interval. Generated e-vapor was collected on the Teflon filter, and then the sample filter was spiked using 2 ul quinoline to have the filnal concentration of 545 µg/ml. Extracted e-vapor with 4 ml of methanol (HPLC grande, ≥99.9%, Sigma, St. Louis, MO, USA) was analyzed using multiple reaction monitoring (MRM) mode using the parameters tabulated in Table S3-2.

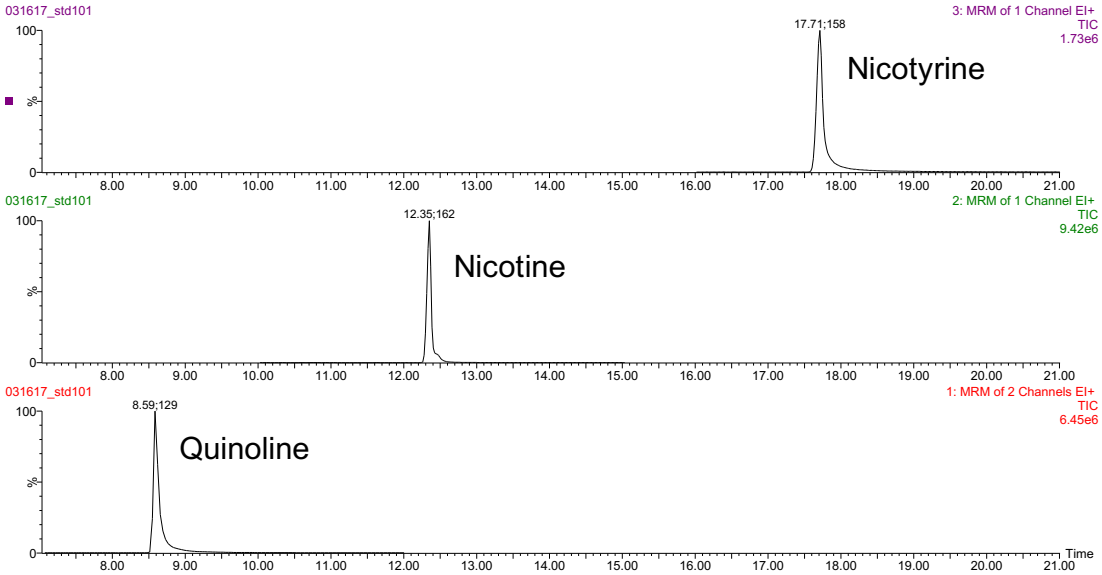

Figure S3-2. Chromatographic profiles of quinoline, nicotine, and nicotyrine

All GC/MS/MS analysis was performed using the Waters Micromass Quattro micro GC (Waters Corporation, Milford, MA, USA) connected with the Agilent 6890N GC oven (Agilent Technologies, Santa Clara, CA, USA). A DB-5ms column (30 m length, 0.25 mm ID, 0.25 μm thickness, Agilent Technologies, Santa Clara, CA, USA) was installed in splitless mode. The GC oven temperature ramp 80 °C for 2 min, 4 °C /min to 125 °C, hold 5 min, 40 °C/min to 240 °C, hold 5min. Constant flow rate was used with a He flow of 2 ml/min. Figure S3-2 shows chromatographic profiles of quinoline, nicotine, and nicotyrine.

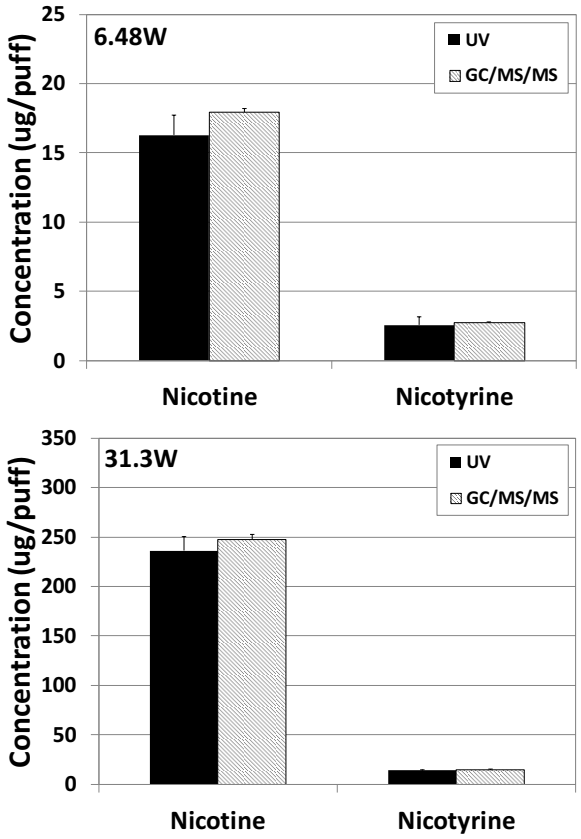

Figure S3-3. Nicotine and nicotyrine concentration measured using UV and GC/MS/MS method (N = 3, and error bars are standard deviations of the 5 independent measurements)

Figure S3-3 shows nicotine and nicotyrine concentration measured using UV and GC/MS/MS method. Average extraction efficiency was 99.4±0.7%. No significant difference was observed between these two methods, with the average difference less than 10%.

IV. Calibration factors for the measurement artifacts

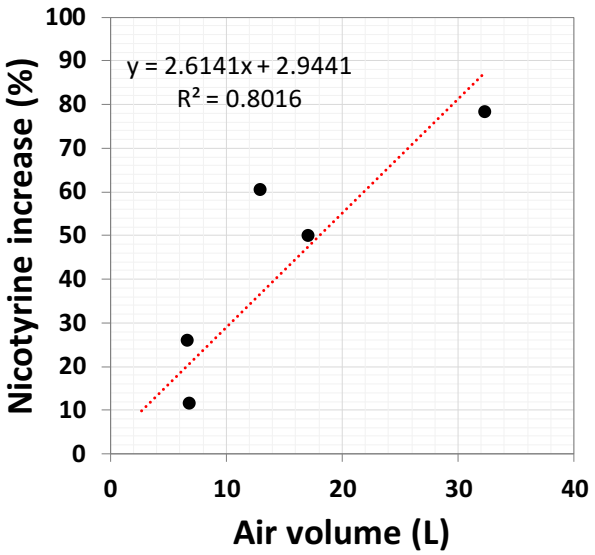

Figure S3-4. Linear regression for the introduced air volume (L) into the sample filter and nicotyrine increment (%)

Table S3-3. Calibration factors for the air introduced into the sample filters

Puff duration	Puff volume		
	35 ml	**90 ml**	**170 ml**
2 sec	0.938	0.890	0.828
3.8 sec	0.910	0.828	0.731

Calibration factors for the measurement artifacts were derived using the relationship between the air introduced into the sample filter and increased nicotyrine (Figure S3-4). Estimated calibration factors were tabulated in Table S3-3. In addition, calibration factors for the e-liquid samples with different nicotine concentrations were 0.423, 0.828, 0.945, and 0.962 for 3, 12, 24, and 36 mg/ml, respectively.

V. Nicotine, nicotyrine and e-vapor mass under different experimental conditions

Table S3-4. Nicotine, nicotyrine, nicotyrine/nicotine ratio, and e-vapor mass of e-cigarette vapor generated from e-liquid with different base material and nicotine contents

E-liquid Base Material	Component	Nicotine Contents			
		3 mg/mL	12 mg/mL	24 mg/mL	36 mg/mL
VG	Nicotine (µg/puff)	3.87±0.51	15.74±2.90	30.45±5.03	45.15±2.67
	Nicotyrine (µg/puff)	0.19±0.06	1.98±0.38	2.55±0.35	2.59±0.43
	Nicotyrine/Nicotine	0.050±0.019	0.126±0.041	0.084±0.019	0.057±0.019
	E-vapor mass (mg/puff)	1.59±0.21	1.53±0.20	1.25±0.05	1.34±0.27
	Nicotine (mg/ml)	1.93±0.36	8.19±1.86	19.26±3.27	26.81±5.68
PG:VG = 1:1	Nicotine (µg/puff)	4.54±1.00	17.33±2.23	29.51±2.08	43.13±4.71
	Nicotyrine (µg/puff)	0.23±0.05	1.67±0.28	2.53±0.19	2.62±0.25
	Nicotyrine/Nicotine	0.050±0.096	0.096±0.046	0.086±0.023	0.061±0.011
	E-vapor mass (mg/puff)	1.33±0.27	1.38±0.42	1.41±0.24	1.31±0.09
	Nicotine (mg/ml)	2.97±0.89	10.90±3.61	18.26±3.38	28.61±3.69
PG	Nicotine (µg/puff)	0.37±0.03	2.13±0.15	3.80±0.36	7.55±0.38
	Nicotyrine (µg/puff)	0.01±0.00	0.24±0.05	0.35±0.11	0.72±0.21
	Nicotyrine/Nicotine	0.025±0.007	0.114±0.035	0.091±0.035	0.096±0.041
	E-vapor mass (mg/puff)	0.18±0.03	0.16±0.02	0.16±0.02	0.20±0.05
	Nicotine (mg/ml)	1.99±0.33	12.72±2.16	23.09±3.88	35.47±8.19

Table S3-5. Nicotine, nicotyrine, nicotyrine/nicotine ratio, and e-vapor mass of e-cigarette vapor generated under different E-cigarette device power outputs

Component	Device Power		
	6.4 W	**14.7 W**	**31.3 W**
Nicotine (µg/puff)	16.29±1.44	137.06±6.72	236.25±13.97
Nicotyrine (µg/puff)	2.11±0.51	12.67±0.34	11.64±0.35
Nicotyrine/Nicotine	0.129±0.043	0.092±0.030	0.049±0.005
E-vapor mass (mg/puff)	1.47±0.22	8.90±2.06	21.55±1.19
Nicotine (mg/ml)	8.82±1.54	8.64±2.10	8.70±0.71

Table S3-6. Nicotine, nicotyrine, nicotyrine/nicotine ratio, and e-vapor mass of e-cigarette vapor under different vaping topographies

Puff duration	Component	Puff volume		
		35 ml	**90 ml**	**170 ml**
2 sec	**Nicotine (µg/puff)**	3.29±0.31	3.05±0.26	3.53±0.39
	Nicotyrine (µg/puff)	0.23±0.02	0.24±0.01	0.23±0.01
	Nicotyrine/Nicotine	0.069±0.014	0.078±0.015	0.064±0.033
	E-vapor mass (mg/puff)	0.31±0.03	0.28±0.03	0.33±0.12
	Nicotine (mg/ml)	8.48±1.18	8.68±1.28	8.43±3.15
3.8 sec	**Nicotine (µg/puff)**	10.80±2.03	16.00±0.74	24.38±1.91
	Nicotyrine (µg/puff)	2.19±0.25	2.28±0.38	2.65±0.25
	Nicotyrine/Nicotine	0.202±0.053	0.142±0.044	0.109±0.017
	E-vapor mass (mg/puff)	0.94±0.09	1.43±0.26	2.25±0.15
	Nicotine (mg/ml)	9.13±1.94	8.91±1.67	8.58±0.88

Appendix 4

Hydroxyl radicals induced by e-cigarette vaping

I. Structure, properties, and occupational exposure limits for the flavoring chemicals

II. The detailed experimental conditions

III. Calibration curve for 2OHTA

I. Structure, properties, and occupational exposure limits for the selected flavouring chemicals

Table S4-1. Characteristics of flavoring chemicals

Name	Flavor	Structure	Property	Occupational exposure limits (mg/m^3)					
				OSHA PEL		ACGIH TLV		NIOSH REL	
				TWA	STEL	TWA	STEL	TWA	STEL
Benzyl alcohol	Fruity		MW: 108.14 g/mol BP: 205.3 °C, VP: 0.18 kPa						
Benzyl acetate	Fruity	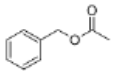	MW: 150.18 g/mol BP: 212 °C, VP: 0.02 kPa	61		61			
Ethyl acetate	Fruity		MW: 88.11 g/mol BP: 77.1 °C, VP: 9.7 kPa	1400		1400		1400	7200
Anethole	Sweet	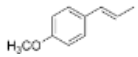	MW: 148.21 g/mol BP: 234 °C, VP: > 1 Pa						
Citral	Citrus	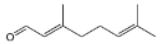	MW: 152.24 g/mol BP: 229 °C, VP: 13.3 Pa			31 (dermal)			
Cinnamaldehyde	Spicy, sweet	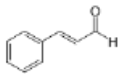	MW: 132.16 g/mol BP: 248 °C, VP: > 1 Pa						
Vanillin	Sweet, Fatty		MW: 152.15 g/mol BP: 285 °C, VP: > 1 Pa						
2,3-butanedione (diacetyl)	Fatty, Buttery	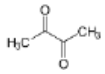	MW: 86.09 g/mol BP: 88 °C, VP: 7.57 kPa			0.035	0.070	0.018	0.088
2,3-pentanedione (Acetylpropionyl)	Fatty, Buttery		MW: 100.12 g/mol BP: 109.9 °C, VP: 2.67 kPa					0.038	0.127

II. The detailed experimental conditions

The e-vapor generation conditions are tabulated in Table S4-2.

Table S4-2. The experimental factors used in the experiments

Experiments	Factors	Settings	Other Settings for Particle Generation
Device setting	Device power (watt)	6.4, 31.3	90 mL puff volume, 3.8 sec puff duration, 12 mg/ml nicotine in VG
	Air hole size (mm)	1, 1.5, 2	
Vaping topography	Puff volume (mL)	35, 90, 170	6.4W, 2 mm air hole and 12 mg/ml nicotine in VG;
	Puff duration (sec)	2, 3.8	
E-liquid base material	Base material	PG, VG, PG&VG (v:v = 1:1)	6.4W, 2 mm air hole, 90 mL puff volume, 3.8 sec puff duration
	Nicotine (mg/ml)	12	
E-liquid flavoring ingredients	Flavor	8 flavors*	6.4W, 2 mm air hole, 90 mL puff volume, 3.8 sec puff duration, VG
	Flavoring level (%)	1 and 10% by volume**	

* Strawberry (Ripe), Dragonfruit, Menthol, Cinnamon, Bubblegum, Bavarian cream, Sweet cream and Graham cracker; ** 0.1 and 1% for cinnamon flavor

III. Calibration curve for 2OHTA

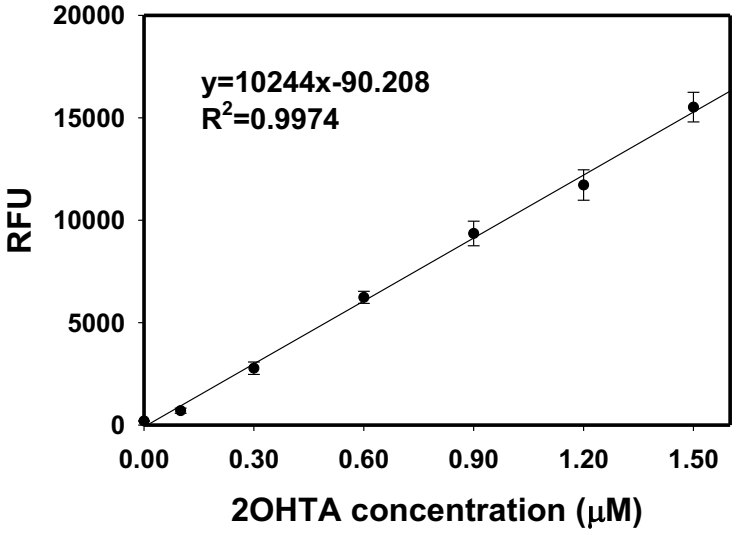

Figure S4-1. Calibration curve for 2OHTA

Appendix 5

Carbonyls emitted from the e-cigarette

I. The detailed experimental conditions

II. The carbonyl sampling system

III. E-cigarette coil setting

I. The detailed experimental conditions

Table S5-1. The experimental factors used in the experiments

Experiments	Factors	Settings	Other Settings
E-liquid flavoring ingredients	Flavor	8 flavors*	6.48 W, 90 mL puff volume, 3.8 sec puff duration, VG
	Flavoring level (%)	10	
E-liquid base material	Base material	VG, PG, PG:VG=1:1 (v/v)	6.48 W, 90 mL puff volume, 3.8 sec puff duration
	Nicotine (mg/ml)	12	
Device setting	Device power (watt)	6.4, 14.7, 31.3	90 mL puff volume, 3.8 sec puff duration, 12 mg/ml nicotine in VG
Vaping topography	Puff volume (mL)	35, 90, 170	6.48 W, 12 mg/ml nicotine in VG
	Puff duration (sec)	2, 3.8	

* Strawberry (Ripe), Dragonfruit, Menthol, Cinnamon, Bubblegum, Bavarian cream, Sweet cream and Graham cracker; **1% for cinnamon flavor

II. The carbonyl sampling system

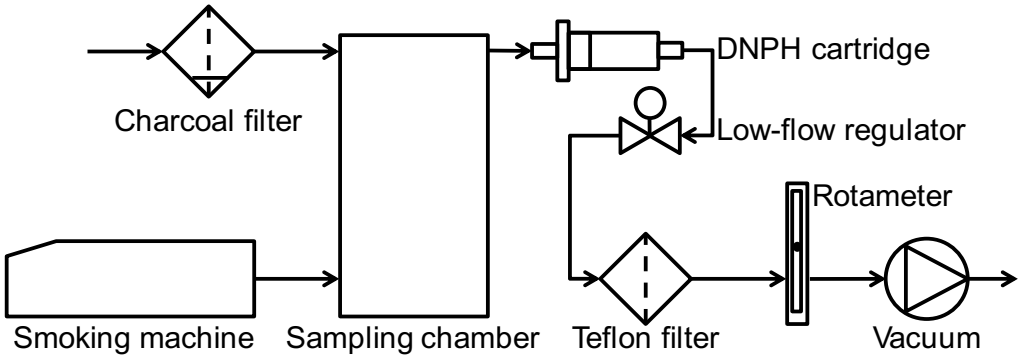

Figure S5-1. Scheme of the carbonyl sampling system

III. E-cigarette coil setting

Figure S5-2. Example of the top and bottom coil settings (obtained from https://www.smokshop.com/blogs/news/15508169-heads-or-tails-bottom-and-top-coils)

Appendix 6

Estimation of the Human Lung Cancer Risks Associated with E-cigarette Vaping

I. Weights to estimate cumulative cancer risks

I. Weights to estimate cumulative cancer risks

Weights for device power output, puff volume, puff duration, and e-liquid base material were determined based on the e-cigarette use patterns observed from the 23 current e-cigarette users.

Table S6-1. Weights for device power output to estimate cumulative cancer risks

Power output (watts)		
6.4W	14.7W	31.3W
0.48	0.26	0.26

Table S6-2. Weights for puff volume to estimate cumulative cancer risks

Puff volume (ml)		
35 ml	90 ml	170 ml
0.13	0.65	0.22

Table S6-3. Weights for puff duration to estimate cumulative cancer risks

Puff duration (seconds)	
2 sec	3.8 sec
0.13	0.87

Table S6-4. Weights for e-liquid base material to estimate cumulative cancer risks

Base material		
VG	PG&VG mixture (PG:VG=1:1 (v/v))	PG
0.61	0.30	0.09

ACKOWLEDGEMENT OF PENDING PUBLICATIONS

I acknowledge that chapter 2, 3, 4, 5, and 6 of this dissertation in whole or in part will be reformatted and published in the Environmental Science & Technology, Journal of Aerosol Science, and other peer reviewed journals.